ABSTRACT

MOORE IV, ARNOLD D. Air Permeability of Nonwoven Fabrics. (Under the direction of Dr. Benoit Maze.)

Air permeability of a nonwoven, the nonwoven's ability to resist the flow of air through the fabric, is an essential property which determines the functionality and end use of the fabric. Though affected by many factors, the two most influential factors influencing air permeability are the fiber diameter and the solid volume fraction of the fabric. This research compares numerous theoretical models that use fiber diameter and solid volume fraction to predict air permeability with the experimental results of the air permeability of carded and needle punched nonwoven fabrics.

The air permeability of samples from different nonwoven fabrics with varying fiber diameters are measured at varying levels of solid volume fraction to assess the influence fiber diameter and solid volume fraction had on the air permeability using two different testing methods. The results of these two testing methods are made comparable through back calculations and the experimental data is compared with the theoretical models.

The theoretical models tended to under predict the air permeability when compared with the experimental results, but this could be because the samples tested were needled punched nonwoven fabric which naturally have a higher permeability than comparable fabrics. In general, the empirical models tended to be limited by the realms in which their experimental work was based and the analytical models based on the flow of air through defined structures failed to predict the behavior of air through such a non-uniform fabric such as a nonwoven. Overall some of the oldest models, the models by Davies, Kuwabara, and Spielman & Goren were found to be most accurate and robust models available.

Air Permeability in Nonwoven Fabrics

by
Arnold D. Moore IV

A thesis submitted to the Graduate Faculty of
North Carolina State University
in partial fulfillment of the
requirements for the Degree of
Master of Science

Textiles

Raleigh, North Carolina

2015

APPROVED BY:

_____	_____
Dr. Behnam Pourdeyhimi	Dr. William Oxenham

_____
Dr. Benoit Maze

BIOGRAPHY

Arnold “Daniel” Moore IV was born in Hickory, North Carolina. He graduated from Newton-Conover High School in 2005 and magna cum laude from Elon University with a Bachelors of Arts in Elementary and Middle Grades Education in 2009. After teaching middle grades mathematics for a few years, he began working towards his Masters of Science in Textiles from North Carolina State University, with a focus in nonwoven fabrics.

ACKNOWLEDGEMENTS

I would like to give a big thank you to my advisors and committee members, Dr. Benoit Maze, Dr. Behnam Pourdeyhimi, and Dr. William Oxenham, for their guidance, support and patience throughout my project. Without their advice, knowledge, and experience, this project would have not been possible.

I would also like to express my gratitude to Amy Minton for her help with the multitude of testing done in this research, to Bruce Anderson for his help with the design and manufacturing of the spacer rings, and to Maryanne Ross for her wisdom with words and help in proofing my written work.

Most of all, I would like to thank my family and friends for their support and inspiration during this arduous process and throughout my academic career.

TABLE OF CONTENTS

LIST OF TABLES

LIST OF FIGURES

1. INTRODUCTION

Air permeability plays a critical role in the application of many nonwoven fabrics. Due to the essential role it plays in its application and since air permeability is dictated by the structure of the fabric and the flow and viscosity of the air, being able to predict and control the air permeability of a nonwoven fabric, it is essential in planning and manufacturing of a nonwoven product. Unfortunately, there are a multitude of theories for predicting the air permeability of a fabric available therefore, resulting in making an easy task in choosing which one very difficult.

The purpose of this research is to analyze the numerous ways of predicting the air permeability of a fabric and to determine which method or methods is the most appropriate to use with a nonwoven fabric. After investigating the variety of ways for predicting air permeability and the factors that affect air permeability, a dual approach was proposed to assess the air permeability of nonwoven samples with theoretical models for predicting air permeability in fabrics. Using two different air permeability testers that incorporated two different methods of testing, polyester carded and needle punched samples of nonwovens were analyzed for the effect that changing fiber diameter and changing solid volume fraction had on the air permeability of the samples.

After instituting a compression system and assessing the difference between the different testing methods with preliminary trials, a means of conversation was established between the different testing methods. The compression system was used to control the solid volume fraction in samples from five different fabrics with varying fiber diameters and the samples were measured at varying solid volume fractions in both testing systems. The

results from using the compression system in both air permeability testers were then back calculated to be comparable to results done according with the ASTM Standard for Air Permeability in a Textile Fabric and then compared with the theoretical models for predicting air permeability.

In the proceeding chapters, Chapter 2 contains a literature review of nonwovens and air permeability, including factors affecting air permeability and the theoretical models for predicting air permeability, Chapter 3 is the problem statement and approach for this research, Chapter 4 is the experimental work and its results, Chapter 5 compares the experimental work to the theoretical models, and Chapter 6 recaps this research with a conclusion and recommendations for possible future works.

2. LITERATURE REVIEW

2.1 Air Permeability

Air permeability is a measurement of how well air can pass through a media, typically a porous or granular material. More specifically it is "the volume of air which passes in unit time, through unit area of the fabric, at a constant pressure difference (Pradaham, 2013, pg. 18)." So in nonwoven fabrics, air permeability, typically represented by the letter *K*, is a measurement of the lack of resistance to air flow through the nonwoven. So nonwovens with a higher air permeability, or higher *K*, will have less resistance to air flow through the material than a nonwoven with a lower air permeability, or lower *K*.

Being inversely proportional to the pressure drop across a nonwoven, air permeability is affected by the structure of the material, the rate of air flow, the pressure of air flow, and the viscosity of the air and can be calculated using Darcy's Law. Ultimately, the air permeability is key factor in determining the end applications that nonwoven fabrics can be used for.

2.1.1 Factors Affecting Air Permeability

The permeability of a fabric is affected by two core areas: the properties of the fabric itself and the properties of air or Newtonian fluid trying to pass through the fabric. The fabric characteristics play a key role in determining the air flow through the material, whereas the properties of the air determine the extent to which the fabric affects the air flow.

2.1.1.1 Media Related Factors

By far the biggest factor affecting the air permeability of a fabric is the structure of fabric. .Almost every aspect of the fabric design and production process can have some effect on the flow of air through the fabric, from fiber selection (fiber fineness, fiber length fiber cross-sectional shape, and fiber crimp) to mode of production, because each aspect can have some effect on the overall structure and pore geometry of the fabric produced. The structure (solid volume fraction, fabric uniformity, fiber orientation, manufacturing and bonding process, basis weight, and thickness) and pore geometry of the fabric determines how air travels through the fabric, which determines the air permeability.

2.1.1.1.1 Fiber Fineness

Fiber fineness is one of the important factors in determining the structure and pore geometry in fabrics, which means it "plays a key role on determining the fluid flow behavior" (Pradham, 2013, pg. 24) within the fabric. Fabrics produced with finer fibers have a larger surface area to mass ratio when compared with similar fabrics produced with coarser fibers, which results in a higher drag resistance and a lower permeability (Pradham, 2013). Besides their effect on drag resistance, fiber fineness can also have an effect on the packing structure and pore size of a fabric. Fabrics produced with finer fibers, typically result with smaller pores and more tortuous and longer flow paths, which results in lower air permeability.

2.1.1.1.2 Fiber Length

Though fiber length can have some effect on the air permeability of a nonwoven fabric, it has been found to have a more limited or indirect effect on the air permeability of nonwoven fabrics through its ability to influence the solid volume fraction of a fabric (Wang, Maze, Tafreshi, & Pourdeyhimi, 2007b). Since shorter fibers can be packed more densely than longer fibers, it is possible to produce more denser, less permeable fabrics with shorter fibers, but if the density or solid volume fraction of the fibers is kept constant, "fiber length has no significant influence on materials' through-plane permeability" (Wang, Maze, Tafreshi, & Pourdeyhimi,2007a, pg. 855) for the range of fiber lengths typically used for nonwoven fabrics (Wang, Maze, Tafreshi & Pourdeyhimi, 2007b; Pradham, 2013).

2.1.1.1.3 Fiber Cross-Sectional Shape

Since fiber cross-sectional shape has an effect on the mean fiber diameter and surface area, the fiber cross-sectional shape will inevitable have some effect on the flow of air through a fabric. Though the exact extent of fiber cross-sectional shape is not well known, due to most research on this area focusing on circular fibers, Labrecque (1967) reported that "there was very little effect of cross-sectional shape on the resistance to the flow of fluids through fiber mats (pg. 2)" when the aspect ratio of the cross section of the fiber was below 3:1. However, Labrecque (1967) found that air permeability decreased when the fiber's cross-sectional aspect ratio was above 3:1.

2.1.1.1.4 Fiber Crimp

Crimp has the ability to affect the flow of air through a fabric through its ability to affect the structure and increase the bulk or loft of a fabric. Higher crimped fibers can be used to produce bulkier, less dense fabrics which will have a higher permeability, but independent of their ability to affect the fabrics structure, fiber crimp or fiber "curvature has a negligible impact on the permeability of the medium (Nabovati, Llewellin, & Sousa, 2009, pg. 868).

2.1.1.1.5 Solid Volume Fraction or Porosity

One of the most significant factors affecting the flow of air through the fabric is the solid volume fraction, or porosity of the fabric. Opposites of each other, solid volume fraction is the percent of the fabric made up by solids or fibers, and porosity is the percent of the volume made up by air (Solid Volume Fraction = 1 – Porosity). According to Wang, Maze, Tafreshi, & Pourdeyhimi (2007b), "pressure drop increases by increasing the solid volume of the material when the fiber diameter is kept constant (pg. 866)," so the more dense the fabric (or the higher solid volume fraction/lower the porosity), the more fibers there are to resist the flow of air through the fabric, which results in a lower air permeability. The opposite can also be said true, the less dense the fabric (or lower solid volume fraction/higher the porosity), the higher air permeability of the fabric.

2.1.1.1.6 Fabric Uniformity

While the uniformity or the consistency of a fabric cannot really have the power to decrease the permeability of a fabric, it does have the ability to increase the permeability of a fabric. Whereas a uniform fabric should have consistent air flow throughout, a non-uniform fabric will have disproportionate flow with increased flow with a smaller pressure drop in the less-dense areas compared to the denser areas of the material. The disproportionate flow throughout a non-uniform fabric will result in a higher permeability than a similar uniform fabric (Jackson & James, 1986; Higdon & Ford, 1996).

2.1.1.1.7 Fiber Orientation

The overall fiber distribution in a fabric is one of the determine characteristics of the fabric structure, and therefore also has an influence on the flow of air through the fabric. According to Mao & Russell (2000), the "fiber orientation is a major factor influencing the anisotropy of permeability (pg. 235)," and an increase in anisotropy, results in an increase in permeability of the fabric (Pradham, 2013). In particular, fiber orientation in the Z-direction results in higher fabric transverse permeabilities, since there is lower pressure drop across the fabric because fibers are aligned parallel with the flow of air and offer less resistance to the flow (Pradham, 2013).

2.1.1.1.8 Basis Weight

There has been much debate on the influence of basis weight on the permeability of a fabric. Kothari and Newton (1976) proposed that basis weight was "the most important

single controlling factor that affects the web air-permeability (pg. 220)." Dent (1976) disagreed with Kothari and Newton, stating that while basis weight was an important factor, its importance was affected by the thickness and density of the web. There is no question that there is some correlation between basis weight and air permeability, especially since the basis weight of the fabric has an influence on the solid volume fraction and porosity of the fabric.

2.1.1.1.9 Thickness

The thickness of a fabric is also important factor determining the flow of air through a fabric, because its ability to affect the mean flow length through the fabric. Vallabh, Banks-Lee, & Seyam (2010) found that in thicker fabrics, the flow path encountered "more fibers, resulting in more tortuous and longer pore channels connecting the pores on the front and back faces (pg. 14)." There is no doubt that thickness has the ability to impact the air permeability of a fabric through its influence on the solid volume fraction or porosity of a fabric, but there are further arguments "that permeability increased with increasing fiberweb thickness with porosity and fiber diameter being constant (Vallabh, Banks-Lee, Seyam, 2010, pg. 14)."

2.1.1.1.10 Manufacturing Process

Since the process or processes used for fabric manufacturing determine the structure of the end fabric, the manufacturing processes can play a huge role on the flow of air through the fabric. The web formation can have huge effect on the fiber orientation, fabric thickness,

and/or uniformity of the end product. For example, a carded fabric's thickness or fiber orientation can be greatly affected if the product is cross-lapped as well, or a spun-laid fabric's uniformity will greatly depend on the speed of production and the efficiency of the manufacturing technology. The bonding processes also affect the structure of the fabric. Thermal calendaring can decrease thickness, lower uniformity, and create a geometrical pattern of bond points in the fabric, whereas thermal through-air bonding typically only affects the fabric by creating bond points at fiber-to-fiber cross-over. Needle punching a fabric particularly increases air permeability by making through channels/pores where the needles pass through the fabric (Lawrence & Liu, 2013; Pradham, 2013).

2.1.1.2 Air Related Factors

Whereas the fabric works to limit the flow of air through the fabric, the power and force behind of the air determines the extent at which air can work its way through the fabric. What goes in, affects what comes out. Two core factors determine the force behind the air: the air viscosity and the air velocity/flow.

2.1.1.2.1 Air Viscosity

The viscosity or thickness of the fluid or air plays a major role in determine the flow of air through a fabric. Since viscosity has to do with the internal friction of the fluid or air, it is no surprise that it will have an effect on the friction or resistance between the fabric and the air. The viscosity of the air is affected by the temperature of the air. The relationship between the temperature of the air and the viscosity, Sutherland's Formula,

$$\mu = \mu_O \left(\frac{T}{T_O}\right)^{3/2} \left(\frac{T_O + C}{T + C}\right)$$

(μ = viscosity, μ_O = reference viscosity, T = absolute temperature [K],

T_O = reference temperature [K], C = Sutherland's constant [K])

shows that as the temperature increases, the viscosity of the air will also increase (Benson, 2014). Somewhat surprisingly, as the viscosity or magnitude of internal friction of the air increases, so does the air permeability of the fabric. Therefore, using a fluid or air with a higher viscosity, will result an increase in air permeability when all other factors are kept constant (Kopenen et al., 1998).

2.1.1.2.2 Air Velocity/Flow

Though it may come as no surprise, the velocity or flow of the air also plays a key role in determining the air permeability of the fabric. The speed or force at which the air enters the fabric will greatly affect how the fabric and individual fibers react to the air. At lower air velocities, air flows around fibers and through open pore channels, but as the velocity and pressure of the air increases this is not the case. At higher velocities, what were once closed pore channels they too have the potential to be forced open, creating further and easier paths at which air can pass through the fabric (Pradham, 2013). Also, at higher Knudsen numbers, the effect that an individual fiber has on the flow of air around it is diminished and would theoretically be negligible if the fiber was small enough and the Knudsen number high enough (Maze, Vahedi Tagreshi, Wang & Pourdeyhimi, 2007). For these reasons, a drastic increase in air velocity should decrease a fabric's ability to limit air flow and therefore increase the air permeability of the fabric.

2.1.2 Calculating Air Permeability

Since air permeability is a measurement of how easily air can pass through a porous or granular material, the air permeability of the material is calculated by measuring the resistance air receives as it passes through the material using measurements of the flow of air and the pressure drop through the fabric. Darcy's Law is then used to relate the flow of air and the pressure drop through the material to derive the specific permeability, *K*, of the material. Because of this relation, air permeability is measured by using a fixed air pressure or air flow and measuring the other.

2.1.2.1 Darcy's Law

$$\frac{Q}{A} = \frac{K\Delta p}{\mu Z}$$

(Q = volumetric flow rate, K = permeability of the material, Δp = pressure difference, A = cross sectional area, μ = viscosity of the fluid, Z = thickness)

Named after the French engineer who discovered it, Henri Darcy, Darcy's Law relates the amount of flow, the viscosity of the fluid, the difference in pressure, the distance, and the permeability of two specific points (Darcy's Law, 2015; FracFocus, 2015). Though it was derived based on Darcy's study of the flow of groundwater in 1856, it has since "has been found valid for any Newtonian fluid (Brown, 2005)." Darcy's Law is essential in determining the specific permeability, *K*, of fabrics from the pressure difference or air flow calculated by air permeability testers.

2.1.2.2 Fixed P

Of the two methods used to calculate air permeability, the more commonly used and approved method uses a fixed pressure differential. In this method "the rate of air flow passing perpendicularly through a known area of fabric is adjusted to obtain a prescribed air pressure differential between the two fabric surfaces (ASTM International, 2012, pg. 1.)." Once the air flow is measured, it can be used with the prescribed air pressure differential and Darcy's Law to determine the fabric's permeability. According to the ASTM *Standard Test Method for Air Permeability of Textile Fabrics,* the pressure drop must be at least 125 Pa.

2.1.2.3 Fixed Q

The second and less commonly used method used to calculate air permeability uses a fixed rate of flow. In this method the pressure differential is adjusted so that a prescribed rate of air flow is passing perpendicular through a known area of fabric. Once the pressure differential is measured and calculated, it can be used with the prescribed air flow and Darcy's Law to determine the fabric's permeability.

2.2 Nonwoven Fabrics

The International Organization for Standardization defines a nonwoven fabric as "a manufactured sheet, web or batt of directionally or randomly orientated fibres, bonded by friction, and/or cohesion and/or adhesion (ISO, 2011)." In simpler terms, a nonwoven is a fabric produced from fibers and polymers rather than yarns and it is not knitted or woven, but an "assembly of fibers held together by bonding and/or interlocking (Shim, 2012a, pg. 5)."

By removing the need to turn fibers into yarn, originally nonwovens grew in popularity because of their cheaper and faster production methods when compared with traditional fabrics. Advancements in manufacturing methods have since turned the nonwoven industry into a multi-billion dollar industry due to their ability to produce highly engineered fabrics, designed with diverse properties and tailored to fit a variety of specific functions in the hygiene, medical, wipe, garment, packaging, automotive, furnishing, agriculture, geotextiles, filtration and a variety of other markets.

2.2.1 Manufacturing of Nonwovens

Nonwoven fabrics, produced from staple fibers or polymers, are manufactured in a variety of methods with a wide range of technologies, but the overall process can be broken down into two key steps: web formation and fiber bonding. Nonwovens produced from staple fibers are produced with dry-laid (carding or air-laid) or wet-laid methods, whereas nonwovens produced with polymers are formed through spun-laid (spunbond or meltblown) processes. Once formed, a fiber web is given integrity through a bonding process, either thermal bonding (calendaring, through-air, infrared, or ultrasonic), chemical bonding (saturating, spraying, printing, foaming, or powdering) and/or mechanical bonding (needling or hydroentangling).

Due to the variety of technologies used to produce nonwoven, a large range of products can be produced with varying properties that will affect their end performance. Each web formation and bonding process will have some effect on the structural elements (fiber orientation distribution, basis weight/density, fiber diameter and its distribution, pore size and

shape, bonding geometry, fiber to fiber crossover, and surface texture) of the nonwoven (Shim, 2012b). Even though the web formation process will have an effect on the fiber orientation of the nonwoven, it is more or less a random assemblage of fibers, allowing no two nonwoven fabrics, or even two samples from the same nonwoven fabric to ever be exactly the same.

2.2.2 Uses of Air Permeability in Nonwovens

Though air permeability in nonwovens is not restricted to particular products, there are some markets where air permeability is vital to the function of the product and other markets where the air permeability is insignificant to its application.

In the apparel and interlining markets it is important to make sure that the nonwoven fabrics have the right insulation so that it is not too permeable that too much heat can escape in cold weather apparel or it is permeable enough to allow cooling in warm weather apparel. In industrial garments, air permeability can be essential to the application in garments, like biohazard suits or medical gowns where permeability could lead to exposure to harmful substances.

Nonwovens used for sound dampening, like those used for linings in the automotive industry, also take air permeability into account since permeability is directly related to the sound absorption of the fabric. In fabrics, an increase in resistance to air flow will result in more sound absorption, so the best nonwovens for acoustic dampening will have a lower air permeability (Jayaraman, 2005).

By far the biggest application of air permeability in nonwoven is in the filtration market, where the air permeability or pressure drop is one of the three parameters used to evaluate a filter's performance (Lawrence & Liu, 2006). In filter medium, the air permeability or pressure drop is related to the energy required to operate the filter. Filters with a low air permeability or high pressure drop will require more energy and therefore more money to operate. Therefore in filter media, a high air permeability and high filtration efficiency are desired in the most effective and efficient filters.

Other applications for air permeability in nonwovens can also be found in the agriculture, geotextiles, and sporting/outdoors markets. In the agriculture market, the nonwoven covers used to protect plants from extreme temperatures must still allow air to pass through the fabric not to suffocate the plants they are guarding, and geotextiles may or may not need to allow gases to escape the surfaces they are covering. Air permeability is also essential in nonwovens used in the sporting and outdoors market in things like parachutes, sails, and mosquito netting.

2.3 Theoretical Models

During the review of previous works on air permeability, numerous models were found that claimed to be able to predict the air permeability of fabrics. While many of these models were based on traditional textiles, the more dominate and proclaimed models were researched to see if they could be extended to use in nonwovens.

These models were broken down into four categories for examination. The first category, the Early Works, contains three of the earliest and widely known methods used for

predicting the air permeability of fabrics. Since there were numerous analytical based models, they were broken down into two separate categories. Models based on the flow of air through two-dimensional arrays were put into one category, and the models based on drag-theory, three-dimensional arrays, and various additional analytical theories were put in the other. The final category contains models that were created using empirical based calculations. Within each category, the models are summarized in chronological order.

2.3.1 The Early Works

Surprisingly, some of the first theories and models on the flow of air through porous media are still some of the mostly widely known and commonly used models today. Whether they are based on the flow through channels or empirical relations, they created the foundation for this area of research and still stand as he key pillars for the prediction of air permeability.

2.3.1.1 Kozeny-Carman

One of the earliest theories on permeability, the Kozeny-Carman equation is based on capillary theory, which "relates the specific permeability to the specific surface area of a unit volume of the medium, and the geometry of the flow channels by including a shape factor and a tortuosity factor (Lawrence & Liu, 2006, pg. 963)." It is based on Kozeny's work in 1927, which was later modified by Carman in 1937 and 1956. Though the Kozeny-Carman equation is one of the most commonly used and widely known models, it relies on the use of Kozeny-Carman constant, k_c, which must be determined experimentally.

$$K = \frac{d^2(1-a)^3}{16k_c a^2}$$

is the more generally used equation, Tomadakis & Robertson (2005) report that for randomly overlapping structures

$$K = \frac{d^2\,(1-a)}{16k_c \ln^2(1-a)}$$

should be used. The Kozeny-Carman model has been reported accurate by various people in almost all porosities but with varying values for the Kozeny-Carman constant.

2.3.1.2 Brinkman

In an attempt to understand the flow of air through porous material at more turbulent conditions, H.C. Brinkman worked to modify Darcy's law to be applicable outside of laminar flow (Chapman, 2010)." Brinkman created a modified Darcy's law that estimated "how the frictional drag given by Stokes Law is modified by the inference of neighboring particles (Carman, 1956, pg. 25)." According to Carman (1956), the Brinkman's equation,

$$K = \frac{d^2}{18}\left[\frac{1}{a} + \frac{3}{4}\left(1 - \sqrt{\frac{8}{a} - 3}\right)\right]$$

works for solid volume fractions below 0.5 and actually agrees with the Kozeny-Carman equation in the 0.2-0.5 solid volume fraction range.

2.3.1.3 Davies

One of the most well-known models for air permeability is the empirical model created by Davies in 1952. Created based on a vast horde of experimental data on a wide

range of fabrics and fiber deniers (0.8 μm to 40 μm) (Jackson & James, 1986), Davies model is "proven to be accurate for a solid volume fraction range of 0.6% to 30% at low Reynolds and Knudsen numbers (Maze, Vahedia Tafreshi, Wang, & Pourdeyhimi, 2007, pg. 555)." Davies model "is widely used to predict the permeability of textile structures due to its simplicity and reasonably good accuracy in prediction (Pradham, 2013, pg. 19)."

$$K = \frac{d^2}{64\alpha^{3/2}(1 + 56\alpha^3)}$$

2.3.2 Cell Based Analytical Models

A vast amount of research on the behavior of air flow through fabrics has been focused on "the flow interference effect of neighboring fibers (Rao & Faghri, 1988)." Due to the fact that a vast majority of textiles produced in the past century have a defined geometrical pattern, there has been an abundant amount of research on the effect the geometry of the structure or ordered matrices have on flow of air. "Based on the assumption that all fibers in the filter experience the same flow field (Wang, Maze, Vahedi Tafreshi, & Pourdeyhimi, 2007a, pg. 4872)," broad range of research has focused on defining the ordered matrices of fabrics into 'cells' and solving the flow field through those cells. Unfortunately, these models tend to struggle to accurately predict air permeability for nonwoven fabrics, since they are based on the flow of air through two-dimensional arrays (Wang, Maze, Vahedi Tafreshi, & Pourdeyhimi, 2007a).

2.3.2.1 Langmuir

Langmuir's paper, published in 1942, was one of the earliest works on cell theory. Langmuir used a circle as his unit cell and considered zero shear stress at the boundary condition (Jackson & James). Langmuir's model,

$$K = \frac{d^2}{16a}\left(-\ln a - \frac{3}{2} + 2a - \frac{a^2}{2}\right)$$

is based on flow parallel to an array of rods.

2.3.2.2 Happel

Similar to Langmuir's model, Happel's models also used a circle as a unit cell and specified zero shear stress at the boundary condition. Though Happel's paper was not published until 1959, it is more well-known than Langmuir model, since it was published in a government document and Happel provided a model for transverse flow as well as parallel flow (Jackson & James, 1986). Happel's models are

$$K = \frac{d^2}{16a}\left(-\ln a - \frac{3}{2} + 2a - \frac{a^2}{2}\right)$$

for parallel flow, and

$$K = \frac{d^2}{16a}\left(-0.5\ln a - 0.5\frac{1-a^2}{1+a^2}\right)$$

for perpendicular/transverse flow. Pradham (2013) found Happel's transverse flow model valid for lower fiber volume structures, but most research shows reports that two-dimensional models under predict air permeability for nonwovens (Lawrence & Liu, 2006; Wang, Maze, Vahedi Tafreshi, & Pourdeyhimi, 2007a).

2.3.2.3 Kuwabara

Also in 1959, Kuwabara produced his "famous cell model (Wang, Maze, Vahedi Tafreshi, & Pourdeyhimi, 2007b, pg. 866" which predicts the transverse air flow around a circular unit cell, but Kuwabara's model unlike Happel's "specified zero vorticity at the boundary instead of zero shear (Jackson & James, 1986, pg. 370)." In earlier works, Kuwabara model was reported as:

$$K = \frac{d^2}{32a}\left(-\ln a + \frac{3}{2} + 2a\right)$$

but more recent works have reported Kuwabara model as:

$$K = \frac{d^2}{16a}\left(-\ln\frac{a}{2} - \frac{3}{4} + a - \frac{a^2}{4}\right)$$

Though Kuwabara's model, is still one of the "the most relevant theoretical models to determine the air permeability of fibrous porous media, (Pradham, 2013, pg.21)," it tends to understate the permeability of nonwoven fabrics (Lawrence & Liu, 2006; Henry & Ariman, 1983; Wang, Maze, Vahedi Tafreshi, & Pourdeyhimi, 2007a).

2.3.2.4 Hasimato

While Happel and Kuwabara were producing their model, Hasimato was also formulating his own models for transverse permeability in 1959. Instead of a circular cell or array, Hasimato's model is based on a square array. Like Kuwabara, Hasimato solved the drag coefficient of the rod using two different methods. Using "a Fourier series method to solve Stokes equation (Jackson & James, 1986, pg. 370-371)," he found:

$$K = \frac{d^2}{32a}(-\ln a - 1.476)$$

Using an elliptical function to solve the drag coefficient of the rod, he found:

$$K = \frac{d^2}{32a}(-\ln a - 1.476 + 2a + Oa^2)$$

Like Happel's and Kuwabara's models, Pradham (2013) reported that Hasimato's was also one of "most relevant theoretical models (pg. 21)" for air permeability.

2.3.2.5 Sangani & Acrivos

Sangani & Acrivos furthered the research into cell theory with their work in 1982. Sangani and Acrivos focused on the transverse flow through square and hexagonal arrays. Using a least-squares technique, "they presented numerical results for the drag co-efficient and checked the accuracy by showing that hey results agreed with values form asymptotic solutions (Jackson & James, 1986, pg. 371)." Their equation for square arrays is:

$$K = \frac{d^2}{32a}(-\ln a - 1.476 + 2a - 1.774a^2 + 4.076a^3 + Oa^4)$$

, and for hexagonal arrays it is:

$$K = \frac{d^2}{32a}(-\ln a - 1.49 + 2a - 0.5a^2 + 4.076a^3 + Oa^4)$$

. Clauge and Phillips (1996) reported that the Sangani & Acrivos asymptotic results for the square arrays were "expected to be valid up to fiber volume fractions of 0.3 (pg. 1568)" and that it agreed with Clague and Phillips own results "up to a volume fraction of 0.3, and is 14% low at a = 0.4 (pg. 1568)."

2.3.2.6 Drummond & Tahir

In 1984, Drummond and Tahir published their extensive research in cell theory in both parallel and transverse flow using a method of distributed singularities (Jackson & James, 1986). For transverse flow, Drummond and Tahir used a square array, but for parallel flow, they derived equations for square, triangular, hexagonal and rectangular arrays. For a square array in transverse flow, their equation is:

$$K = \frac{d^2}{32a}(-\ln a - 1.476 + 2a - 1.774a^2 + Oa^3)$$

For flow parallel to the arrays, their solutions "are:

$$K = \frac{d^2}{16a}(-\ln a - 1.476 + 2a - 0.5a^2 + Oa^4)$$

for a square array,

$$K = \frac{d^2}{16a}(-\ln a - 1.498 + 2a - 0.5a^2 + Oa^6)$$

for an equilateral triangular array,

$$K = \frac{d^2}{16a}(-\ln a - 1.354 + 2a - 0.5a^2 + Oa^3)$$

for a hexagonal array, and

$$K = \frac{d^2}{16a}(-\ln a - 1.130 + 2a - 1.197a^2 + Oa^3)$$

for a two-by-one rectangular array (Jackson & James, 1986, pg. 370)." According to Jackson and James (1986), Drummond and Tahir's equation for transverse permeability closely agrees with the work of Kuwabara, Hasimato, and Sangani and Acrivos below solid volume fractions of 50%.

2.3.2.7 Tamayol & Bahrami

Tamayol and Bahrami (2010) proposed four analytical models for predicting the transverse air permeability "related to the porosity, fiber diameter, and tortuosity of the medium (Tamayol & Baharami, 2010, pg. 1)." Tamayol and Baharami's models are for the creeping flow regime and "assumed a parabolic velocity profile of fluid through the fibers (Pradhan, 2013, pg. 21)." Tamayol and Baharami's first three models, which assumed zero-velocity at the boundary condition, are:

$$K = \frac{0.16d^2\left(\frac{\pi}{4a} - 3\sqrt{\frac{\pi}{4a}} + 3 - \sqrt{\frac{4a}{\pi}}\right)}{\sqrt{1-a}}$$

for a square array,

$$K = \frac{0.16d^2\left(\frac{\pi}{2\sqrt{3a}} - 3\sqrt{\frac{\pi}{2\sqrt{3a}}} + 3 - \sqrt{\frac{2\sqrt{3a}}{\pi}}\right)}{\sqrt{1-a}}$$

for a staggered (triangular) array, and

$$K = \frac{0.16d^2\left(\frac{\pi}{3\sqrt{3a}} - 3\sqrt{\frac{\pi}{3\sqrt{3a}}} + 3 - \sqrt{\frac{3\sqrt{3a}}{\pi}}\right)}{\sqrt{1-a}}$$

for a hexagonal array. Tamayol and Baharami also proposed a model for a two-dimensional structure,

$$K = 0.008d^2\sqrt{(1-a)}\left[\left(\frac{\pi}{4a}\right)^2 - 2\frac{\pi}{4a} + 1\right]$$

The constant, 0.008, was "found through comparison with experimental data collected from different sources (Tamayol & Baharami, 2010, pg. 5).

2.3.2.8 Gebart

Gebart (1992) studied the permeability of fiber webs used for reinforcement in resin transfer molding. After studying quadratic and hexagonal packing matrices and the flow of air through the 'slots' between the matrices in creeping flow, Gebart proposed analytic solutions to predict transverse air permeability, somewhat similar to the Kozeny-Carman equation, except that it incorporated a shape factor instead of the Kozeny constant (Gebart, 1992). For quad racking packing matrices, Gebart proposed:

$$K = \frac{4d^2}{9\sqrt{2\pi}}\left(\sqrt{\frac{\pi}{4a}} - 1\right)^{\frac{5}{2}}$$

And for hexagonal packing matrices he proposed:

$$K = \frac{4d^2}{9\sqrt{6\pi}}\left(\sqrt{\frac{\pi}{2a\sqrt{3}}} - 1\right)^{\frac{5}{2}}$$

Although Gebart (1992) reported that his analytical solutions worked best in the 35% to 65% range, after using numerical calculations and experimental testing to verify his theories, he reported that the effective fiber radius needed to be adjusted "to a value about four times larger than the real fiber radius" in order for his permeability equations to be agreeable with his experimental findings.

2.3.3 Non-Cell Based Analytical Models

This section contains models based on non-cell based analytical means. Similar to Kozeny-Carman, Lawrence and Liu used capillary theory in their model for air permeability, and like Brinkman, Spielman and Goren and Pich studied drag theory as a basis for their

work. Somewhat comparable to the cell-based models, Jackson and James and Higdon and Ford studied the flow of air through three-dimensional lattices before coming up with their theories. While some of these works used similar methods to previous mentioned works, two models used more unique approaches in creating their analytical models. The Conduction model was based on the electrical conduction principal and Das, Ishtiaque, Rao, and Pourdeyhimi studied the structure of nonwovens before basing their model on nonwoven structure parameters. Other than Jackson and James' and Higdon and Ford's theoretical, these models should ideally be more appropriate to use with nonwoven fabrics since they are based outside of clearly defined structures.

2.3.3.1 Spielman & Goren

Spielman and Goren utilized another analytical method, now known as 'swarm theory', to predict air permeability in their research in 1968. "Their idea was that flow through a fibrous porous medium can be modelled by the flow around a single circular cylinder surrounded by an infinite homogenous porous medium (Jackson & James, 1986, pg.371)." Their theory, which utilized the Brinkman-Debye- Bueche equation, allowed them to avoid the Stokes' paradox and produce models using a modified Bessel function (Jackson & James, 1986). Their first model,

$$\frac{1}{2}+\frac{2\sqrt{K}}{d}\frac{k_1\left(\frac{d}{2\sqrt{K}}\right)}{k_0\left(\frac{d}{2\sqrt{K}}\right)}=\frac{1}{4\alpha}$$

(where k_1 and k_0 are modified Bessel functions of the second kind), based on a two dimensional fabric and valid for solid volume fractions below 50%, is a "very successful

analytical model capable of predicting the permeability of fibrous materials with different spatial fiber orientations (Wang, Maze, Vahedi Tafreshi, & Pourdeyhimi, 2007b, pg. 865; Jackson & James, 1986).” Spielman and Goren also solved for a three dimensional medium by solving “the problem of a rod oblique to the superficial velocity by allowing the permeability to have different values in the directions parallel and perpendicular to the flow,” and “then, by averaging over all rod directions (Jackson & James, 1986, pg. 372). Their three-dimensional model,

$$\frac{1}{3}+\frac{5}{3}\frac{\sqrt{K}}{d}\frac{k_1\left(\frac{d}{2\sqrt{K}}\right)}{k_0\left(\frac{d}{2\sqrt{K}}\right)}=\frac{1}{4\alpha}$$

(where k_1 and k_0 are modified Bessel functions of the second kind), is valid for solid volume fractions below 75%.

2.3.3.2 Pich

Similar to Spielman and Goren’s research, Pich’s (1966, 1971) research focused on the behavior of air flow around a single fiber within a media with high porosity. Pich employed the use of drag theory to analyze the drag force and slip on the surface of a fiber (Pich, 1966). “By considering the slippage at the surface of (Pradhan, 2013, pg. 21)” a fiber and the total drag force on fibers in a media, Pich was able to develop a model that predicted the pressure drop of said media. Pradhan (2013) reported Pich’s model as being

$$K=\frac{8d^2a\left(1+1.966\frac{2a}{d}\right)}{-\ln a+2a-\frac{a^2}{2}-\frac{3}{2}+1.966\frac{2a}{d}\left(\ln a+\frac{a^2}{2}-\frac{1}{2}\right)}$$

, but there are some discrepancies between this model and the one Pich gave in his paper in 1966. Pradhan made numerous mistakes in his conversation of the Pich model and incorrectly calculated Knudsen's number as the solid volume fraction divided by the radius of the fiber. The correctly converted relation for predicting the pressure drop, combined with Darcy's Law, can be used to obtain the Pich based air permeability model:

$$K = \frac{d^2\left(-\ln a + 2a - \frac{a^2}{2} - \frac{3}{2} + 1.966Kn(-\ln a + \frac{1}{2}a^2 - \frac{1}{2}\right)}{8(1 + 1.966Kn)}$$

2.3.3.3 Jackson & James

Jackson and James published their cubical lattice model in 1982, based on their belief "that the permeability of a random medium…is equivalent to the permeability of a cubical lattice formed of the same material (Jackson & James, 1986, pg. 372)." By utilizing Happel's and Drummond and Tahir's relations and equations for square arrays, Jackson and James combined the transverse and parallel flow to create their prediction for a three-dimensional medium,

$$K = \frac{3d^2(-\ln a - 0.931 + O(\ln a)^{-1})}{80a}$$

, which agrees well with Spielman and Goren's model for a three dimensional medium (Jackson & James, 1986). Gervais, Bardin-Monnier, and Thomas (2012) reported that Jackson & James model was in agreement with their experimental findings below a solid volume fraction of 25%, and Tomadakis and Robertson (2005) reported that it was in good agreement with their experimental data in the 5% to 30% solid volume fraction range.

2.3.3.4 Conduction

The conduction model for predicting air permeability is based on electrical conduction principals. The original proposed equation,

$$K = \frac{\Lambda^2}{8F}$$

, was proposed by Johnson, Koplik, and Swartz in 1986 and utilized the formation factor, *F*, "a measure of the relative resistance to transport through the fluid and the fluid-saturated porous medium," and *Λ*, "a weighted pore volume-to-surface ratio, a characteristic length directly related to transport (Tomadkis & Robertson, 2005, pg. 167)". Later, Tomadkis and Robertson (2005) used Archie's law to modify the original equation to predict the air permeability of randomly overlapping fiber structures in parallel and transverse air flow. Using Archie's law parameters, they proposed

$$K = \frac{d^2(1-a)}{32\ln^2(1-a)} \times \frac{((1-a)-0.11)^{2.521}}{(0.89)^{0.521}[(1.521)(1-a)-0.11]^2}$$

for two-dimensional structures in parallel flow,

$$K = \frac{d^2(1-a)}{32\ln^2(1-a)} \times \frac{((1-a)-0.11)^{2.785}}{(0.89)^{0.785}[(1.785)(1-a)-0.11]^2}$$

for two-dimensional structures in transverse flow, and

$$K = \frac{d^2(1-a)}{32\ln^2(1-a)} \times \frac{((1-a)-0.037)^{2.661}}{(0.963)^{0.661}[(1.661)(1-a)-0.037]^2}$$

for three-dimensional structures. Tomadkis and Robertson (2005) reported that of the conduction based models, the three-dimensional model tends to work best, but that all the conduction based models tended to over predict the air permeability, especially at lower solid volume fractions.

2.3.3.5 Higdon & Ford

Higdon and Ford's research, published in 1996, focused on the flow of air through three-dimensional ordered networks of three different cubic lattices: simple cubic (SC), body-centered cubic (BCC), and face-centered cubic (FCC). Higdon and Ford "used a boundary element method to estimate the viscous permeability of 3-d networks of cylindrical fibers ordered in regular SC, BCC, and FCC cubic lattices (Tomadakis & Robertson, 2005, 1972). By using "slender-body theory and lubrication approximations (Higdon & Ford, 1996, pg.341)," they arrived at this analytical, asymptotic solution:

$$K = \frac{d^2}{4\left[a \ln a^{-1/2} + O\left(\frac{a}{\ln a^{-1/2}}\right)^2\right]}$$

for their prediction of air permeability. Tomadakis & Robertson (2005) reported that Higdon and Ford's SC model agreed well with their experimental data for media that had a solid volume fraction above 10%.

2.3.3.6 Lawrence & Liu

Lawrence & Liu (2006) studied "the relation between the structure, permeability and filtration performance of needled nonwoven filter media (pg. 957)." They studied a range of nonwoven fabrics with varying solid volume fractions (5% to 24%) and fiber diameters (13.1 μm to 23.5μm), as well as surface treated and untreated fabrics. Based on their experimental work, Lawrence & Liu proposed a new model for predicting the air permeability based upon capillary theory, similar to that of Kozeny-Carman. "By using the effective pore diameter for

deriving the hydraulic radius as a substitute for the flow-average pore diameter in the Hagen-Poiseulle equation, (Lawrence & Liu, 2006, pg.966)," they arrived at the following equation:

$$K = \frac{(1-a)^2 d^2}{128a^2}$$

, which fit well with their experimental work.

2.3.3.7 Das, Ishtiaque, Rao & Pourdeyhimi

In 2013, Das, Ishtiaque, Rao & Pourdeyhimi published their analytical model on predicting air permeability specifically for nonwoven fabrics. Their research focused on non-uniform nature of nonwoven fabrics and its effect on air permeability. Their model,

$$K = \frac{g\pi^2 d^4}{16p^2} \frac{(1-a)^{2h+1}}{a^{2h}}$$

(where g & h are constants and p is the fiber perimeter), incorporates the use of the fiber perimeters and "two parameters that characterize the structure of the fibrous porous media (Das, Ishtiaque, Rao, & Pourdeyhimi, 2013, pg. 495)." Unfortunately, the two parameters, k and a, "must be determined empirically from experimental data (Neckar & Ibrahim, 2003, pg. 617)." Das, Ishtiaque, Rao, & Pourdeyhimi reported that their model was valid within the solid volume ranges they tested (between 25% to 40%) (Das, Ishtique, Rao, & Pourdeyhimi, 2013).

2.3.4 Empirical Based Models

While all of these models studied the flow of air through fabrics, using various methods to predict its behavior, and some analyzed previously postulated methods for

predicting air permeability, all of these models, ended up using an empirical-based solution to predict the air permeability of the fabrics. Since they were empirical based, these models were found to be accurate to a certain degree within their range of fabrics or comparable with the models they were based upon.

2.3.4.1 Henry & Ariman

In their "An Evaluation of the Kuwabara Model," Henry and Ariman (1983) compared "the Kuwabara flow field to the that obtained by a numerical solution of Stokes' flow over an array of cylinders (Henry & Ariman, 1983, pg. 1)." By considering 30°, 45°, and 60°staggered arrays at 5% and 10%, Henry and Ariman were able to make "numerical predictions of the variation of stream function and vorticity for the three array configurations (Henry & Ariman, 1983, pg. 10)." From these numerical calculations, Henry and Ariman used a method of least squares to create a third order polynomial to predict the pressure drop within a staggered array of cylinders, which was used to derive this air permeability model:

$$K = \frac{d^2}{2.446\alpha + 38.16\alpha^2 + 138.9\alpha^3}$$

Henry & Ariman (1983) did warn that though their numerical model produced results similar to that of the Kuwabara model (for media with a solid volume fraction range between ~3% - ~15%), "that a staggered array of cylinders may not be an accurate approximation of fibrous (pg. 17)" media.

2.3.4.2 Rao & Faghri

Rao and Faghri (1988) worked to define the transverse flow through an inline array of parallel cylinders. By using the "finite volume differencing methods developed (Rao & Faghri, 1988, pg. 138)" by Patankar, Rao and Faghri were able to calculate the flow field through the array, assuming laminar flow and zero shear boundary conditions. Using their calculated flow field, Rao and Faghri used a method of least squares to create a third-order polynomial to define their prediction for pressure drop for fibrous media that have a solid volume fraction between 2.9% to 13.6% (Rao & Faghri, 1988). Based upon their predictions for the pressure drop, the following relation for air permeability can be calculated:

$$K = \frac{d^2}{2.653a + 39.34a^2 + 144.5a^3}$$

Rao & Faghri (1988) reported that "the results obtained from the inline array model agree well with those obtained from Kuwabara-Hashimoto model, and the staggered array model of Henry and Ariman (pg. 143)," but that the results were "considerably higher than the experimental measurements of Davies (pg. 144)." Rao & Faghri (1998) went on to postulate that the higher estimates of the theoretical models could be due to the fact that fibrous media does not have a regular geometry and the "non-uniformity decreases the flow resistance (pg. 144)."

2.3.4.3 Johnston

In Johnston's paper (1998), he focuses on the use of the gamma distribution to predict the pore-size distribution and permeability in laminar flow of random fiber beds and random particle beds. Based on "empirical data showing how random fibrous mats, containing fibers

of known diameter, decrease in permeability with increased packing density (Johnston, 1998, pg. 289)" from previous works, Johnston proposed the following empirical function to predict the air permeability of fibrous mats:

$$K = 0.00266d^2\left(\frac{(1-a)(2-a)}{a}\right)^2$$

According to Tomadakis & Robertson (2005), this model described the data collected for transverse flow of fiber mats above a solid volume fraction of 15%.

2.3.4.4 Kopenen et al

Kopenen et al. (1998) developed an empirical based model for predicting air permeability after studying lattice-Boltzmann "simulations of creeping flow through large three-dimensional random fiber webs that closely resemble fibrous sheets such as paper and nonwoven fabrics (pg. 716)." These simulations included webs with a wide range of solid volume fractions (from 5% to 60%), constructed by the random placement of fibers in the x and y directions without overlapping (Kopenen et al., 1998). Kopenen et al. "report that the permeability of such materials is exponentially dependent on the porosity and independent of whether the fibers were place randomly or not (Nabovati, Llewellin, & Sousa, 2009, pg.861)." Kopenen et al. (1998) reported that their air permeability simulated results were in excellent agreement with the experimental work of similar materials (paper and nonwoven fabrics), and though they had no theoretical arguments to support their claim, they found that the empirical relation,

$$K = \frac{5.5d^2}{4(e^{10.1(a)} - 1)}$$

fit well with their simulated results.

2.3.4.5 Navobati, Llewellin & Sousa

Similar to Kopenen et al., Nabovati, Llewellin, and Sousa (2009) studied the behavior of air flow in the creeping flow regime using a lattice-Boltzmann simulation and simulated three-dimensional fabrics. By allowing overlapping in their simulation, Nabocati, Llewellin, and Sousa were able to simulate a larger range a large range of solid volume fractions (from 1% to 92%) compared with that of Kopenen et al. Using the lattice-Boltzmann simulation and a computer statistical analysis pack for the best fit, Nabovati, Llewellin, and Sousa developed a semi-empirical equation, based on Gebart's (1992) equation for the permeability of a hexagonal array. Based on their simulations, Nabovati, Llewellin, and Sousa (2009) found that their equation,

$$K = \frac{0.491d^2}{4}\left(\sqrt{\frac{0.9257}{1-a}} - 1\right)^{2.31}$$

, "has a tendency to slightly under-predict permeability at low porosities and to over-predict at high porosity (pg. 865)." It was also reported that there was a small standard deviation (~10%) at very high solid volume fractions and large standard deviation (~50%) at low solid volume fractions.

2.3.4.6 Vallabh, Banks-Lee & Seyam

Vallabh, Banks-Lee, and Seyam (2010) research focused on the effect that tortuosity had on the transverse air permeability of highly fibrous porous media, like nonwovens. By

studying layered configurations of nonwoven fabrics, they were able to collect the air permeability of a wide variety of samples, with solid volume fractions that ranged from 10% to 35% and with fiber diameters that ranged from 7.7 μm to 25.3μm. Based on their data, they used statistical analysis software to produce an empirical relationship to predict the air permeability of a nonwoven that incorporated the thickness, as well as the solid volume fraction and the fiber diameter.

$$K = (6.82 * 10^{-6})\left(\frac{d}{a}\right) - (2.2 * 10^{-11})(\ln t) + (1.64 * 10^{-4})(da^2) - (1.71 * 10^{-9})a - 6.66 * 10^{-10}$$

Vallbh, Banks-Lee, and Seyam (2010) reported that though their equation had a similar trend as the conduction based, the Davies, and the Kopenen et al models, their equation produced slightly higher values when compared with those models, which could be due to the layered configuration of their samples.

3. PROBLEM STATEMENT & APPROACH

3.1 Problem Statement

There are numerous theories and model used to predict the air permeability of fabrics, but choosing the right one to use to predict or control the air permeability of a nonwoven fabric can be much more complicated than expected. Though most every model has been proven accurate by their author or authors, they have only been proven situationally accurate. As can be seen in the literature review, most models come with specific circumstances in which that theory should be correct, whether it be for a defined range of solid volume fractions, air flow from only one direction, certain fiber sizes, the rate of air flow or air pressure, or the patterns formed by the fibers. All of these parameters limit when and where the various models can be used accurately.

Choosing the correct model to use is even further complicated when used with nonwoven fabrics because of the very nature in which nonwovens are produced. Whereas woven or knitted fabrics which are produced with uniform yarns and fibers in designed patterns, this is not the case with nonwoven fabrics. Depending on the processes used to create them, samples taken from the same fabric can have inconsistences in fiber size, basis weight, solid volume fraction, and pore structure. Even the most uniform nonwoven fabrics will be found to have minor differences between samples. These inconsistencies in the nonwoven fabrics structure means the air flow through no two samples of nonwoven fabric will ever be exactly the same.

This lack of uniformity limits the ability to predict any of the exact properties of a nonwoven fabric, so no one model on air permeability is ever going to be able to accurately predict or calculate the exact air permeability of every nonwoven fabric. Between the parameters in which the models must be used and the non-uniformity of nonwoven fabrics, choosing which model to use is less about which one is correct, but more about which model is the most appropriate for the circumstance.

Furthermore, even proving the accuracy of these models with nonwoven fabrics is complicated due to differing methods established to calculate air permeability. As stated in the literature review, there are two established methods for measuring air pressure, either with a fixed pressure or a fixed flow. Both methods use Darcy's Law,

$$\frac{Q}{A} = \frac{K\Delta p}{\mu Z}$$

(Q = volumetric flow rate, K = permeability of the material, Δp = pressure difference, A = cross sectional area, μ = viscosity of air, Z = thickness)

nevertheless depending on the method used, the flow rate of the air and/or the pressure used will affect the behavior of air through the material. It's likely that measuring nonwoven fabrics at higher or lower flow rates or pressures can affect the flow of air through the nonwoven by opening or closing pore channels within the nonwoven, which could have some effect on the air permeability of the nonwoven fabric.

3.2 Approach

To get a better understanding of the limitations of the various air permeability models and their practicality with nonwoven fabrics, a dual approach was used to explore the two

main factors affecting air permeability in nonwovens, solid volume fraction and fiber diameter. Approach #1 focuses on the effect changing fiber diameter has on the air permeability of nonwovens, while Approach #2 focuses on the effect changing solid volume fraction has on the air permeability of the nonwovens. To this end, five different carded and needle punched PET nonwoven fabrics with varying deniers of fibers, but with approximately the same solid volume fraction (~4%) were chosen.

To focus on just the effect of fiber diameter on air permeability, the first approach keeps the solid volume fraction of the nonwoven samples relatively constant while concentrating on the changing fiber diameter controlled by the denier of the sample used in the experiment.

In the second approach, fiber diameter was kept constant, while controlling the thickness of the nonwoven samples was used to vary the solid volume fraction of the nonwoven samples, since solid volume fraction is a function of thickness and basis weight. By compressing the varying numbers of the samples to the thickness of one sample, it was possible to focus on the effect solid volume fraction at five different levels (~4%, ~8%, ~12%, ~16% & ~20%) while keeping the fiber diameter and overall structure of the nonwovens constant. A breakdown of these approaches can be found in Figure 3.1.

To further establish the accuracy of these models, the air permeability of the nonwoven samples was measured with both air permeability testing methods, using fixed flow and a fixed pressure. The KES-F8 Air Permeability tester was used to measure the air permeability of the samples at a fixed flow and at varying lower air pressures (0.8 – 77 Pa). The FX 3300 Air Permeability tester was used to measure the air permeability of the samples

in accordance with the standard testing method of air permeability (ASTM D737-04) at a fixed air pressure (125 Pa) and varying flow rates. Using both methods of air permeability should help establish the accuracy of the models somewhat independent of the rate of flow or air pressure used in the measuring of the experimentation.

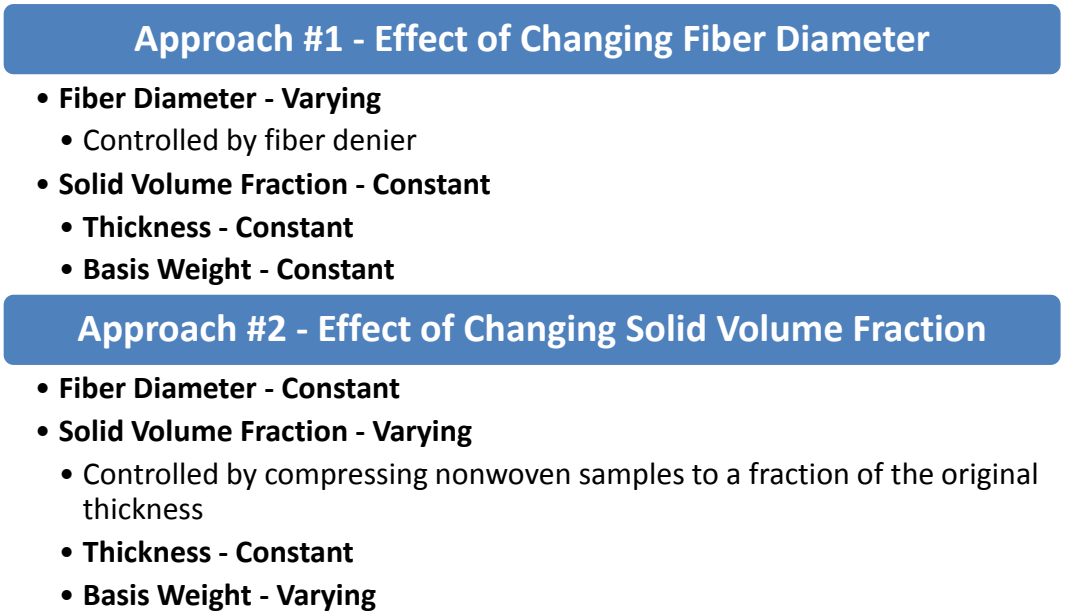

Figure 3.1: Experimental Approaches

4. EXPERIMENTAL WORK

This chapter presents the experimental work and results done during this study, including the equipment and samples used to facilitate the dual approach of this research. After establishing a means for controlling the fiber diameter and solid volume fraction on both a fixed pressure and a fixed flow air permeability testers and a means of comparison between the different testing methods, back calculations were used to assess the results.

4.1 Equipment

To achieve the dual approach of this study using both methods for testing air permeability two different air permeability machines were used. The FX-3300 was used to test the air permeability using a fixed pressure and the KES-F8 was used to test the air permeability using a fixed flow. Along with the two machines, a compression tube and spacer rings were used as a means to control the thickness and therefore the solid volume fraction of the samples.

4.1.1 FX-3300 Tester

The FX-3300 LabAir, pictured in Figure 4.1, is an air permeability tester produced by TexTest Instruments, a German based company, specializing in "Testing Instruments for Quality Control (TexTest, n.d.)." The FX-3300 LabAir "measures the air permeability of all kinds of flat materials as well as foam cubes (TexTest, n.d.)," by means of a fixed pressure differential, which can be fixed between 20 to 2,500 Pa. In typical use, a flat material or fabric is placed underneath the test head and clamping arm and the air flow through the

material is determined at the specified pressure differential. For this research, the 38 cm^2 testing apparatus and head is used. If need be, the test head can be removed from the clamping arm in order to allow the FX-3300 tester to measure the air permeability of fabrics that would be affected by the testing head or to measure materials that cannot fit under the clamping arm. Unfortunately, the removal of the testing head has the potential to allow for the movement of fabric samples and to allow edge leakage to be introduced into the system.

Figure 4.1: FX-3300 LabAir Permeability Tester

4.1.2 KES-F8 Tester

The KES-F8, pictured in Figure 4.2, is a permeability tester designed in 1987 by the Chinese Company, Kato tech Co., Ltd. The KES-F8 utilizes the fixed flow method for measuring air permeability. In the KES-F8 tester, a fabric is placed under the 2π cm^2 vent

pressing plate, clamped down, and "the pressure loss due to the sample (at a constant flow rate of 4 cc/cm^2/sec. for standard measurements) is measured using a semiconductor type differential gauge (Kato Tech Co., Ltd., 2007)." After testing and measuring the resistance twice, the KES-F8 averages the results and displays the measured resistance as "R," which can be converted to the pressure differential with the following equation.

$$R = \frac{P}{V}$$

R = air resistance (K Pa s/m), P = pressure difference (pa),
V = 0.04 m^3/m^2/s = Rate of the air flow per unit area (m^3/m^2/s)

Figure 4.2: KES-F8 Air Permeability Tester

The KES-F8 tester also comes with an optional compression tube attachment which can be screw clamped on top of the vent pressing plate and is discussed in more detail in the next section.

4.1.3 Compression Tube

The KES-F8 air permeability tester comes with an optional compression tube attachment which will be utilized throughout these experiments. The compression tube, pictured below in Figure 4.3, consists of two cylinders, a larger, outer cylinder and a smaller, inner cylinder. The smaller cylinder, with an inner diameter of ~81.1 mm, fits perfectly inside the larger cylinder, with an inner diameter of ~89.1 mm, and each cylinder has a square screen on their bottom faces made of perforated metal. The cylinders were designed so that a lofty or bulky fabric could be placed in between the two cylinders and compressed to a desired thickness. To help with the control of the thickness, a ruler is attached to the outer cylinder and each cylinder has two small holes so that nuts and bolts can be used to lock the cylinders at the desired thickness.

Figure 4.3: Compression Tube

Once the desired thickness has been set with the nuts and bolts, the compression tube can be tightened on top of the KES-F8 tester and be used to measure the air permeability of the fabric. Figure 4.4 shows the compression tube being used with the KES-F8 tester. Since the compression tube (20π cm^2) has a larger area than the vent plate (2π cm^2), the KES-F8 instructions specify that the results will read one tenth of the actual resistance.

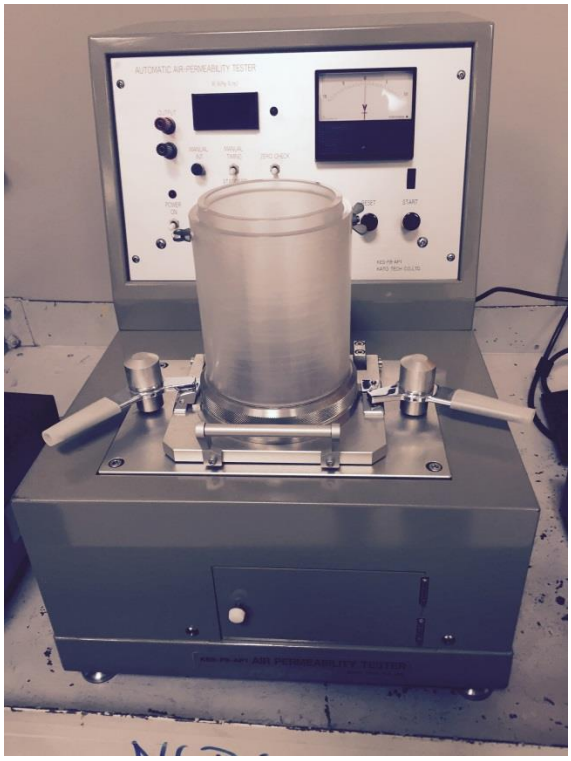

Figure 4.4: The Compression Tube Being Used with the KES-F8 Tester

In an attempt to understand the air permeability of the samples at higher pressure differentials and used the fixed pressure method of testing air permeability, the compression tube was also used FX-3300. So that the compression tube could fit on top of the testing orifice, the FX-3300 test head was removed when the compression tube was used with that

system. There was some concern that leakage could occur between the compression tube and the FX-3300 testing orifice, so a thin layer of rubber sheeting was placed between the compression tube and the testing orifice to prevent leakage from occurring. To accommodate the difference in area between the FX-3300 orifice (38 cm^2) and the inner cylinder of the compression tube (16.443025π cm^2), the results displayed on the FX-3300 for flow will need to be multiplied by $\frac{38}{16.443025\pi}$. The compression tube being used with the FX-3300 and the rubber sheeting can be seen in Figure 4.4.

Figure 4.5: The Compression Tube Being Used with the FX-3300 Tester & Rubber Sheeting

4.1.4 Spacer Rings

Unfortunately, the ruler on the side of the compression tube is not accurate enough for this research, as a result another measure was needed to control the thickness of the samples at much smaller and more finite levels. To this end, the spacer rings, pictured below in Figure 4.6, were designed and manufactured using a digital 3-D printer. The spacer rings were designed to the specifications of the inner and outer cylinders of the compression tube. The spacer rings were designed to have the same outer diameter of the inner cylinder so that it could fit perfectly inside the outer cylinder. The inner diameter of spacer rings (85.1 mm) were designed to be larger than the inner diameter of the smaller, inner cylinder so that they could still allow samples to be larger than the inner cylinder of the compression tube, therefore still allowing the inner cylinder to compress the sample and prevent leakage on the outside of the samples. Figure 4.7 is a bottom view of the compression tube with a spacer ring in between the inner and outer cylinders. A preliminary ring was manufactured to be used as a stencil for the fabrics samples, but the thickness of the spacer rings used in testing were determined based on the average thickness of the samples of each of the five fabrics used in these experiments with the spacer rings.

4.2 Fabrics

Five fabrics from a series of pre-made fabrics were used for this experiment. Each of the five carded and needle-punched fabrics, composed of 90% PET and 10% FT201, were manufactured to be roughly 200 grams per square meter and have solid volume fraction of

Figure 4.6: Spacer Rings

Figure 4.7: Bottom View of a Ring inside the Compression Tube

about 4%, but each fabric was produced with varying deniers of fibers (1.5 denier, 3 denier, 6 denier, 9 denier, and 15 denier). This series of fabrics were chosen for this experiment for three reasons. First, their consistencies in structure but varying fiber denier provide the appropriate variables for the first approach, the effect of changing fiber diameter. Secondly,

polyester is known for is resilience which will help the fabric samples keep and return to their shape throughout the manipulation of the samples in this research. Finally being produced by means of mechanical bonding allows the fabric to be compressed to varying thickness and therefore allows for change in the structure and solid volume fraction of the fabrics, where as if the fabrics had been produced with thermal or chemical bonding, the fibers would be bonded together and therefore the structure of the fabric would be somewhat fixed. Since the fibers and structure in mechanically bonded fabrics is not fixed, it makes the use of needle-punched fabrics widely appropriate for the second approach, the effect of changing solid volume fraction.

4.2.1 100 cm^2 Samples

In order to determine the approximate solid volume fraction of the five fabrics, five samples from each of the five fabrics, for a total of twenty-five samples, were cut using the 100 cm^2 die cutter. The mass and thickness of each sample was measured, and the solid volume fraction of each sample was determined using the following formula:

$$SVF = \frac{w/xyz}{\rho}$$

(w = fabric mass, $p = 1.38\,{}^{\mathrm{g}}/_{\mathrm{cm}^3}$ = fiber mass density, x = fabric length, y = fabric width, z = fabric thickness)

This data, along with the average solid volume fraction for each fabric, can be found in Table 1.

Table 1: Fabric Solid Volume Fractions

Sample #	Denier	Mass (g)	Thickness (mm)	SVF	SVF $_{average}$
1	1.5	2.49	4.65	3.88%	3.80%
2		2.31	4.21	3.98%	
3		2.4	4.69	3.71%	
4		2.28	4.36	3.79%	
5		2.37	4.70	3.65%	
6	3	2.24	4.03	4.02%	4.02%
7		2.29	3.92	4.23%	
8		2.2	4.11	3.88%	
9		2.15	3.89	4.00%	
10		2.18	3.98	3.97%	
11	6	2.14	4.09	3.79%	3.82%
12		2.1	4.10	3.71%	
13		2.17	4.12	3.82%	
14		2.12	3.85	3.99%	
15		2.14	4.09	3.79%	
16	9	2.2	4.12	3.87%	3.88%
17		2.24	4.17	3.90%	
18		2.35	4.29	3.97%	
19		2.3	4.30	3.88%	
20		2.12	4.04	3.80%	
21	15	2.21	4.69	3.41%	3.42%
22		2.13	4.45	3.47%	
23		2.07	4.34	3.46%	
24		2.08	4.43	3.40%	
25		2.11	4.51	3.39%	

4.2.2 56.9 cm^2 Samples

To create samples that could be used in both the air permeability machines (FX 3300 and KES-F8) and that would fit inside the compression tube and spacers rings, five samples from each of the five fabrics (totaling twenty-five samples) were cut using a spacer rings as a stencil. These samples had an approximate diameter of 85.1 mm, giving them an

approximate area of 56.9 cm^2. Since these samples were stenciled and cut by hand and the area of the stenciled samples could not be accurately estimated or measured, the average solid volume fractions calculated from the 100 cm^2 samples was assumed accurate for their corresponding fabrics. Table 2 contains the thickness of the 56.9 cm^2 samples and the corresponding average of each sample fabric.

Table 2: Thickness of the 56.9 cm^2 Samples and Fabric Thickness Averages

Sample #	**Denier**	**Thickness** (mm)	**Thickness** $_{avg.}$ (mm)
1	1.5	4.55	4.567
2		4.43	
3		4.77	
4		4.53	
5		4.55	
6	3	4.14	3.993
7		4.08	
8		4.01	
9		3.79	
10		3.94	
11	6	3.71	3.807
12		3.70	
13		3.80	
14		3.85	
15		3.97	
16	9	3.93	4.333
17		4.51	
18		4.31	
19		4.39	
20		4.52	
21	15	4.68	4.501
22		4.41	
23		4.34	
24		4.53	
25		4.54	

4.2.2 Woven Sample

To help get a better understanding between the different machines and configurations used throughout this research, a very tightly woven fabric was used to compare the different testing methods. Since the woven fabric would have consistent air permeability, due to its defined geometrical structure, it was used as a way to gauge and compare the different readings of air permeability between the FX-3300 tester and KES-F8 tester and with and without the use of the compression tube. The woven fabric had a thickness of 0.16 mm.

4.1 Experimental Trials

In order to establish the accuracy of the effect of changing fiber diameter and changing solid volume fraction independent of the testing method and testing devices, three different trials were tested using both the fixed pressure differential method (FX-3300) and the fixed flow method (KES-F8).

4.1.1 First Preliminary Trials

The first set of preliminary trials were conducted to determine the air permeability of the five fabrics and the woven sample using both air permeability testers (FX-3300 and KES-F8) in typical operating conditions, without the compression tube or the spacer rings. These first trials were conducted for multiple purposes. First, these trials were conducted to determine the air permeability of the all samples using the ASTM D737 Standard Test Method for Air Permeability of Textile Fabrics. Secondly, these trials were used to determine the difference between the different test methods and machines and to determine if

there was any correlation between the FX-3300 tester and KES-F8 tester in typical operating conditions. Finally, these trials were in alignment with our first approach of determining the effect changing fiber diameter had on the air permeability of nonwoven fabrics, since all the fabrics except the woven sample had varying fiber diameters and a constant solid volume fraction, around 4%.

For the first preliminary trials, each of the five 56.9 cm^2 samples, from each of the five fabrics and the woven sample, were tested individually to determine their air permeability. On the FX-3300 tester, testing procedures followed ASTM D737 Standard Test Method for Air Permeability of Textile Fabrics, and samples were placed underneath the test head and clamping arm and the results were recorded once the air flow had been stabilized at a pressure differential of 125 pa. On the KES-F8 tester, samples were placed underneath the vent pressing plate, subjected to the discharge process and the resistance to air flow was recorded at the end of the cycle. Due to variance between testing cycles of the same sample on the KES-F8 tester, each sample was subject to five cycle measurements, and the mean of these results was used to determine the resistance and pressure differential of each sample. It should be noted that the original test done on the KES-F8 conflicted with the results obtained by the FX-3300. After further investigation, it became apparent that the KES-F8 machine needed to be calibrated. Once the KES-F8 tester had been re-calibrated, the tests in the preliminary trial were re-done, and those results are the ones reported in this research. The measurements on air flow from the FX-3300, the mean resistance and pressure differential, and their corresponding air permeability calculated using Darcy's Law can be

found below in Table 3. Figure 4.8 compares the air permeability calculated using the FX-3300 tester versus the KES-F8.

Table 3: Air Permeability Measurements of Single Fabric Samples FX-3300 and KES-F8
(w/o the Compression Tube or Spacer Rings)

Sample #	**Denier**	Q/A^2* (m^3/m^2 s)	K* (m^2)	R_{mean}** (K pa s/m)	Δp** (pa)	K** (m^2)
1	1.5	129	8.493E-10	0.1834	7.3344	4.488E-10
2		133	8.538E-10	0.1837	7.3480	4.368E-10
3		136	9.400E-10	0.1896	7.5856	4.556E-10
4		137	8.993E-10	0.1777	7.1096	4.616E-10
5		136	8.954E-10	0.1742	6.9696	4.723E-10
6	3	251	1.505E-09	0.0845	3.3808	8.866E-10
7		258	1.524E-09	0.0784	3.1344	9.424E-10
8		250	1.453E-09	0.0855	3.4208	8.494E-10
9		263	1.445E-09	0.0752	3.0096	9.125E-10
10		250	1.426E-09	0.0832	3.3288	8.569E-10
11	6	386	2.075E-09	0.0440	1.7600	1.528E-09
12		380	2.036E-09	0.0446	1.7832	1.502E-09
13		373	2.052E-09	0.0477	1.9080	1.442E-09
14		373	2.081E-09	0.0502	2.0064	1.390E-09
15		367	2.108E-09	0.0454	1.8168	1.581E-09
16	9	477	2.717E-09	0.0318	1.2712	2.240E-09
17		448	2.923E-09	0.0371	1.4848	2.197E-09
18		460	2.873E-09	0.0327	1.3080	2.388E-09
19		464	2.952E-09	0.0330	1.3216	2.407E-09
20		473	3.096E-09	0.0319	1.2744	2.568E-09
21	15	604	4.093E-09	0.0243	0.9728	3.483E-09
22		628	4.013E-09	0.0201	0.8048	3.970E-09
23		623	3.915E-09	0.0207	0.8296	3.788E-09
24		618	4.057E-09	0.0220	0.8800	3.730E-09
25		643	4.227E-09	0.0208	0.8304	3.958E-09
26	woven	2.8375	6.574E-13	9.0880	363.52	3.187E-13

*from FX-3300 ** from KES-F8

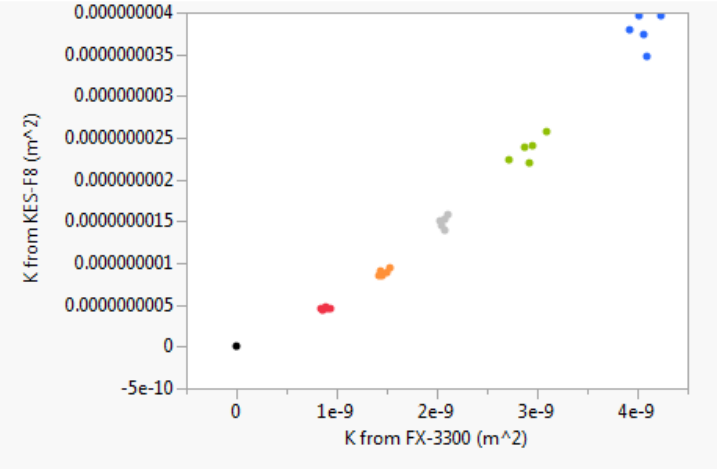

Sample	
1.5 denier	**red**
3 denier	**orange**
6 denier	**grey**
9 denier	**green**
15 denier	**blue**
woven	**black**

Figure 4.8: Comparison of *K* from FX-3300 vs. *K* from KES-F8
(both w/o the Compression Tube or Spacer Rings)

4.1.2 Second Preliminary Trials

The second set of preliminary trials were similar to the first preliminary set, except that the second set of preliminary trials incorporated the use of the compression tube and the spacer rings with both the FX-3300 and the KES-F8 tester. This second set of trials were conducted to be compared with the results collected in the first preliminary trials, so that the effect the compression tube and the spacer ring had on each of the testers could be established, and to determine the correlation between the testers when used with the compression tube and spacer rings and the correlation between each tester when used with and without the compression tube and spacer rings.

Like the first set of preliminary trials, the second set of trials involved individually testing each of the five 56.9 cm^2 samples, from each of the five fabrics, and the woven sample on both the FX-3300 machine and the KES-F8 machine. To prepare the samples to be used with the compression tube and spacer rings, each sample was positioned in the middle of the spacer ring with the appropriate thickness, and the spacer ring and sample were

placed between the two cylinders of the compression tube. The two cylinders of the compression tube were fully compressed, limited and controlled by the spacer ring, and then locked into place using the nuts and bolts. Table 4gives the thickness values of the spacer ring used for the nonwoven fabrics. The woven fabric was particularly tricky to use with the compression tube and spacer ring because it was so thin. In order to prevent leakage around the outside of the woven fabric in the compression tube, the woven fabric had to be wrapped up the sides of a spacer ring and then placed inside the compression tube.

Table 4: Spacer Ring Thickness

Fabric	Spacer Ring Thickness
1.5 denier	4.56 mm
3 denier	4.00 mm
6 denier	3.80 mm
9 denier	4.34 mm
15 denier	4.50 mm

(determined and manufactured with a 3-D digital printer based on the mean value of the five 56.9 cm^2 samples rounded to the nearest fiftieth of a millimeter)

When configured, the compression tube, containing the spacer ring and sample, could be used with the FX-3300 or KES-F8 machines. After the test head had been removed from the clamping arm of the FX-3300, the compression tube was placed on top of the rubber sheeting in the center of the testing orifice of the FX-3300. Once the air flow had been stabilized at the fixed pressure differential, 125 pa, the air flow was recorded and then adjusted by multiplying by $\frac{38}{16.443025\pi}$ to accommodate for the larger area of the compression tube.

For the KES-F8 machine, the compression tube was used by sealing it to the vent pressing plate, by twisting the compression tube into its predesigned clamps. Once the

compression tube was clamped into place, the KES-F8 tester was used to obtain five cycle measurements which were recorded, multiplied by ten to factor for the change in area per the KES-F8 instructions, and used to obtain the mean resistance and pressure differential of each sample.

Since the spacer rings limited the maximum thickness of the fabric samples, the spacer ring's thickness was substituted for the fabric thickness when calculating air permeability with Darcy's Law, if the fabric thickness exceeds the thickness of the spacer ring. Table 5 contains the results for adjusted air flow from the samples using the FX-3300 with the compression tube and spacer ring, the adjusted mean resistance and pressure differential from the samples using the KES-F8 with the compression tube and spacer ring, and their corresponding air permeability calculated using Darcy's Law. A comparison of the air permeability calculated by the FX-3300 and the KES-F8 using the compression tube and spacer rings can be found in Figure 4.9. Figures 4.10 and 4.11 compare the results of the FX-3300 and the KES-F8 machines with the use of the compression tube and spacer ring to the results of the first preliminary trial without the use of the compression tube and spacer ring.

Table 5: Air Permeability Measurements of Single Fabric Samples FX-3300 and KES-F8 with the Compression Tube or Spacer Rings

Sample #	**Denier**	Q/A^{2}* (m^3/m^2 s)	K* (m^2)	R_{mean}** (K pa s/m)	Δp** (pa)	K** (m^2)
1	1.5	141	9.250E-10	0.2242	8.9680	3.671E-10
2		143	9.208E-10	0.2070	8.2800	3.876E-10
3		156	1.030E-09	0.1786	7.1440	4.621E-10
4		146	9.609E-10	0.2104	8.4160	3.900E-10
5		151	9.928E-10	0.2066	8.2640	3.983E-10
6	3	258	1.496E-09	0.1068	4.2720	6.779E-10
7		237	1.372E-09	0.1080	4.3200	6.704E-10
8		250	1.449E-09	0.1112	4.4480	6.511E-10
9		263	1.447E-09	0.1166	4.6640	5.888E-10
10		252	1.439E-09	0.1082	4.3280	6.591E-10
11	6	375	2.017E-09	0.0704	2.8160	9.547E-10
12		372	1.994E-09	0.0620	2.4800	1.080E-09
13		362	1.991E-09	0.0756	3.0240	9.098E-10
14		377	2.072E-09	0.0724	2.8960	9.500E-10
15		352	1.939E-09	0.0790	3.1600	8.706E-10
16	9	447	2.543E-09	0.0540	2.1600	1.318E-09
17		432	2.714E-09	0.0542	2.1680	1.449E-09
18		448	2.798E-09	0.0594	2.3760	1.314E-09
19		441	2.769E-09	0.0588	2.3520	1.336E-09
20		444	2.788E-09	0.0456	1.8240	1.723E-09
21	15	545	3.552E-09	0.0396	1.5840	2.057E-09
22		554	3.540E-09	0.0438	1.7520	1.824E-09
23		554	3.481E-09	0.0366	1.4640	2.146E-09
24		547	3.561E-09	0.0368	1.4720	2.213E-09
25		552	3.595E-09	0.0436	1.7440	1.868E-09
26	woven	4	8.286E-13	8.8280	353.12	3.280E-13

*from FX-3300 ** from KES-F8

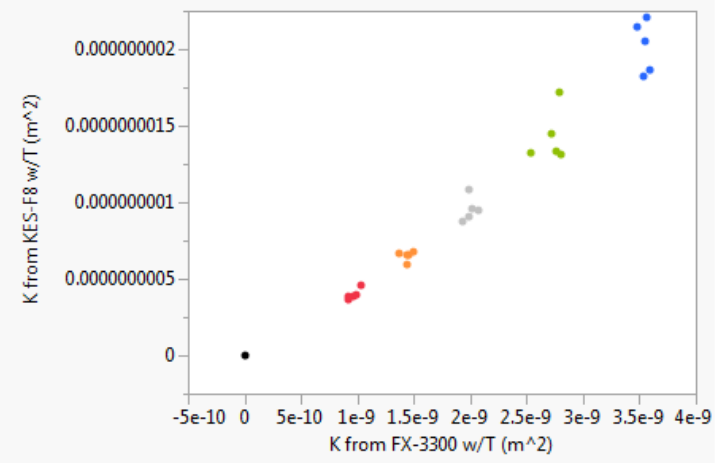

Sample	
1.5 denier	**red**
3 denier	**orange**
6 denier	**grey**
9 denier	**green**
15 denier	**blue**
woven	**black**

Figure 4.9: Comparison of *K* from FX-3300 vs. *K* from KES-F8
(both with the Compression Tube and Spacer Rings)

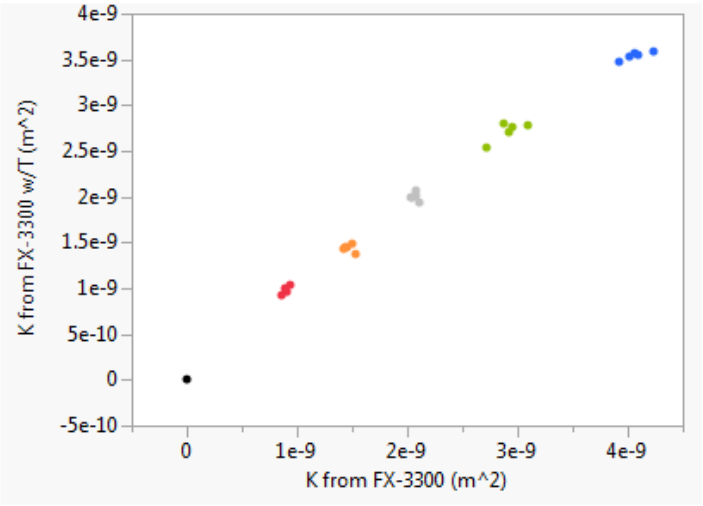

Sample	
1.5 denier	**red**
3 denier	**orange**
6 denier	**grey**
9 denier	**green**
15 denier	**blue**
woven	**black**

Figure 4.10: Comparison of *K* from FX-3300 w/o the Compression Tube and Spacer Ring vs.
K from FX-3300 with the Compression Tube and Spacer Ring

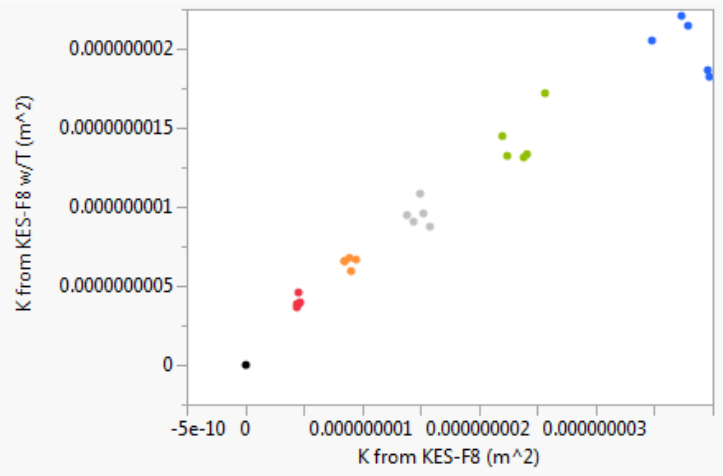

Sample	
1.5 denier	**red**
3 denier	**orange**
6 denier	**grey**
9 denier	**green**
15 denier	**blue**
woven	**black**

Figure 4.11: Comparison of *K* from KES-F8 w/o the Compression Tube and Spacer Ring vs. *K* from KES-F8 with the Compression Tube and Spacer Ring

4.1.3 Primary Trials

While the preliminary trials offered insight into the air permeability of the single samples and on the functioning of the testing equipment, the primary trials were a focused attempt on determining the effect of changing fiber diameter and solid volume fraction had on the air permeability of the nonwoven fabrics.

To target the first approach, the effect of changing fiber diameter, experiments were organized to look at how the air permeability would change as the fiber diameter increased between our five levels (1.5, 3, 6, 9 & 15 denier) while the solid volume fraction was kept constant. By compressing the fabrics, to manipulate the solid volume fraction of the samples, it was possible to study the effect of fiber diameter at five different solid volume fractions (~4%, ~8%, ~12%, ~16% & ~20%). To this end, five series of experiments were created, each with five levels, to target the first approach. Table 6 contains a breakdown of the experiments targeted at the first experimental approach.

Table 6: Experimental Design for the Effect of Changing Fiber Diameter

Series	Level 1	Level 2	Level 3	Level 4	Level 5
~ 4%	1.5 denier	3 denier	6 denier	9 denier	15 denier
~ 8%	1.5 denier	3 denier	6 denier	9 denier	15 denier
~ 12%	1.5 denier	3 denier	6 denier	9 denier	15 denier
~ 16%	1.5 denier	3 denier	6 denier	9 denier	15 denier
~ 20%	1.5 denier	3 denier	6 denier	9 denier	15 denier

To target the second approach, the effect of changing solid volume fractions, a second, similar set of experiments were designed to target how air permeability was affected as solid volume fraction varied at five different levels (~4%, ~8%, ~12%, ~16% & ~20%). By studying just one of the fabrics at a time, it was possible to compress the samples of that fabric to create the different levels of solid volume fraction, while keeping the fiber diameter constant (controlled by the denier of fabric selected). By creating a series of experiments for each of the five different fabrics, it was possible to design experiments that targeted the second experimental approach of this research. A breakdown of these series of experiments can be found in Table 7.

Table 7: Experimental Design for the Effect of Changing Solid Volume Fraction

Series	Level 1	Level 2	Level 3	Level 4	Level 5
1.5 denier	~ 4%	~ 8%	~ 12%	~ 16%	~ 20%
3 denier	~ 4%	~ 8%	~ 12%	~ 16%	~ 20%
6 denier	~ 4%	~ 8%	~ 12%	~ 16%	~ 20%
9 denier	~ 4%	~ 8%	~ 12%	~ 16%	~ 20%
15 denier	~ 4%	~ 8%	~ 12%	~ 16%	~ 20%

Though designed based on differing approaches, it became apparent that the same experimental works could be used to satisfy both designs and that they only differed in their

organization and breakdown/analysis of the data collected. A combined experimental design that incorporates both experimental approaches can be found in Table 8.

Table 8: Combined Experimental Design for Dual Approach on Air Permeability

		Solid Volume Fraction				
	Levels	**1**	**2**	**3**	**4**	**5**
Fiber Diameter	**1**	1.5 denier @ ~ 4%	1.5 denier @ ~ 8%	1.5 denier @ ~ 12%	1.5 denier @ ~ 16%	1.5 denier @ ~ 20%
	2	3 denier @ ~ 4%	3 denier @ ~ 8%	3 denier @ ~ 12%	3 denier @ ~ 16%	3 denier @ ~ 20%
	3	6 denier @ ~ 4%	6 denier @ ~ 8%	6 denier @ ~ 12%	6 denier @ ~ 16%	6 denier @ ~ 20%
	4	9 denier @ ~ 4%	9 denier @ ~ 8%	9 denier @ ~ 12%	9 denier @ ~ 16%	9 denier @ ~ 20%
	5	15 denier @ ~ 4%	15 denier @ ~ 8%	15 denier @ ~ 12%	15 denier @ ~ 16%	15 denier @ ~ 20%

For these experiments, controlling the fiber diameter was easy enough and involved selecting samples based on the fabric's fiber denier. Controlling the solid volume fraction was a little more difficult and involved the use of the compression tube and spacer rings as in the second preliminary trials. The primary trials only differed from that of second preliminary trials in how the compression tube containing the spacer ring and sample(s) was prepared prior to being used with the FX-3300 and the KES-F8 machines. Once assembled, the compression tube containing the spacer ring and sample(s) was used exactly the same with the FX-3300 and the KES-F8 machines as in the second preliminary trials. Testing the samples at solid volume fraction of 4% was simple and involved just testing one sample at a time, which had already been done in the second preliminary trial. Testing the samples at the other solid volume fraction involved using multiple samples from the same fabric denier with

their corresponding spacer ring at the same time. To simulate a fabric with about 8% solid volume fraction, two samples from the same fabric were placed in the center of the compression ring. The spacer ring and both samples were then placed between the two cylinders of the compression tube, compressed fully, and then fixed into place with the nuts and bolts. By this compression, the fabric samples were temporarily compressed to half of their normal volume, simulating twice the normal solid volume fraction. In this manner, ~12% solid volume fraction was simulated using three fabrics at once, ~16% solid volume fraction was simulated using four fabrics, and ~20% solid volume fraction was simulated using five fabrics at once. To maximize the data collected every combination possible of the five samples for each fabric. So for each of the five fabric deniers, there were five test at 4% SVF, ten test at 8% SVF, ten test at 12% SVF, five test at 16%, and one test at 20%. Table 9 contains the means of these results and their coefficient of variation.

Table 9: Air Permeability Measurements of Multiple Samples in Tube & Ring

Denier	~SVF	# of Combinations	$\bar{K}$* (m^2)	CV*	$\bar{K}$** (m^2)	CV**
1.5	4%	5	9.659E-10	4.78%	4.010E-10	8.99%
	8%	10	4.992E-10	3.79%	2.134E-10	3.94%
	12%	10	2.273E-10	1.11%	9.388E-11	2.39%
	16%	5	1.514E-10	3.76%	5.987E-11	3.60%
	20%	1	1.049E-10	-	4.288E-11	-
3	4%	5	1.440E-09	3.07%	6.495E-10	5.45%
	8%	10	8.457E-10	1.72%	3.605E-10	3.47%
	12%	10	4.388E-10	1.93%	2.020E-10	7.98%
	16%	5	2.931E-10	1.46%	1.340E-10	0.54%
	20%	1	2.267E-10	-	9.507E-11	-
6	4%	5	2.004E-09	2.40%	9.531E-10	8.27%
	8%	10	1.245E-09	1.22%	5.629E-10	5.40%
	12%	10	6.768E-10	2.58%	3.496E-10	2.73%
	16%	5	4.671E-10	1.80%	2.402E-10	3.80%
	20%	1	3.526E-10	-	1.751E-10	-
9	4%	5	2.722E-09	3.87%	1.428E-09	12.16%
	8%	10	1.764E-09	1.65%	8.833E-10	7.90%
	12%	10	1.035E-09	1.93%	4.909E-10	2.62%
	16%	5	7.295E-10	1.97%	3.251E-10	3.89%
	20%	1	5.547E-10	-	2.360E-10	-
15	4%	5	3.546E-09	1.17%	2.022E-09	8.43%
	8%	10	2.377E-09	1.17%	1.302E-09	6.52%
	12%	10	1.480E-09	1.60%	7.436E-10	3.19%
	16%	5	1.083E-09	0.83%	5.015E-10	3.30%
	20%	1	8.484E-10	-	3.659E-10	-

*from FX-3300 ** from KES-F8

4.4 Back Calculations

Since multiple testing methods were used throughout this research, some back calculations were needed in order to compare the data collected independent of the configuration used to obtain the data. Not only did these back calculations make it possible

to relate the data collected from the different trials regardless of the equipment used, but it also allowed for the abstraction of the systematic error introduced by the use of the compression tube and spacer rings used in the primary trials. Through these back calculations, it was possible to forecast the air permeability of the samples had they been tested with any of the other according to the ASTM Standard Test Method for Air Permeability of Textile Fabrics.

4.4.1 Explanation of Back Calculations

Part of the intent of the two preliminary trials was to assess the relationship between the different test methods and to determine if any correlation existed between the various testing methods. The first preliminary trial worked to establish a relationship between the two testers, FX-3300 and KES-F8, without the use of the compression tube or spacer ring. As can be seen in Figure 4.12a, there is almost a linear relationship between the two testers. The second preliminary trial analyzed the effect the compression tube and spacer ring had on each testing machine and attempted to further establish a relation between the various testing methods. Though effected by the use of the compression tube and the spacer ring, the results of the second preliminary trial, seen in Figure 4.12d, proved that there was still a correlation between the two testing machines even when used with the compression tube and spacer ring. Further correlations were also seen when comparing the results without the use of the compression tube and spacer ring in the first preliminary trials with the results using the compression tube and spacer rings in the second preliminary trial. Figure 4.12b demonstrates another almost linear correlation between the results on the FX-3300 with and without the

use of the compression tube and spacer rings, and Figure 4.12c demonstrates a similar association between the results on the KES-F8 machine with and without the use of the compression tube and spacer rings. There is even a similar relation between the results from the FX-3300 without the compression tube and spacer ring and the KES-F8 with the compression tube and spacer ring, as seen in Figure 4.12e,

To further define the relation between the various testing methods, JMP Pro, data analysis software, was used to define the relations between the four different testing methods. Though all five relations, seen in Figures 4.12a, 4.12b, 4.12c, 4.12d and 4.12e, appeared almost linear, the linear relationships established by the JMP software were unable to accurately describe the relationship between the measurements of the different testing methods at low air permeability values, even though the coefficient of determination for each relation of best fit was at least 95%. It was found that second degree polynomials more accurately fit the data and better defined the relation between the testing methods, even at lower air permeability values.

It should be noted, that the results from the FX-3300 tester and the results without the compression tube and the spacer ring were used as the independent variables, since the trials conducted with those test methods had the least amount of systematic error and most closely aligned with the ASTM Standard Test Method for Air Permeability of Textile Fabrics. The best fit equations for these relations and their coefficient of determination can be found in Table 10. Figure 4.13 shows how these relations can be used to convert between the various test methods.

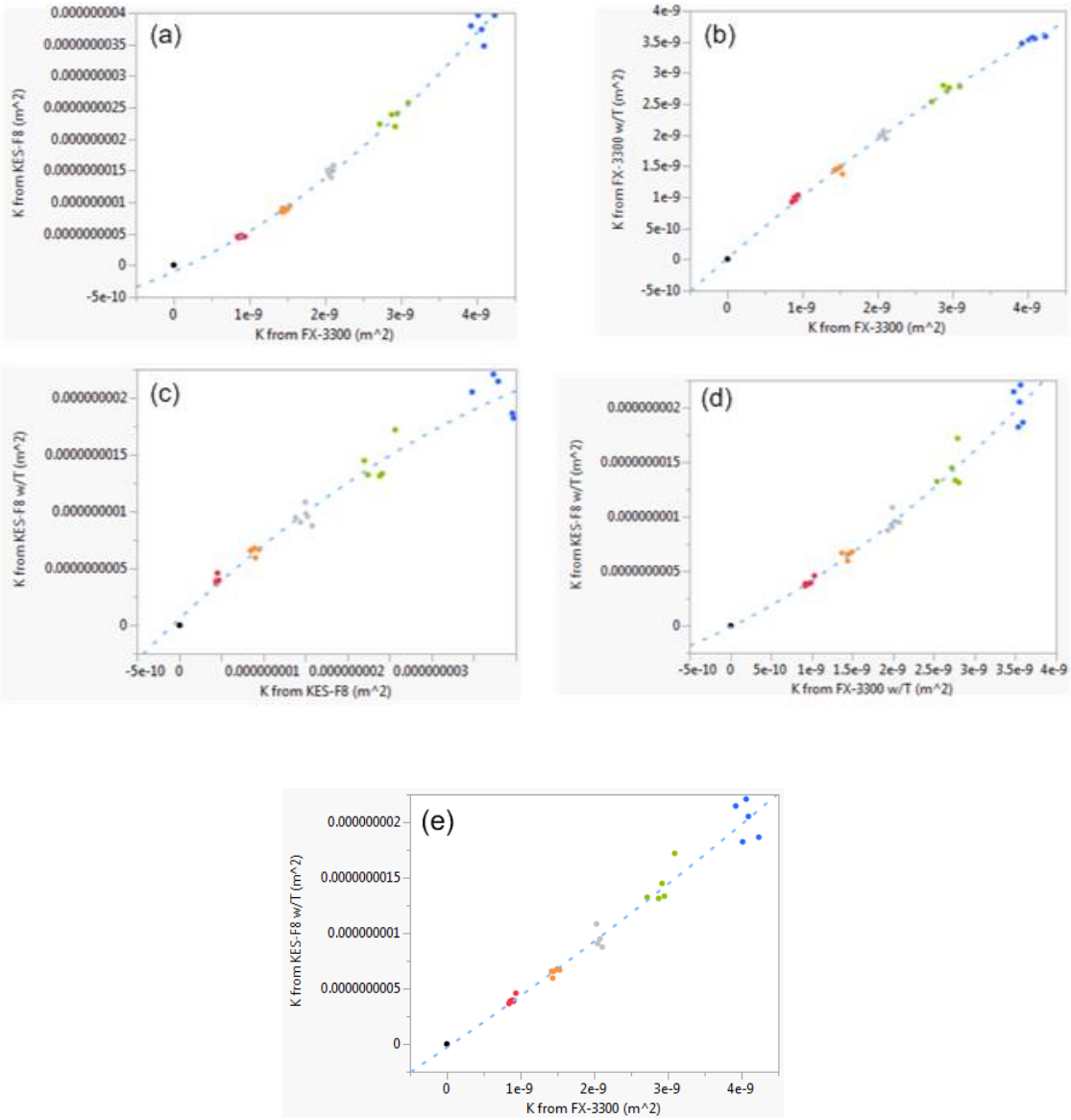

Figure 4.12: Correlation Between Various Test Methods
(a) Correlation of K from FX-3300 vs. K from KES-F8
(b) Correlation of K from FX-3300 vs. K from FX-3300 w/T
(c) Correlation of K from KES-F8 vs. K from KES-F8 w/T
(d) Correlation of K from FX-3300 w/T vs. K from KES-F8 w/T
(e) Correlation of K from FX-3300 vs. K from KES-F8 w/T
*w/T = with Compression Tube and Spacer Rings

Table 10: Relation between Various Test Methods

	Relation		Coefficient of determination
K from FX-3300 vs. K from KES-F8	$K_{KES} = 101844681(K_{FX} - 2.19 \times 10^{-9})^2 + 0.9861455(K_{FX}) - 5.77 \times 10^{-10}$	(1)	0.991731
K from FX-3300 vs. K from FX-3300 w/T	$K_{FX\,w/T} = -45186374(K_{FX} - 2.19 \times 10^{-9})^2 + 0.8502169(K_{FX}) + 2.52 \times 10^{-10}$	(2)	0.997094
K from KES-F8 vs. K from KES-F8 w/T	$K_{KES\,w/T} = -48668898(K_{KES} - 1.73 \times 10^{-9})^2 + 0.5282683(K_{KES}) + 2.083 \times 10^{-10}$	(3)	0.965487
K from FX-3300 w/T vs. K from KES-F8 w/T	$K_{KES\,w/T} = 56533511\left(K_{FX\,w/T} - 2.05 \times 10^{-9}\right)^2 + 0.603274\left(K_{FX\,w/T}\right) - 2.45 \times 10^{-10}$	(4)	0.971681
K from FX-3300 vs. K from KES-F8 w/T	$K_{KES\,w/T} = 12252068(K_{FX} - 2.19 \times 10^{-9})^2 + 0.5079901(K_{FX}) - 8.22 \times 10^{-11}$	(5)	0.971683

*w/T = with Compression Tube and Spacer Rings

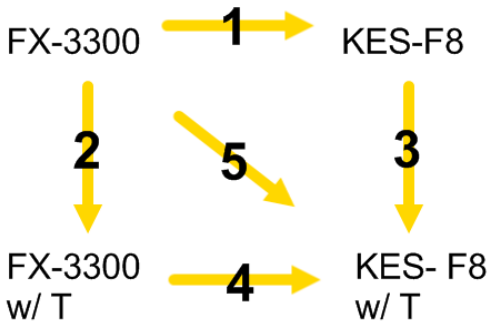

Figure 4.13: Graphical Representation of how Equations #1-5 Correlate Between the Various Test Methods
*w/T = with Compression Tube and Spacer Rings

In order to use these relations for back calculation purposes, each of the relations in Table 10 were converted so that they dependent variable could be used to solve for the independent variable in the relation. It should be noted that when each of these relations was solved for their independent variable, two equations were created, but with each relation, one solution made K positive and one solution made K negative. Since air permeability must be positive, only one of the two equations was feasible with air permeability, therefore the equation that made air permeability positive was picked for each relation. Table 11 contains the relations solved for the independent variable and Figure 4.14 is graphical representation of how these relations can be used to back calculate between the various methods of testing.

Table 11: Relation between Various Test Methods – Solved for the Independent Variable

	Relation
K from FX-3300 vs. K from KES-F8	$K_{FX} = \sqrt{\frac{K_{KES}+8.854273\times10^{-11}}{101844681} + 7.030035 \times 10^{-18}} - 2.651421 \times 10^{-9}$ (6)
K from FX-3300 vs. K from FX-3300 w/T	$K_{FX} = -\sqrt{1.345116 \times 10^{-16} - \frac{K_{FX\,w/T}-3.528163\times10^{-11}}{45186374}} + 1.159791 \times 10^{-8}$ (7)
K from KES-F8 vs. K from KES-F8 w/T	$K_{KES} = -\sqrt{5.122501 \times 10^{-17} - \frac{K_{KES\,w/T}-6.263886\times10^{-11}}{48668898}} + 7.157165 \times 10^{-9}$ (8)
K from FX-3300 w/T vs. K from KES-F8 w/T	$K_{FX\,w/T} = \sqrt{\frac{K_{KES\,w/T}+7.41792\times10^{-12}}{56533511} + 1.07948 \times 10^{-17}} - 3.285543 \times 10^{-9}$ (9)
K from FX-3300 vs. K from KES-F8 w/T	$K_{FX} = \sqrt{\frac{K_{KES\,w/T}-2.343786\times10^{-11}}{12252068} + 3.4347609 \times 10^{-16}} - 1.854079 \times 10^{-8}$ (10)

*w/T = with Compression Tube and Spacer Rings

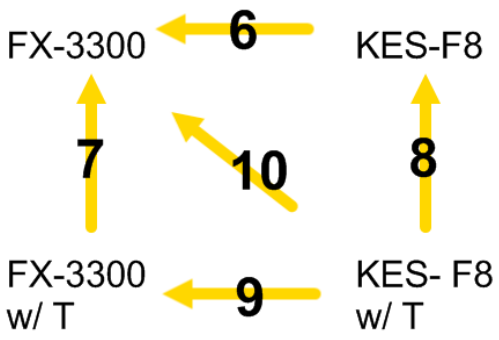

Figure 4.14: Graphical Representation of how the Back Calculating Equations (#6-10) Convert Between the Various Testing Methods
*w/T = with Compression Tube and Spacer Rings

4.4.2 Back Calculated Results

Through the use of the formulas found in in Table 11, it was possible to back calculate the results of the experimental trials so that the data collected was comparable regardless of the equipment and testing method used. For the purpose of comparison, the data collected in the experimental trails was back calculated to be equivalent to the testing done on the FX-3300 without the use of the compression tube and spacer rings, since this method is aligned with the standard testing method of testing the air permeability of a nonwoven fabric. Figure 4.15, a comparison of the results of the 6 denier fabric samples tested with the compression tube and spacer ring in both the FX-3300 and the KES-F8 back calculated to as if they had been measured using the FX-3300 without the compression tube and spacer ring testing configuration, demonstrates that though some noise still exist, it is limited and as expected as with all testing with nonwoven fabrics.

Figures 4.16 and 4.17 are a graphical representation of the back calculated results of all the data collected on all the nonwoven samples with the compression tube and spacer ring in both the FX-3300 and the KES-F8 testers.

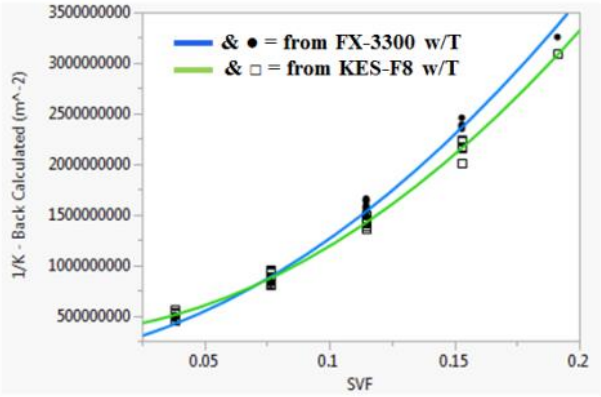

Figure 4.15: Comparison of Back Calculated Results for the 6 Denier Fabric Samples

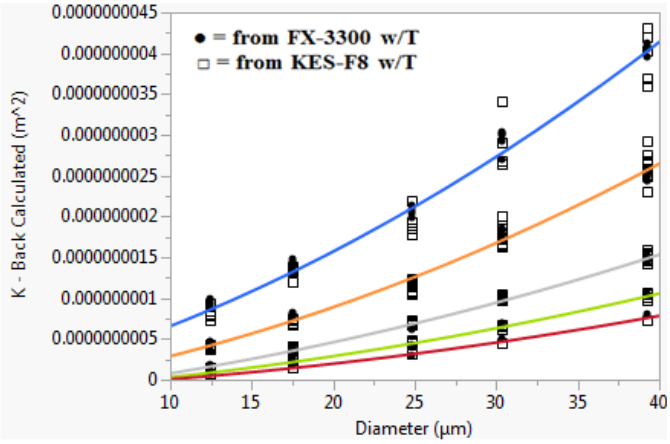

~SVF	
4 %	blue
8 %	orange
12 %	grey
16 %	green
20 %	red

Figure 4.16: Back Calculated Results Show the Effect of Changing Fiber Diameter

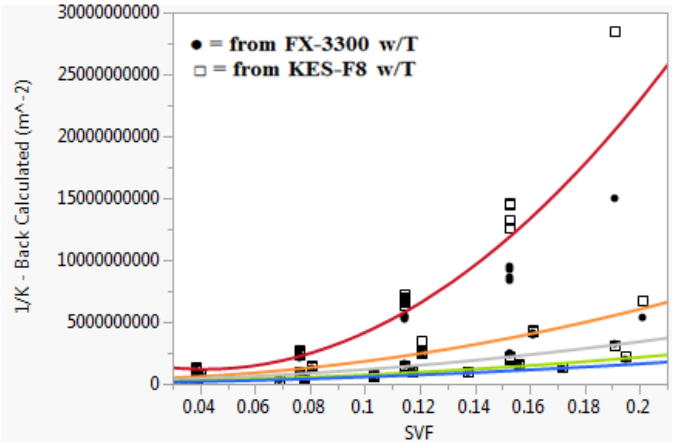

Sample	
12.401 µm	red
17.537 µm	orange
24.801 µm	grey
30.375 µm	green
39.214 µm	blue

Figure 4.17: Back Calculated Results Show the Effect of Changing Solid Volume Fraction

4.5 Effect of Changing Fiber Diameter and Changing Solid Volume Fraction

As expected, changing fiber diameter and changing solid volume fraction played critical roles on the air permeability of the nonwoven samples in this study. Figure 4.16 demonstrates how as the size of fibers in the nonwoven samples increased, the air permeability also increased and Figure 4.17 shows that the air permeability of the samples

also increased, when the solid volume fraction of the samples was lowered, agreeing well with previous research and literature on the effect of changing fiber diameter and changing solid volume fraction. Since decreasing the fiber diameter, decreases pore size, creating more tortuous and longer flow paths, and increased the surface area to mass ratio of the fibers, resulting in a higher drag resistance, it came as no surprise that finer fibers related in a lower air permeability. Likewise, the effect of changing solid volume fraction was not shocking, since an increase in solid volume fraction, resulted in few paths for the air to flow through and more fiber per volume area to resist the flow of air through the nonwoven.

This research and both Figures 4.16 and 4.17 further prove that neither the fiber diameter nor the solid volume fraction of the nonwovens is enough to predict the air permeability of a nonwoven alone, and that both, fiber diameter and solid volume fraction, need to be factored in to accurately predict the air permeability of a nonwoven fabric.

5. MODEL TO EXPERIMENTAL COMPARISON

The following data is a comparison of the experimental results with the theoretical models. These results are split up in the same manner of the literature review, into four categories based upon the method in which they were created. For each model, except for the models that had negative predictions or relied on a constant or structure parameters, two graphs were plotted. The first graph examines the effect changing fiber diameter had on the model and the experimental results. The second graph shows how air permeability was affected by changing solid volume fraction. For the second graph, the reciprocal of the air permeability is graphed to compensate the effect the uneven number of repetitions for each level of solid volume fraction had on the analysis.

5.1 The Early Works

5.1.1 Brinkman

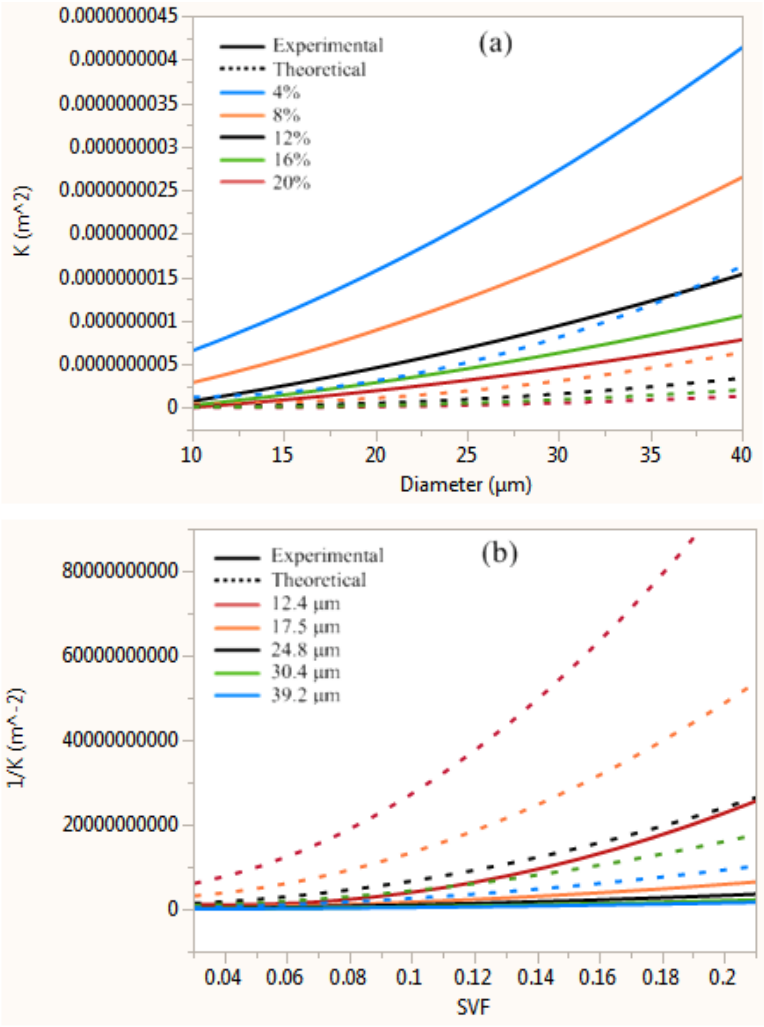

Figure 5.1: Comparison of the Experimental Air Permeability with the Brinkman Theoretical
(a) Air permeability by fiber diameter (b) The reciprocal of the air permeability by solid volume fraction

5.1.2 Davies

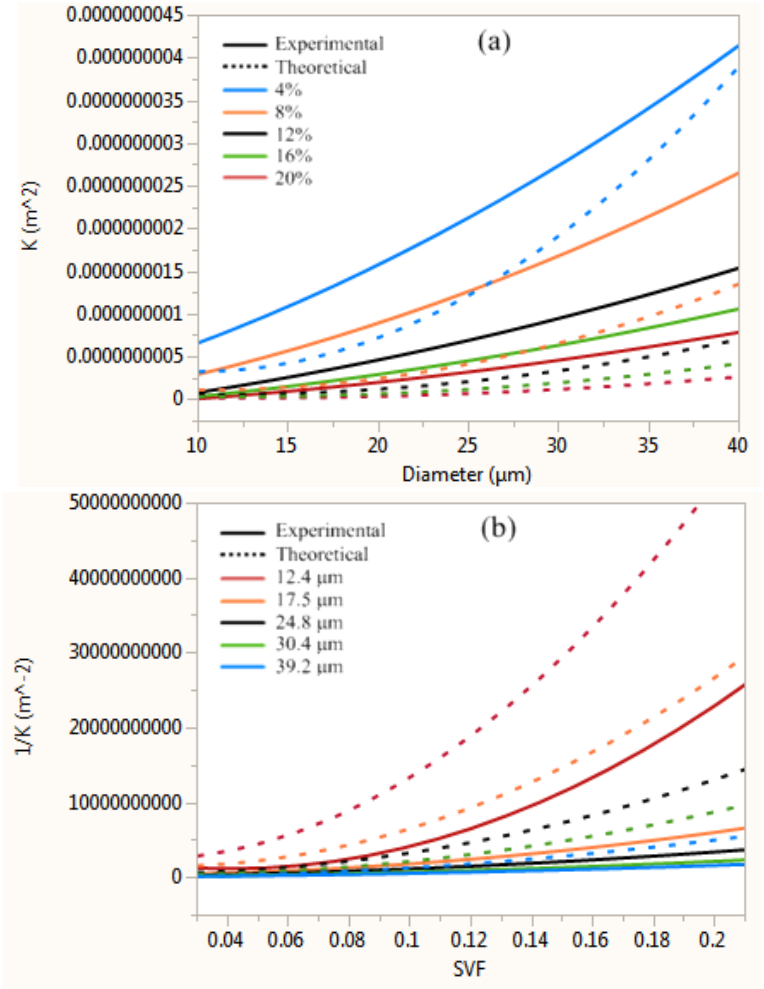

Figure 5.2: Comparison of the Experimental Air Permeability with the Davies Theoretical
(a) Air permeability by fiber diameter (b) The reciprocal of the air permeability by solid volume fraction

5.1.3 Kozeny-Carman

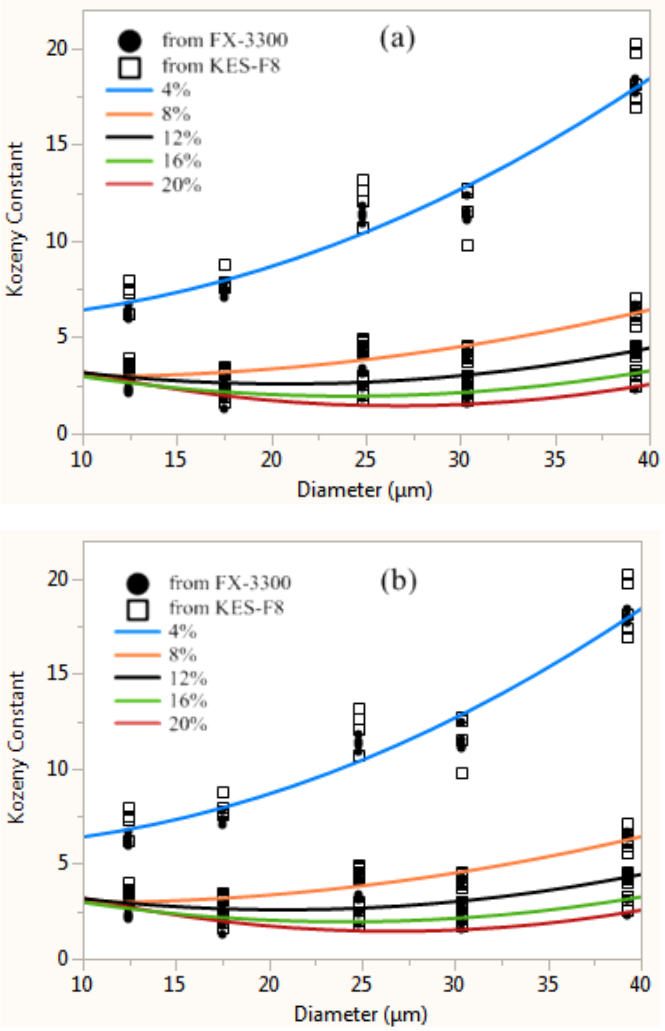

Figure 5.3: Comparison of the Kozeny-Constant for the Experimental Results
(a) using $K = \frac{d^2(1-a)^3}{16k_c a^2}$ (b) using $K = \frac{d^2(1-a)}{16k_c \ln^2(1-a)}$

5.1.4 Analysis

Of the comparison of three of the earliest works in predicting the air permeability, Kozeny-Carman, Brinkman, and Davies, Davies' empirical model was the closest at predicting the air permeability of the nonwoven samples tested in this research. Figures 5.1 and 5.2 show that though both the Davies' model and Brinkman's drag-force based model, under predicted the permeabilities of the nonwoven samples, the Davie's model had a similar trend when compared with the experimental results.

The Kozeny-Carman, channel-based theories, could be somewhat accurate at predicting the air permeability of a nonwoven fabric, if the Kozeny constant was known. Unfortunately, as can be seen in Figure 5.3, the Kozeny constant changes depending on the nonwoven fabric and its fiber diameter and solid volume fraction, and since the Kozeny constant is determined based on the air permeability of the fabric, it essentially means the Kozeny-Carman equations are only useful at predicting the air permeability of a fabric. That is if the air permeability of the fabric is already known.

5.2 Cell Based Analytical Models

5.2.1 Langmuir

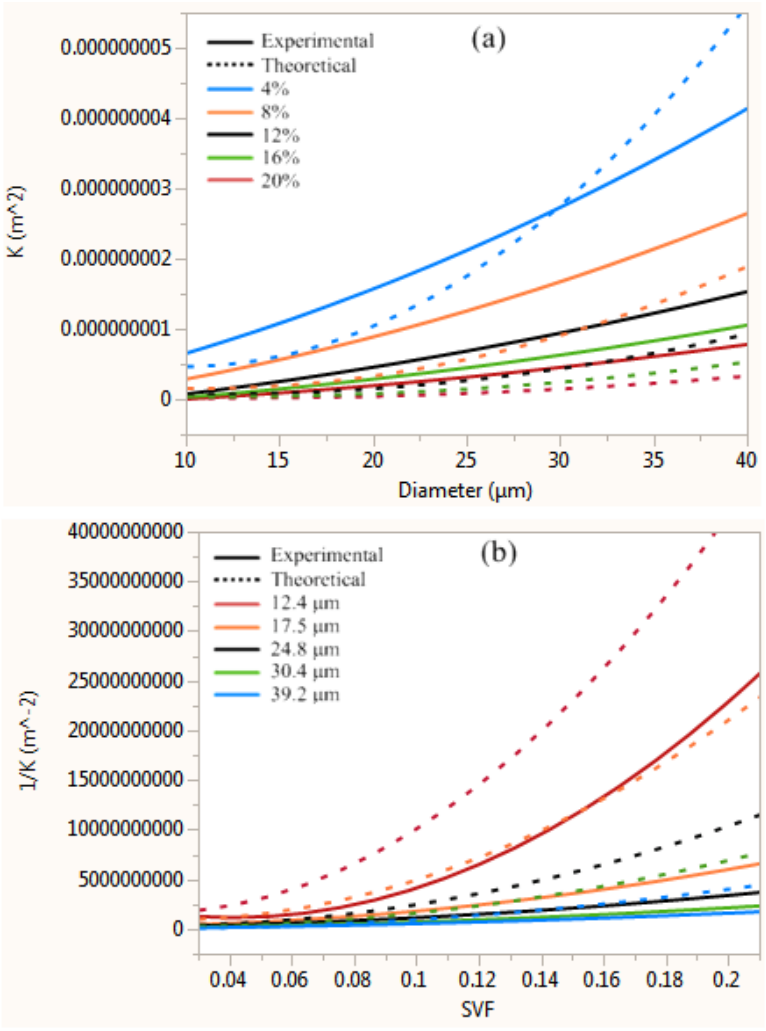

Figure 5.4: Comparison of the Experimental Air Permeability with the Langmuir Theoretical
(a) Air permeability by fiber diameter (b) The reciprocal of the air permeability by solid volume fraction

5.2.2 Happel

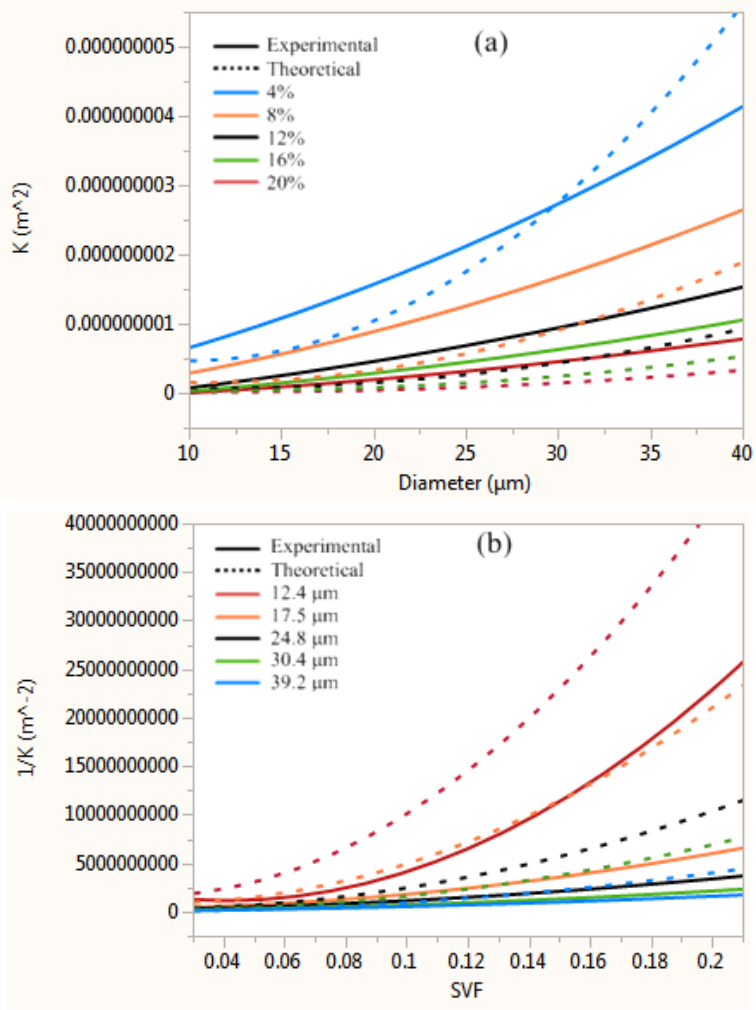

Figure 5.5: Comparison of the Experimental Air Permeability with the Happel Theoretical for Parallel Flow
(a) Air permeability by fiber diameter (b) The reciprocal of the air permeability by solid volume fraction

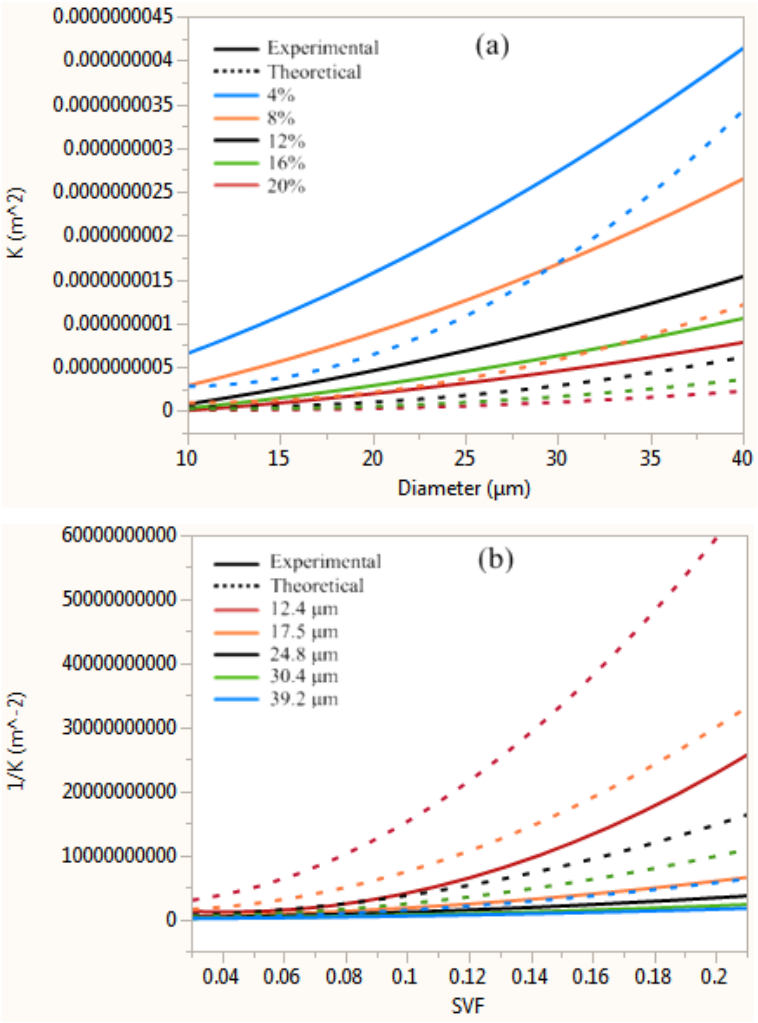

Figure 5.6: Comparison of the Experimental Air Permeability with the Happel Theoretical for Transverse Flow
(a) Air permeability by fiber diameter (b) The reciprocal of the air permeability by solid volume fraction

5.2.3 Kuwabara

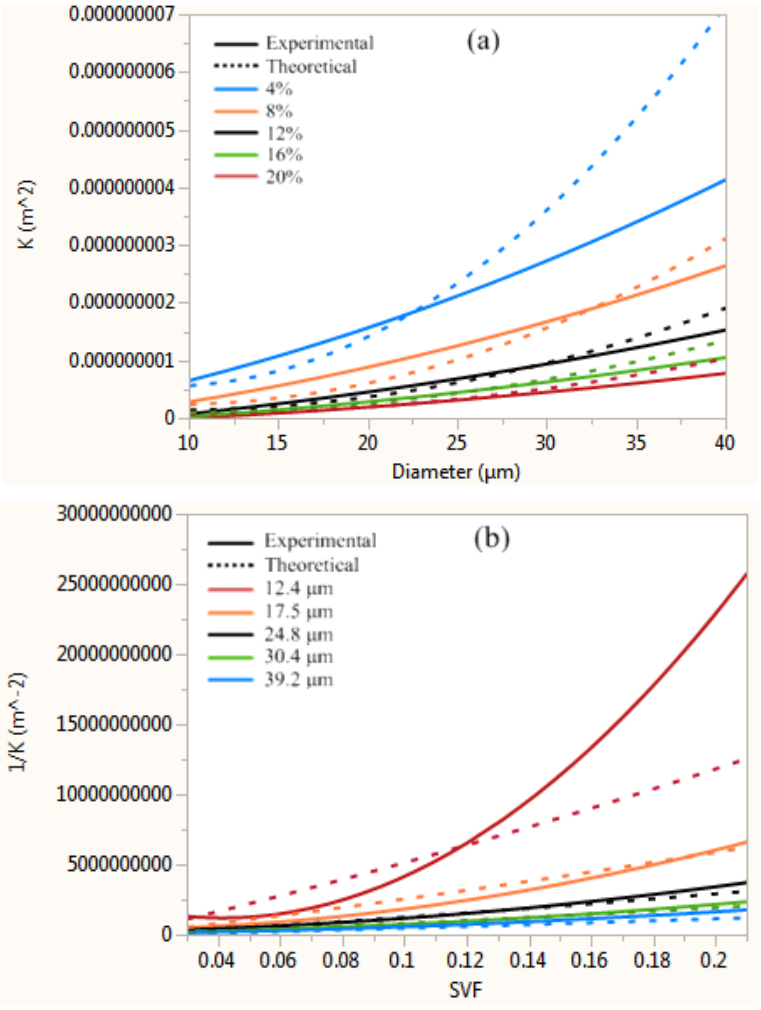

Figure 5.7: Comparison of the Experimental Air Permeability with the Kuwabara Theoretical for $K = \frac{d^2}{32a}\left(-\ln a + \frac{3}{2} + 2a\right)$
(a) Air permeability by fiber diameter (b) The reciprocal of the air permeability by solid volume fraction

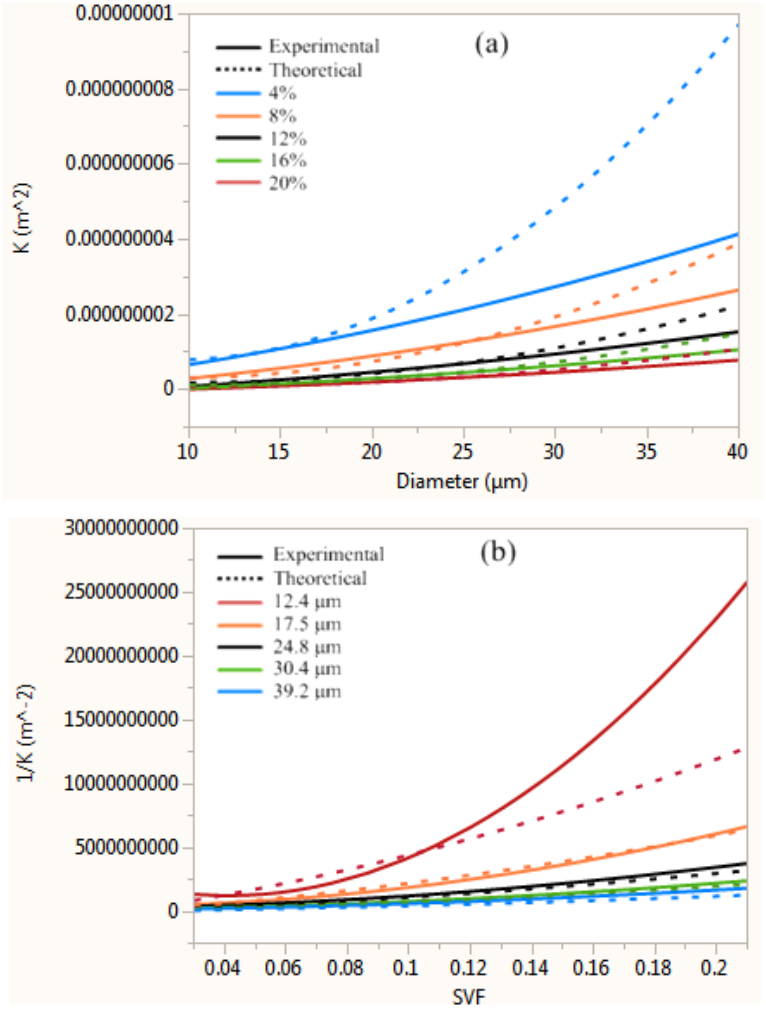

Figure 5.8: Comparison of the Experimental Air Permeability with the Kuwabara Theoretical for $K = \frac{d^2}{16a}\left(-\ln\frac{a}{2} - \frac{3}{4} + a - \frac{a^2}{4}\right)$

(a) Air permeability by fiber diameter (b) The reciprocal of the air permeability by solid volume fraction

5.2.4 Hasimato

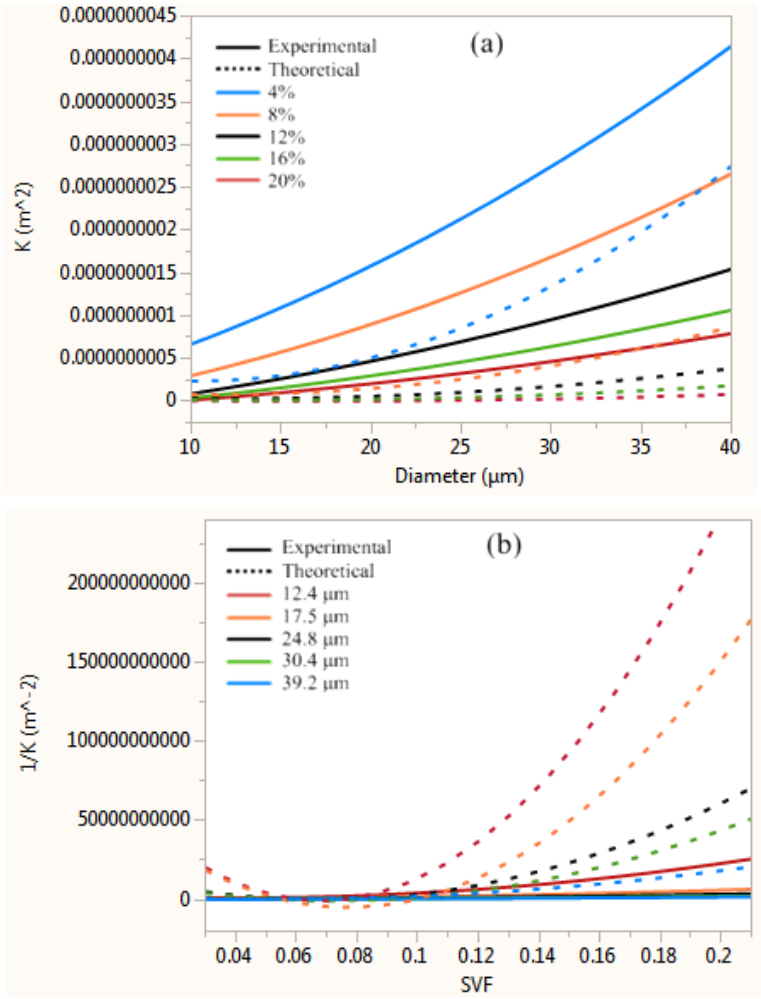

Figure 5.9: Comparison of the Experimental Air Permeability with the Hasimato Theoretical for $K = \frac{d^2}{32a}(-\ln a - 1.476)$

(a) Air permeability by fiber diameter (b) The reciprocal of the air permeability by solid volume fraction

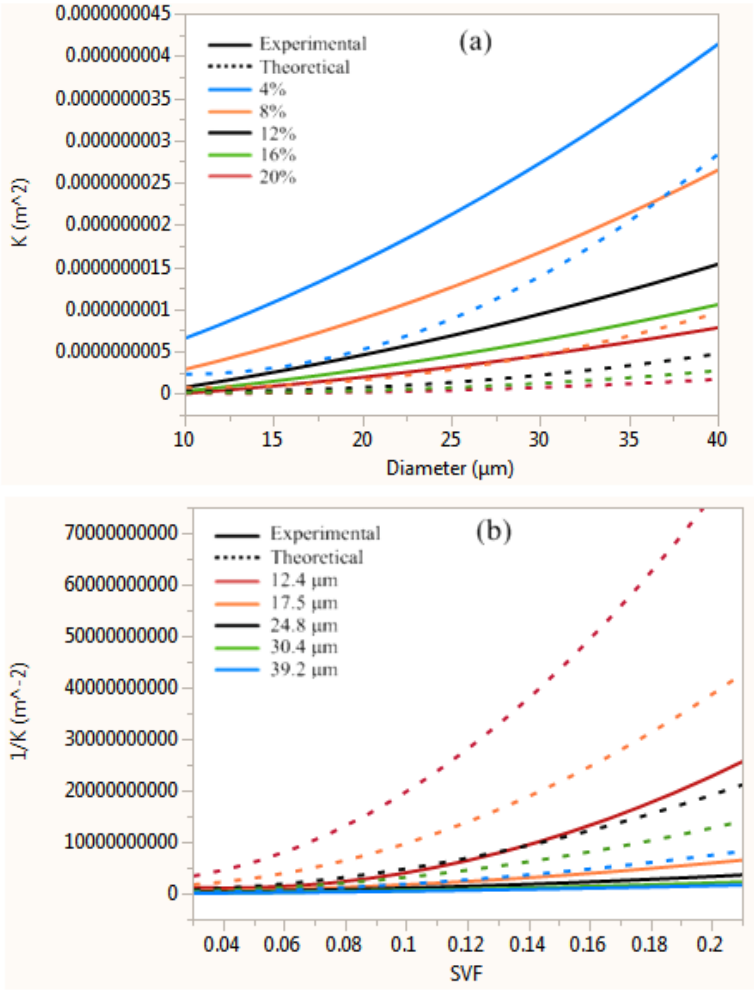

Figure 5.10: Comparison of the Experimental Air Permeability with the Hasimato Theoretical for $K = \frac{d^2}{32a}(-\ln a - 1.476 + 2a + Oa^2)$

(a) Air permeability by fiber diameter (b) The reciprocal of the air permeability by solid volume fraction

5.2.5 Sangani & Acrivos

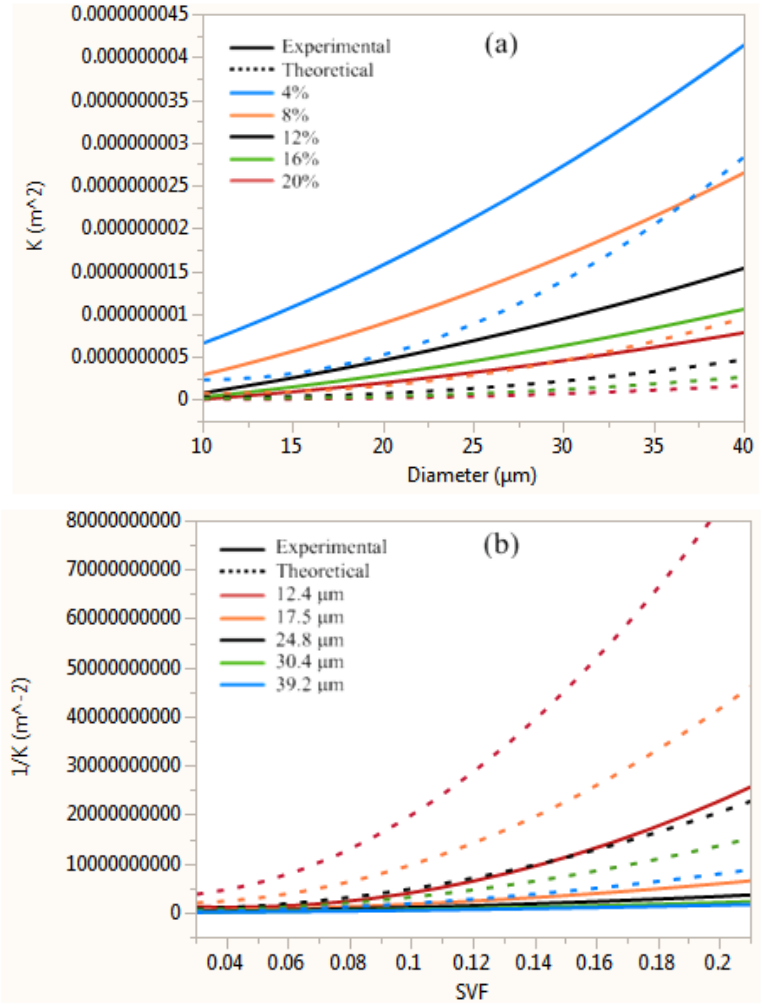

Figure 5.11: Comparison of the Experimental Air Permeability with the Sangani & Acrivos Theoretical for a Square Array
(a) Air permeability by fiber diameter (b) The reciprocal of the air permeability by solid volume fraction

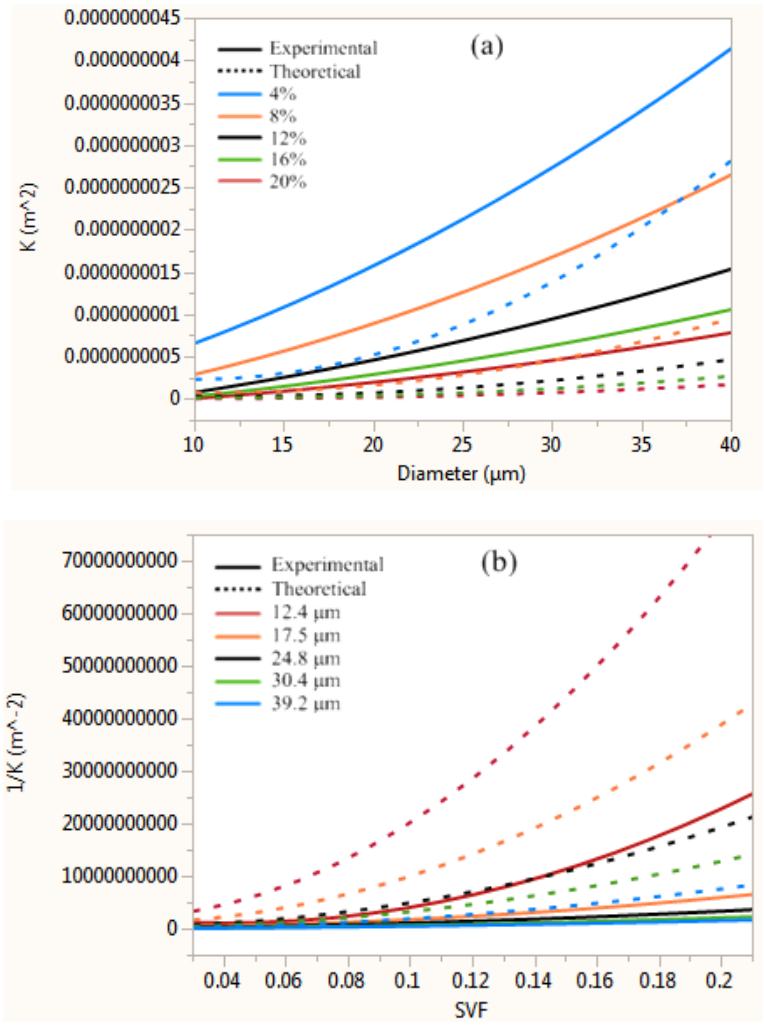

Figure 5.12: Comparison of the Experimental Air Permeability with the Sangani & Acrivos Theoretical for a Hexagonal Array
(a) Air permeability by fiber diameter (b) The reciprocal of the air permeability by solid volume fraction

5.2.6 Drummond & Tahir

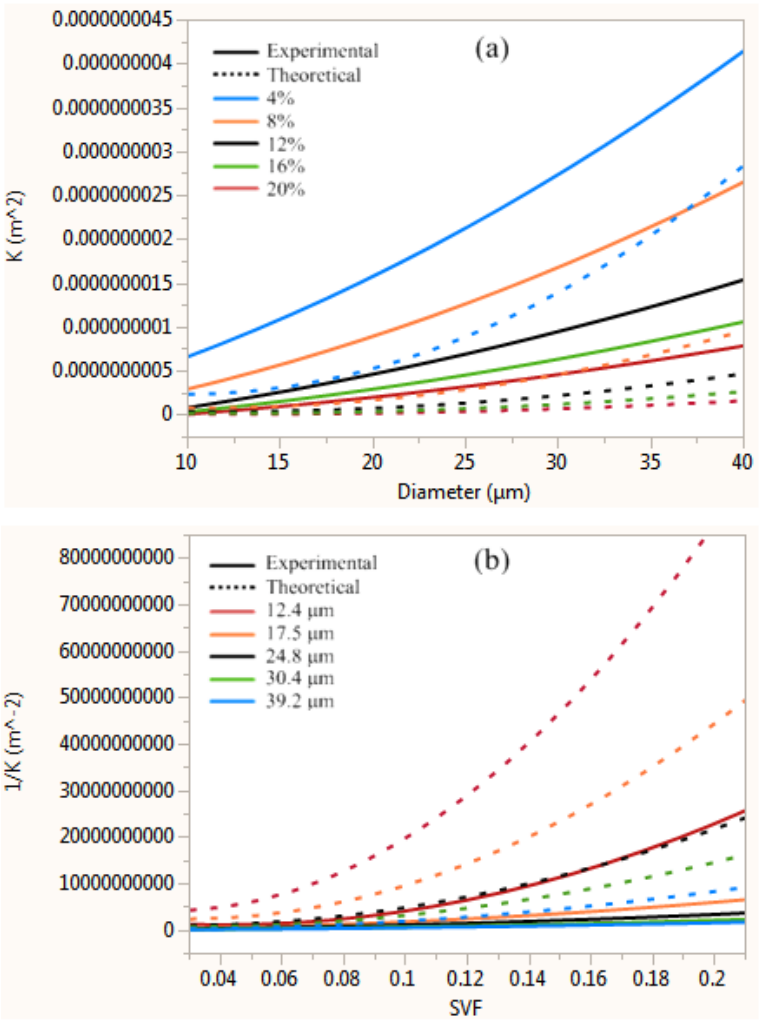

Figure 5.13: Comparison of the Experimental Air Permeability with the Drummond & Tahir Theoretical for Transverse Flow through a Square Array
(a) Air permeability by fiber diameter (b) The reciprocal of the air permeability by solid volume fraction

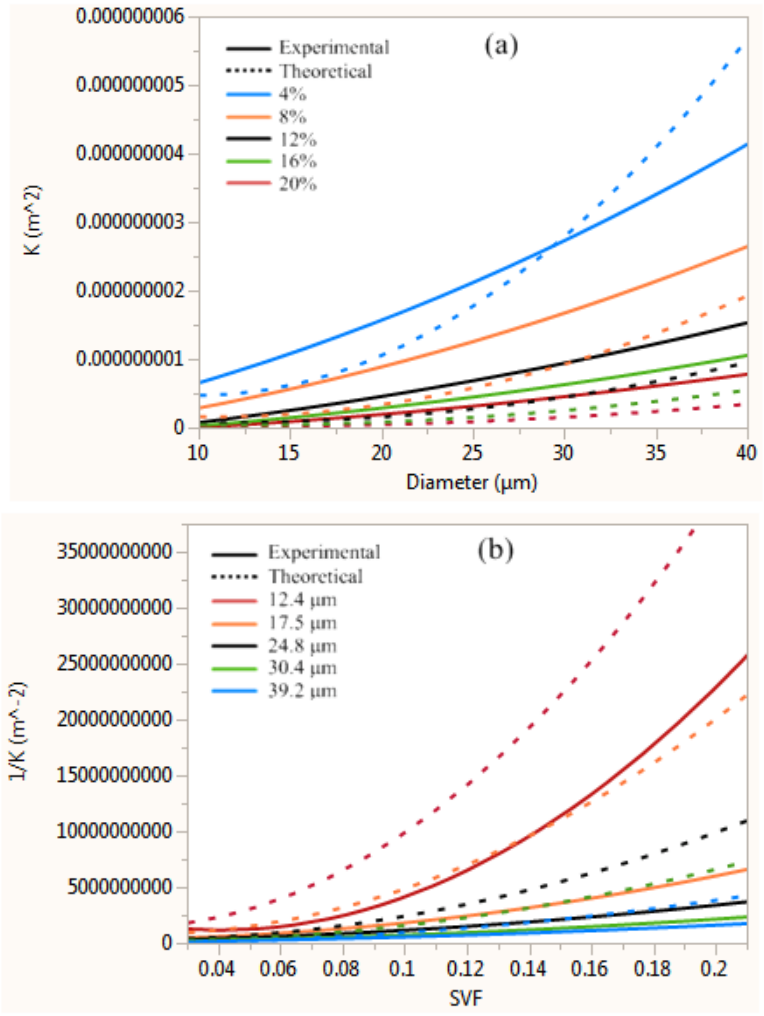

Figure 5.14: Comparison of the Experimental Air Permeability with the Drummond & Tahir Theoretical for Parallel Flow through a Square Array
(a) Air permeability by fiber diameter (b) The reciprocal of the air permeability by solid volume fraction

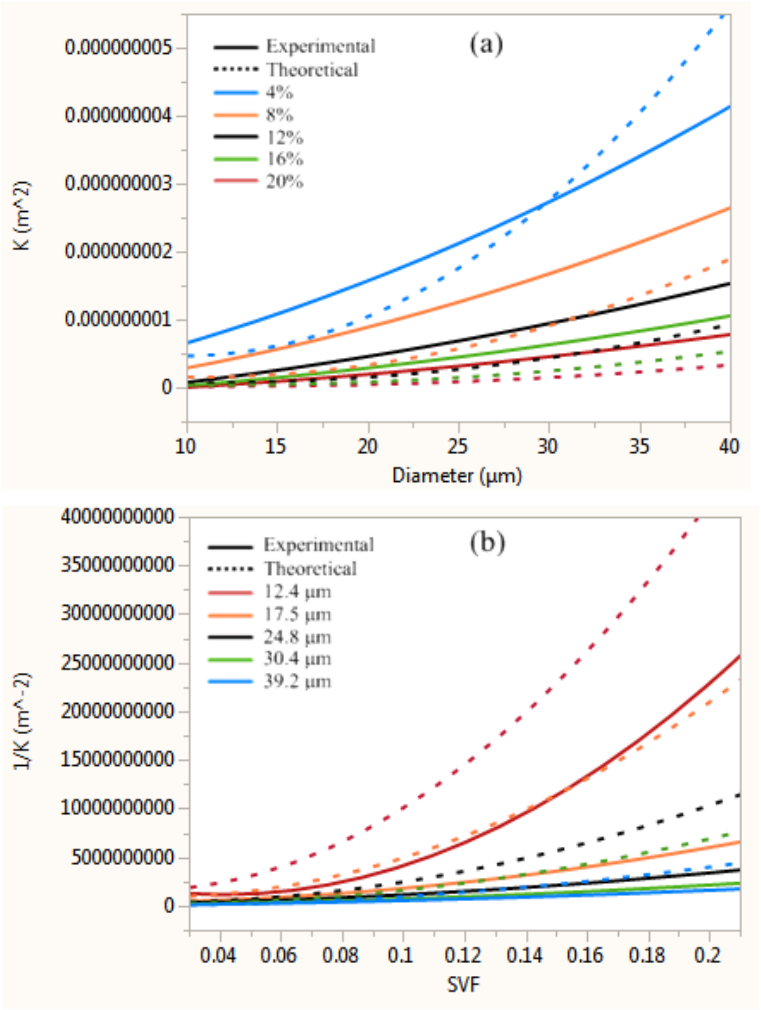

Figure 5.15: Comparison of the Experimental Air Permeability with the Drummond & Tahir Theoretical for Parallel Flow through a Triangular Array
(a) Air permeability by fiber diameter (b) The reciprocal of the air permeability by solid volume fraction

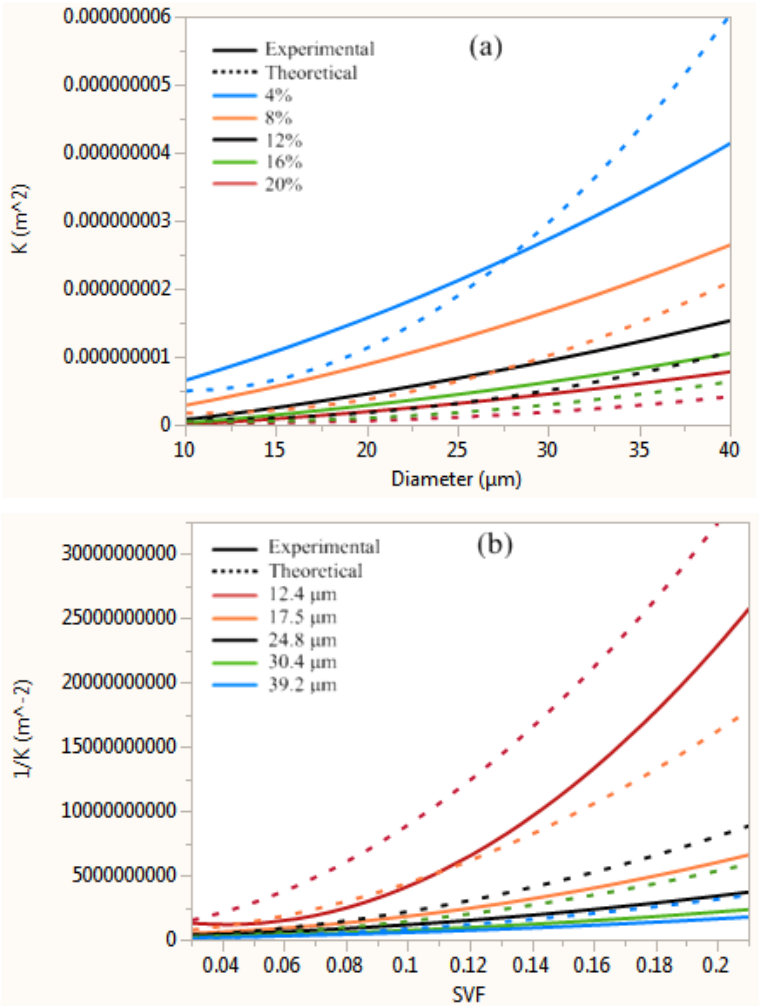

Figure 5.16: Comparison of the Experimental Air Permeability with the Drummond & Tahir Theoretical for Parallel Flow through a Hexagonal Array
(a) Air permeability by fiber diameter (b) The reciprocal of the air permeability by solid volume fraction

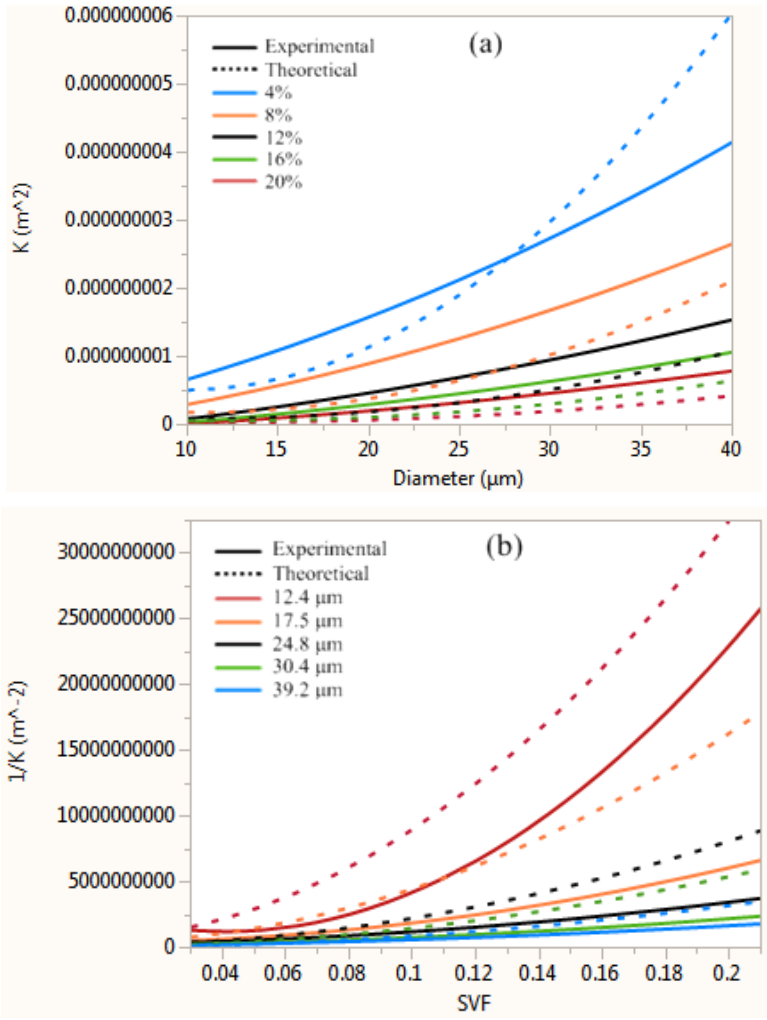

Figure 5.17: Comparison of the Experimental Air Permeability with the Drummond & Tahir Theoretical for Parallel Flow through a Rectangular Array
(a) Air permeability by fiber diameter (b) The reciprocal of the air permeability by solid volume fraction

5.2.7 Tamayol & Bahrami

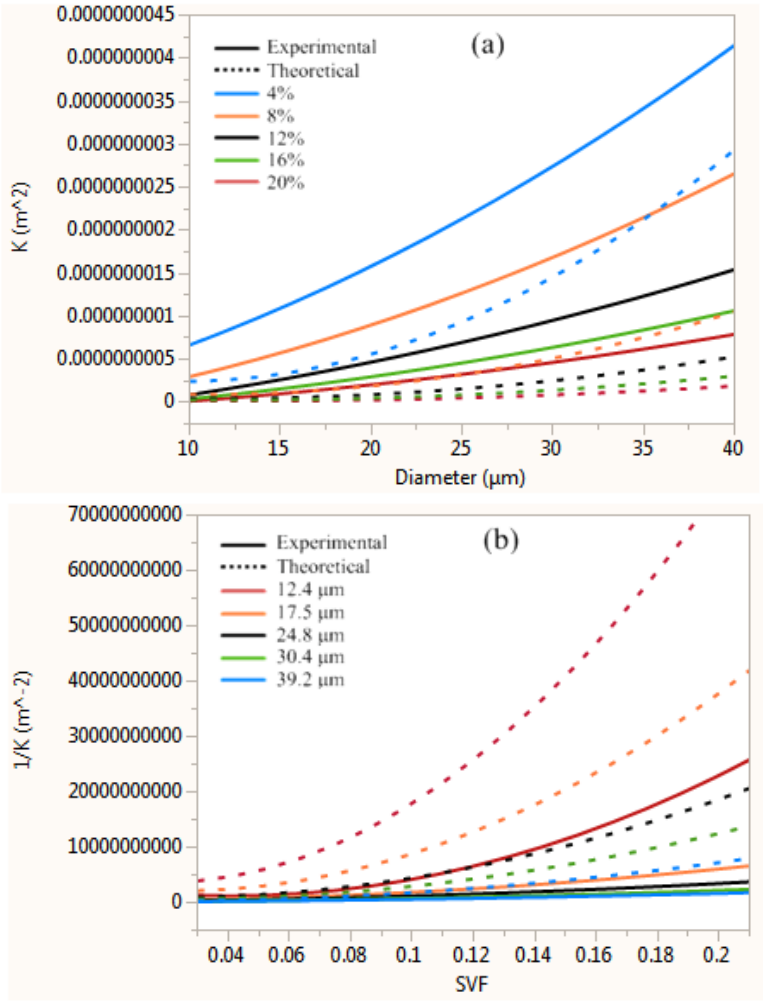

Figure 5.18: Comparison of the Experimental Air Permeability with the Tamayol & Bahrami Theoretical for a Square Array
(a) Air permeability by fiber diameter (b) The reciprocal of the air permeability by solid volume fraction

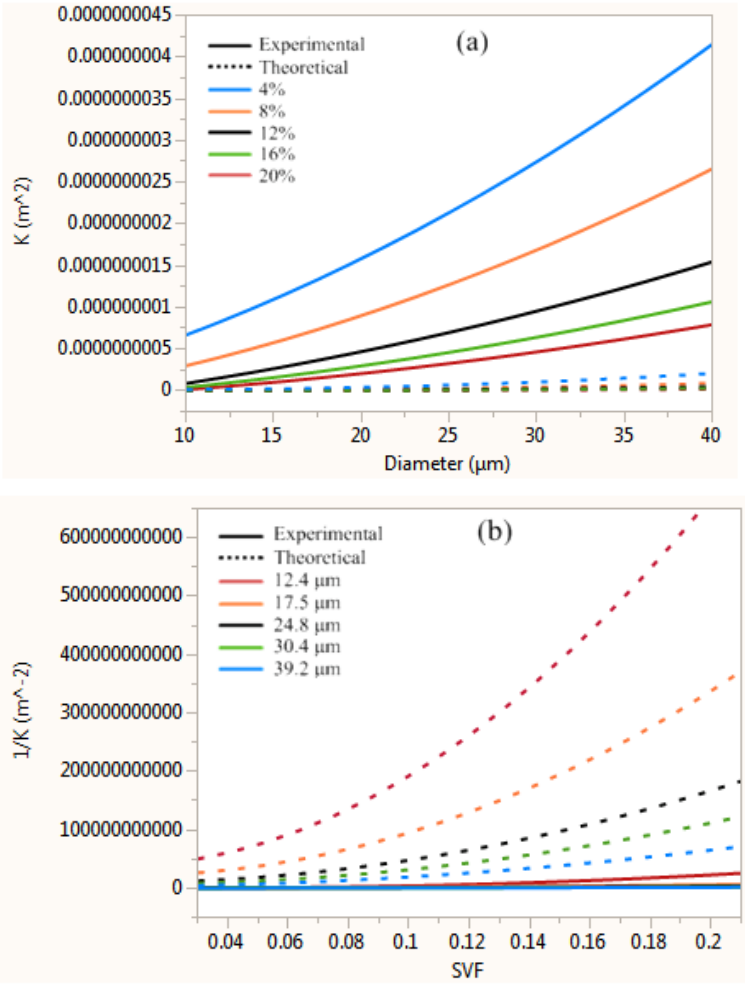

Figure 5.19: Comparison of the Experimental Air Permeability with the Tamayol & Bahrami Theoretical for a Triangular Array
(a) Air permeability by fiber diameter (b) The reciprocal of the air permeability by solid volume fraction

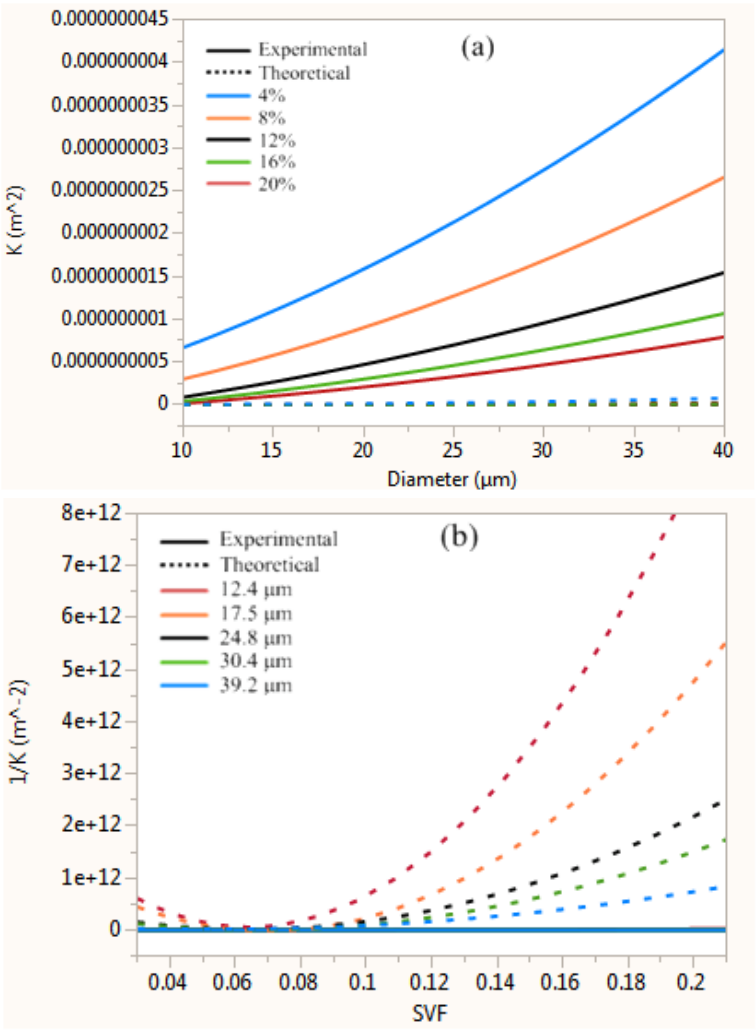

Figure 5.20: Comparison of the Experimental Air Permeability with the Tamayol & Bahrami Theoretical for a Hexagonal Array
(a) Air permeability by fiber diameter (b) The reciprocal of the air permeability by solid volume fraction

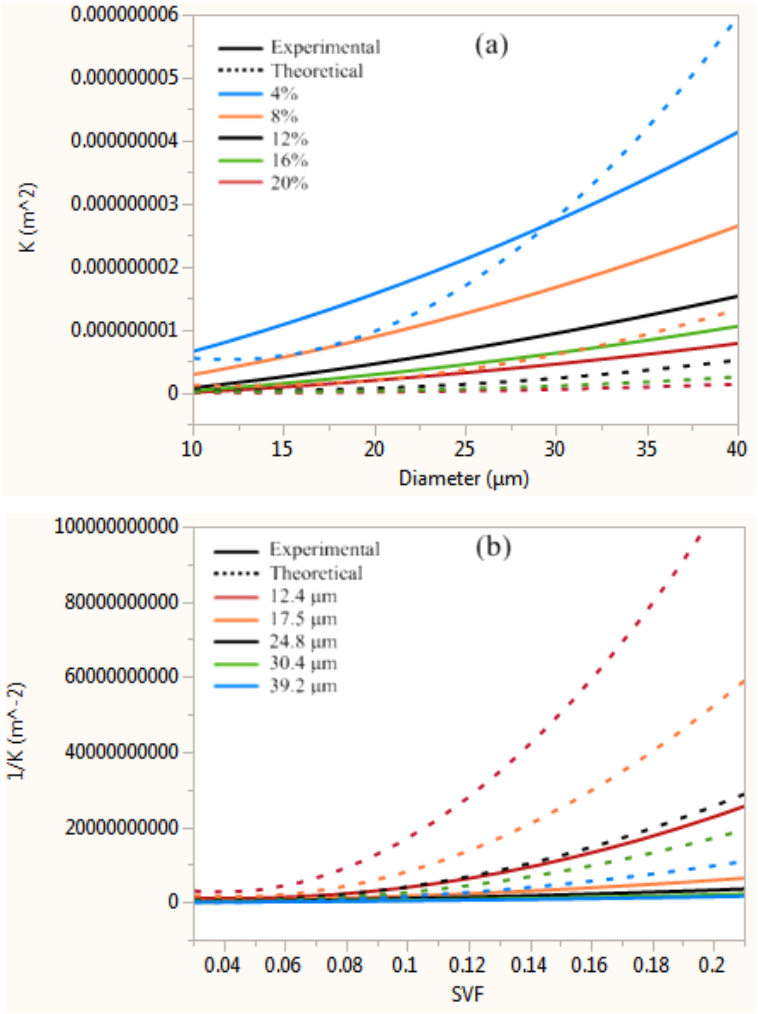

Figure 5.21: Comparison of the Experimental Air Permeability with the Tamayol & Bahrami Theoretical for a Two-Dimensional Structure
(a) Air permeability by fiber diameter (b) The reciprocal of the air permeability by solid volume fraction

5.2.8 Gebart

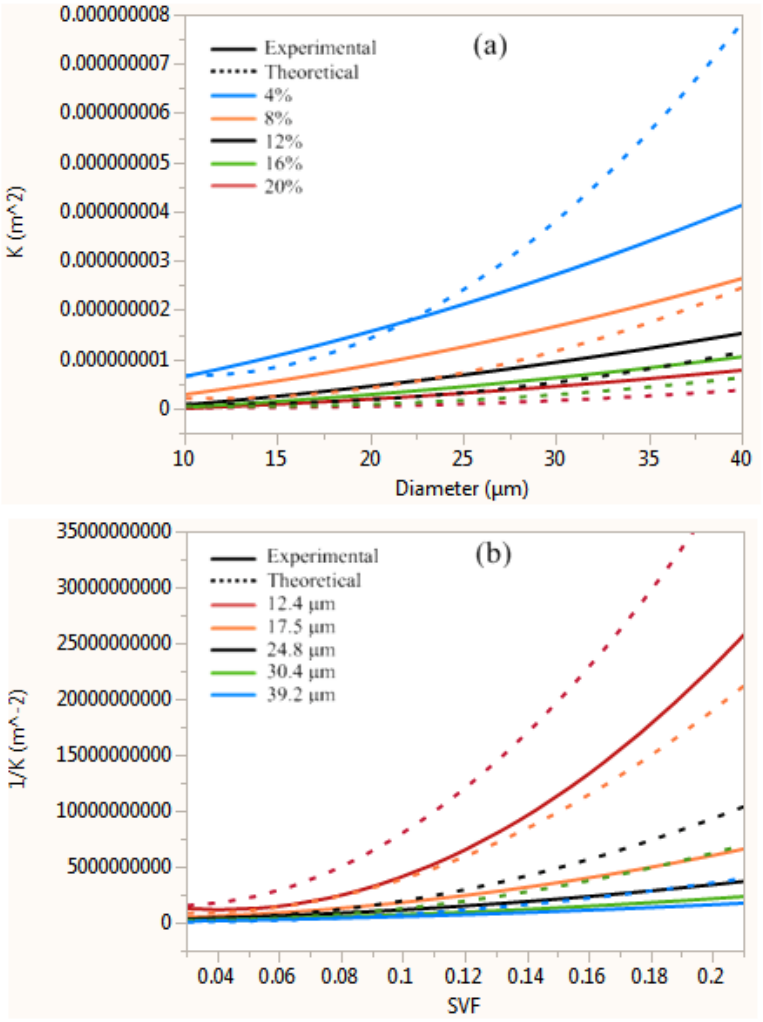

Figure 5.22: Comparison of the Experimental Air Permeability with the Gebart Theoretical for Quad Racking Packing Matrices
(a) Air permeability by fiber diameter (b) The reciprocal of the air permeability by solid volume fraction

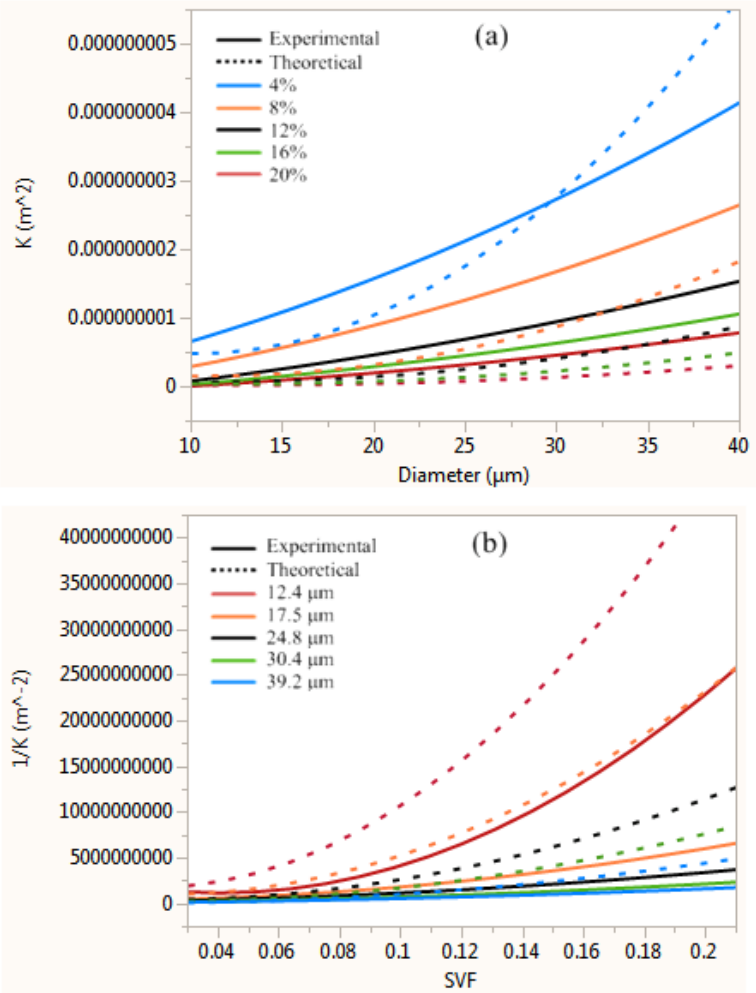

Figure 5.23: Comparison of the Experimental Air Permeability with the Gebart Theoretical for Hexagonal Packing Matrices
(a) Air permeability by fiber diameter (b) The reciprocal of the air permeability by solid volume fraction

5.2.9 Analysis

As anticipated in the literature review, the cell-based models had a general tendency to under predict the air permeability of the nonwoven samples when compared with the experimental data. As seen in Figures 5.4 – 5.23 most of the cell-based model followed a similar trend as the experimental data, though the models that predicted the permeability of the flow parallel to an array of rods along with both of the Kuwabara models, both of Gebart

models, and the Tamayol and Bahrami model for a two-dimensional structure had a tendency to over predict the air permeability in the nonwoven samples with larger fiber diameters and at higher solid volume fractions. The only models that did not follow an even somewhat similar trend with the experimental data and the rest of the theoretical models were Tamayol and Bahrami's models for triangular and circular arrays, which tremendously under predicted the experimental data and the rest of the theoretical models.

Unsurprisingly, some of the more well-known models, the Happel and Kuwbara models for the transverse permeability of circular arrays did the best job at predicting air permeabilities and coincide with the results of this research. Though Kuwabara's models predicted higher air permeabilities at higher fiber diameters and lower solid volume fractions, Kuwabara's models did a better job than Happel's model at predicting the effect changing fiber diameter and solid volume fraction had on the experimental results, and of the two, Kuwbara's model published in more recent works,

$$K = \frac{d^2}{16a}\left(-\ln\frac{a}{2} - \frac{3}{4} + a - \frac{a^2}{4}\right)$$

was the best. Besides the Tamayol and Bahrami models for triangular and circular arrays, the rest of the models for predicting the transverse permeability of a fabric seem like they could have some basis for use in predicting the air permeability of a nonwoven fabric. Other than the fact that they under predicted the air permeability of the samples, all the models for the air permeability of fabrics in transverse flow in square arrays and Sangani and Acrivos model for hexagonal arrays, followed similar trends with the experimental results.

Since all of the cell based models were designed on the premise of predicting the flow of air through fibers making up specific geometrical patterns and since the nonwoven samples and most nonwovens samples have no specific geometrical pattern, it is not difficult to see why some variation existed between the experimental results and the predictions of the different cell based-models.

5.3 Non-Cell Based Analytical Models

5.3.1 Spielman & Goren

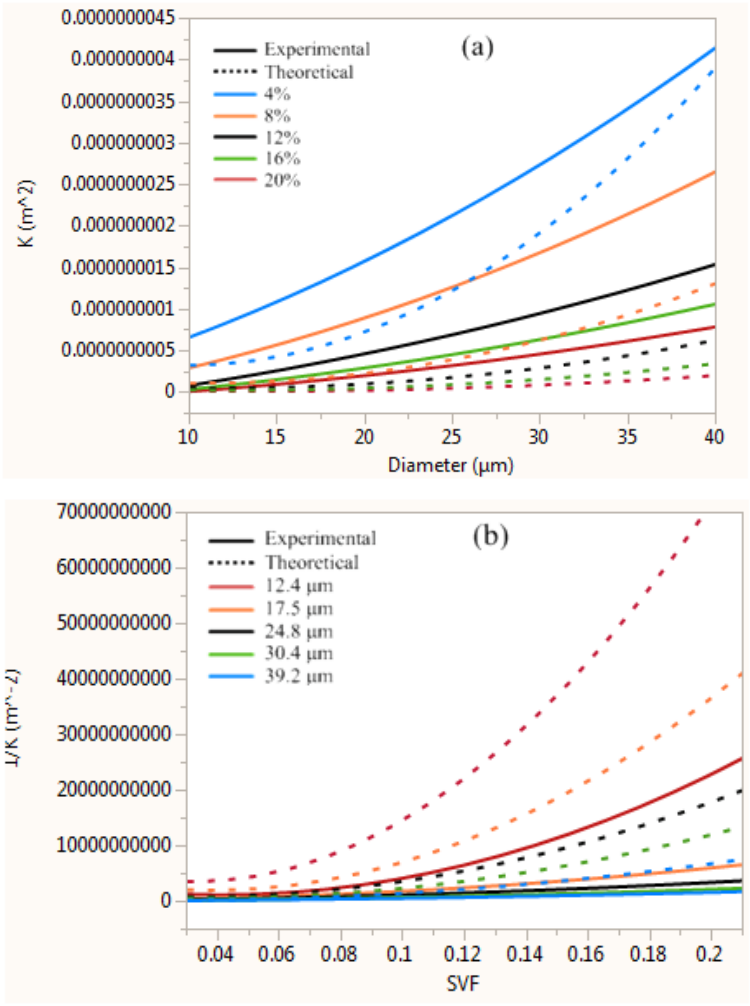

Figure 5.24: Comparison of the Experimental Air Permeability with the Spielman & Goren Theoretical for a Two-Dimensional Fabric
(a) Air permeability by fiber diameter (b) The reciprocal of the air permeability by solid volume fraction

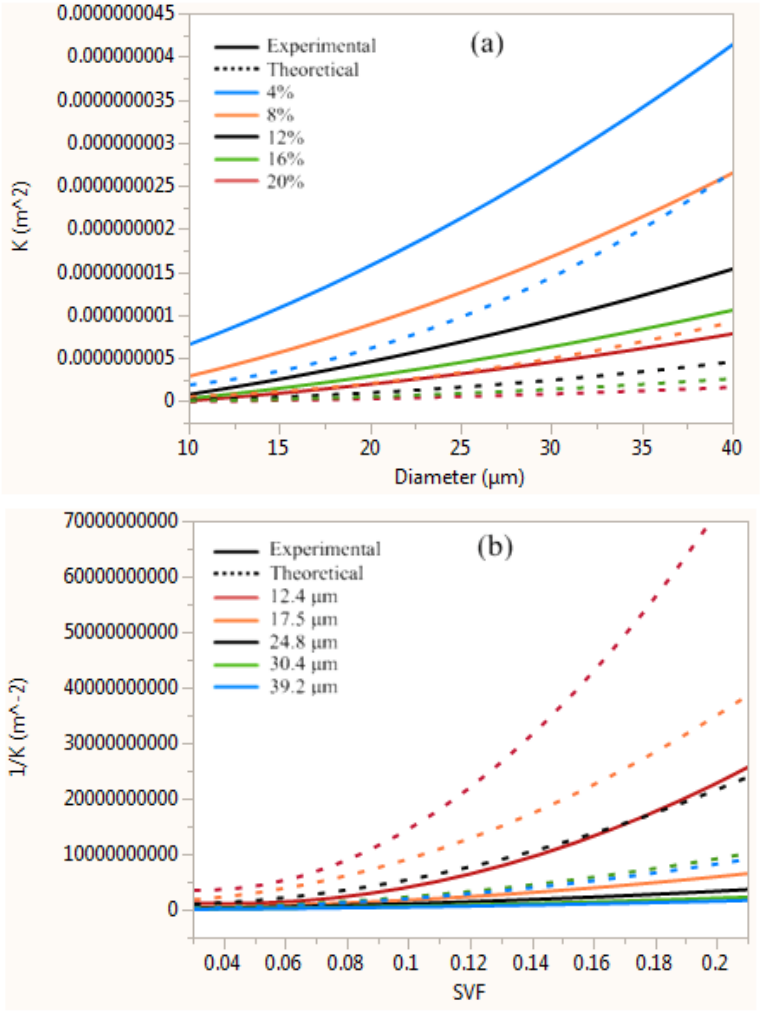

Figure 5.25: Comparison of the Experimental Air Permeability with the Spielman & Goren Theoretical for a Three-Dimensional Fabric
(a) Air permeability by fiber diameter (b) The reciprocal of the air permeability by solid volume fraction

5.3.2 Pich

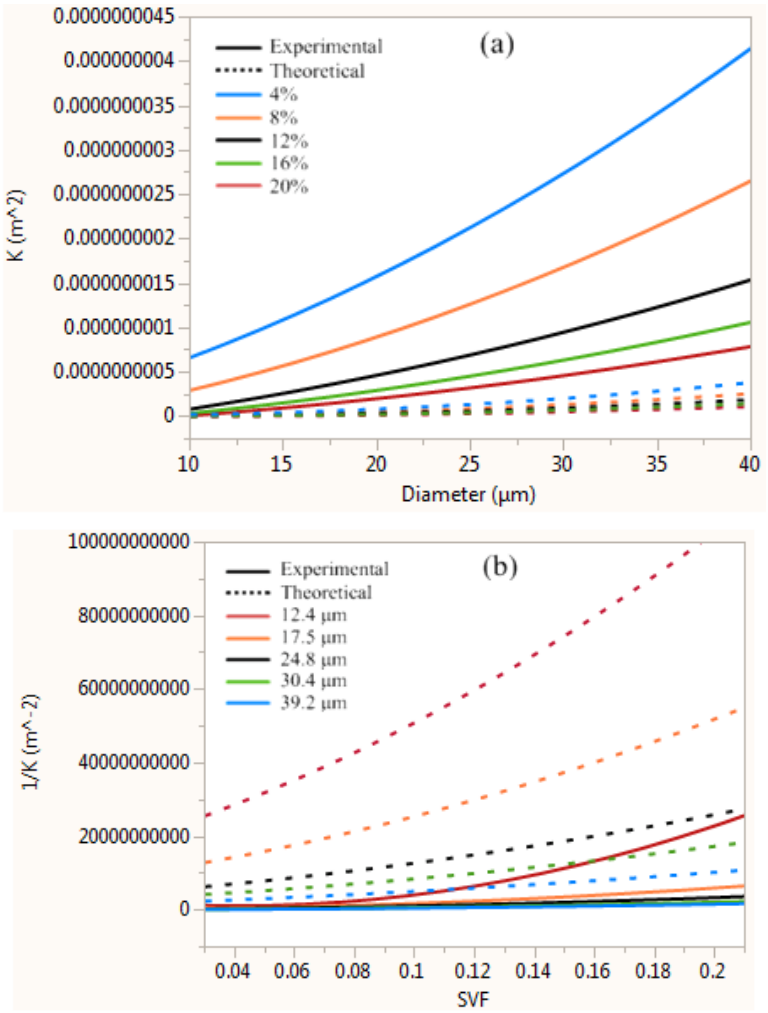

Figure 5.26: Comparison of the Experimental Air Permeability with the Pich Theoretical
(a) Air permeability by fiber diameter (b) The reciprocal of the air permeability by solid volume fraction

5.3.3 Jackson & James

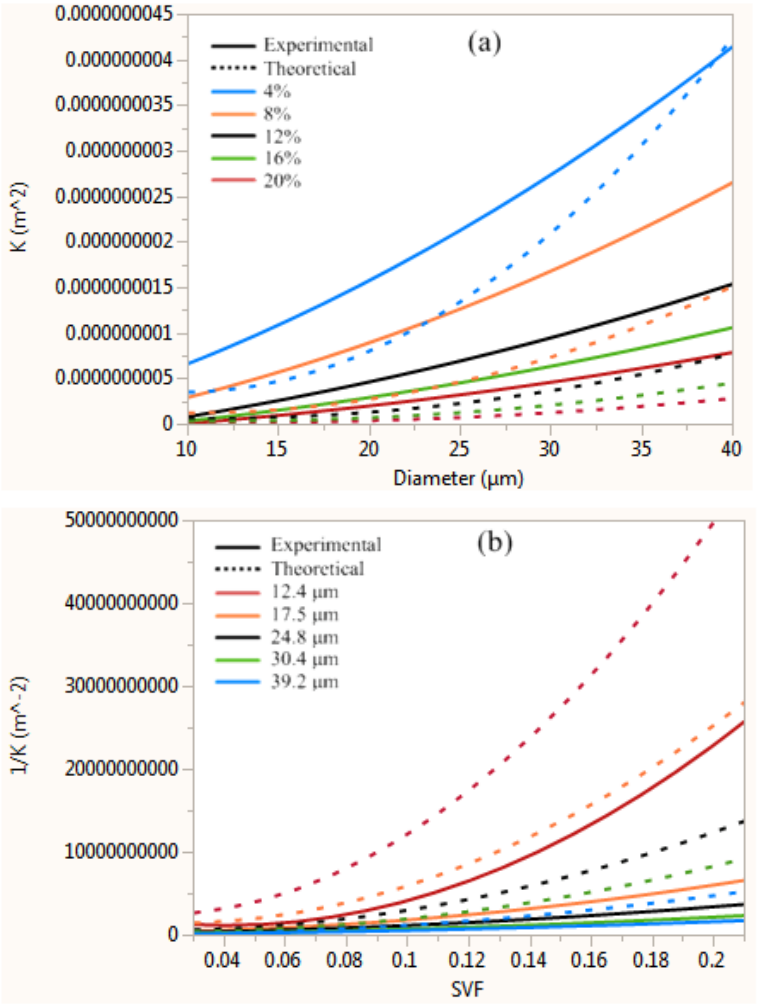

Figure 5.27: Comparison of the Experimental Air Permeability with the Jackson & James Theoretical (a) Air permeability by fiber diameter (b) The reciprocal of the air permeability by solid volume fraction

5.3.4 Conduction

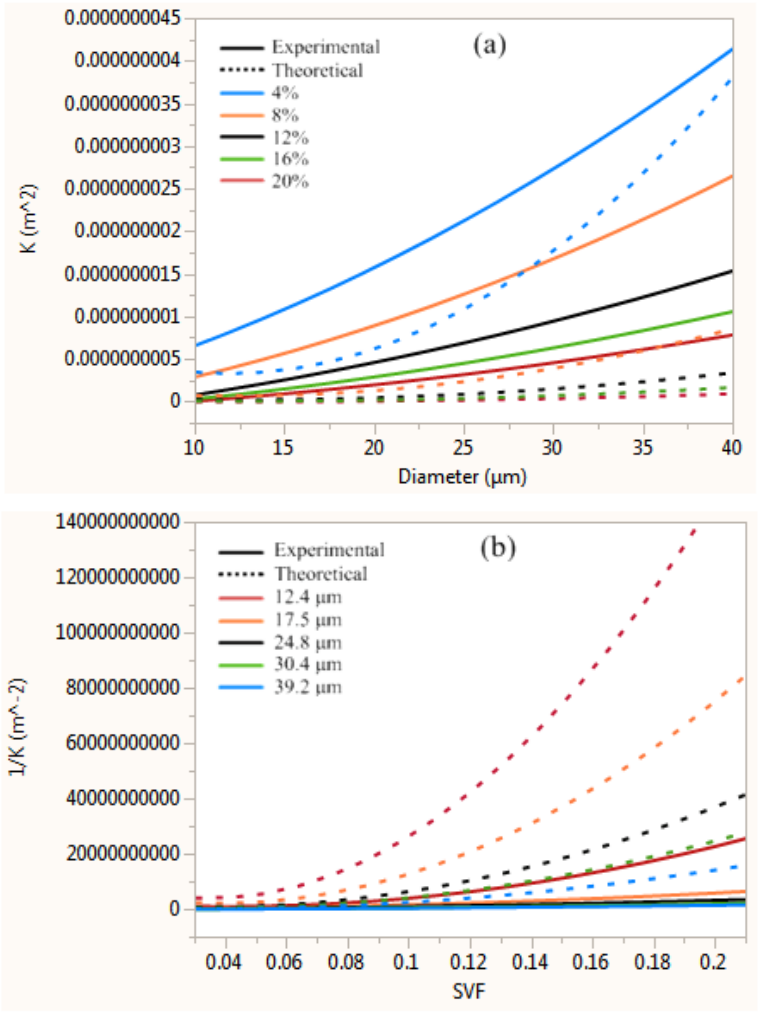

Figure 5.28: Comparison of the Experimental Air Permeability with the Conduction Theoretical for Parallel Flow in a Two-Dimensional Structure
(a) Air permeability by fiber diameter (b) The reciprocal of the air permeability by solid volume fraction

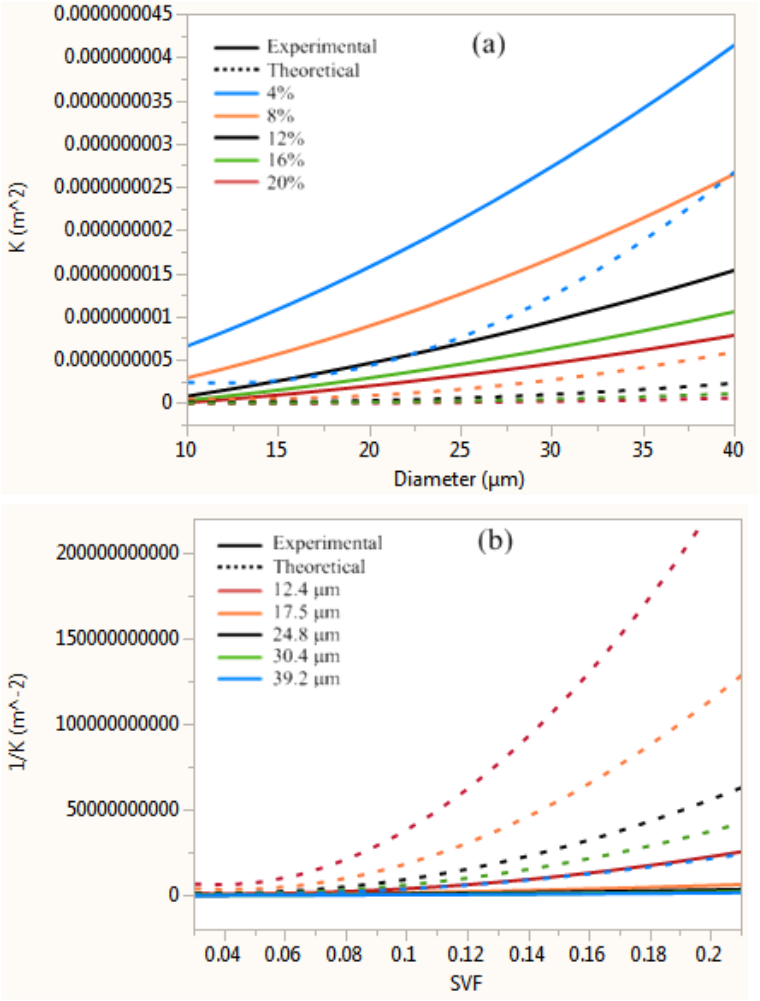

Figure 5.29: Comparison of the Experimental Air Permeability with the Conduction Theoretical for Transverse Flow in a Two-Dimensional Structure
(a) Air permeability by fiber diameter (b) The reciprocal of the air permeability by solid volume fraction

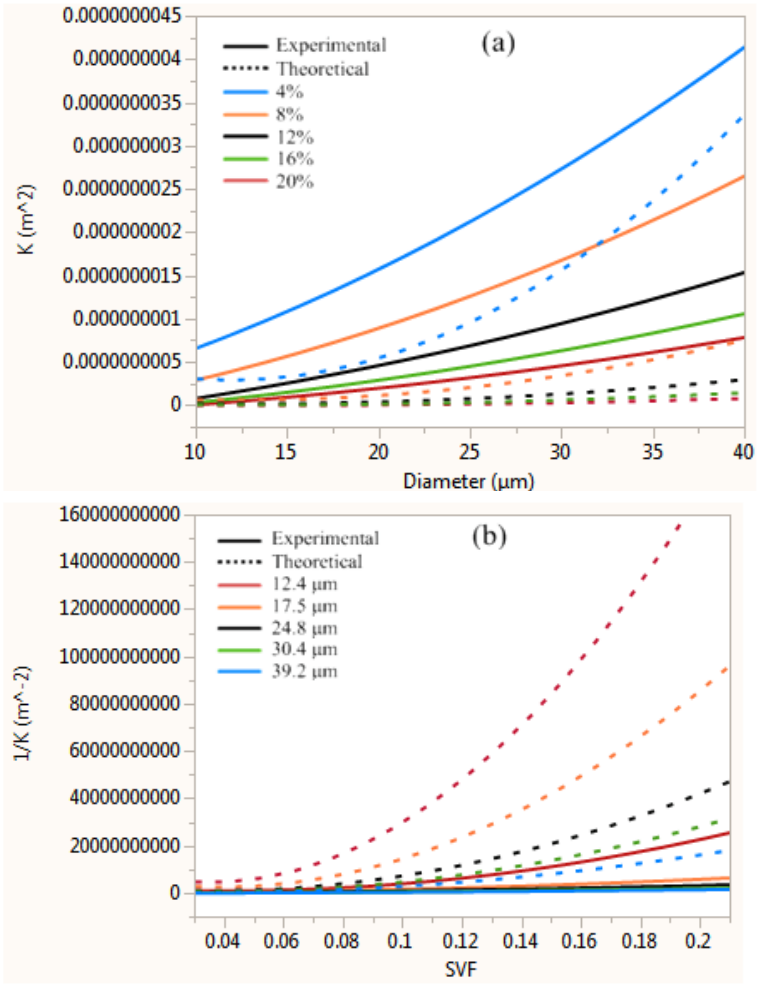

Figure 5.30: Comparison of the Experimental Air Permeability with the Conduction Theoretical for a Three-Dimensional Structure
(a) Air permeability by fiber diameter (b) The reciprocal of the air permeability by solid volume fraction

5.3.5 Higdon & Ford

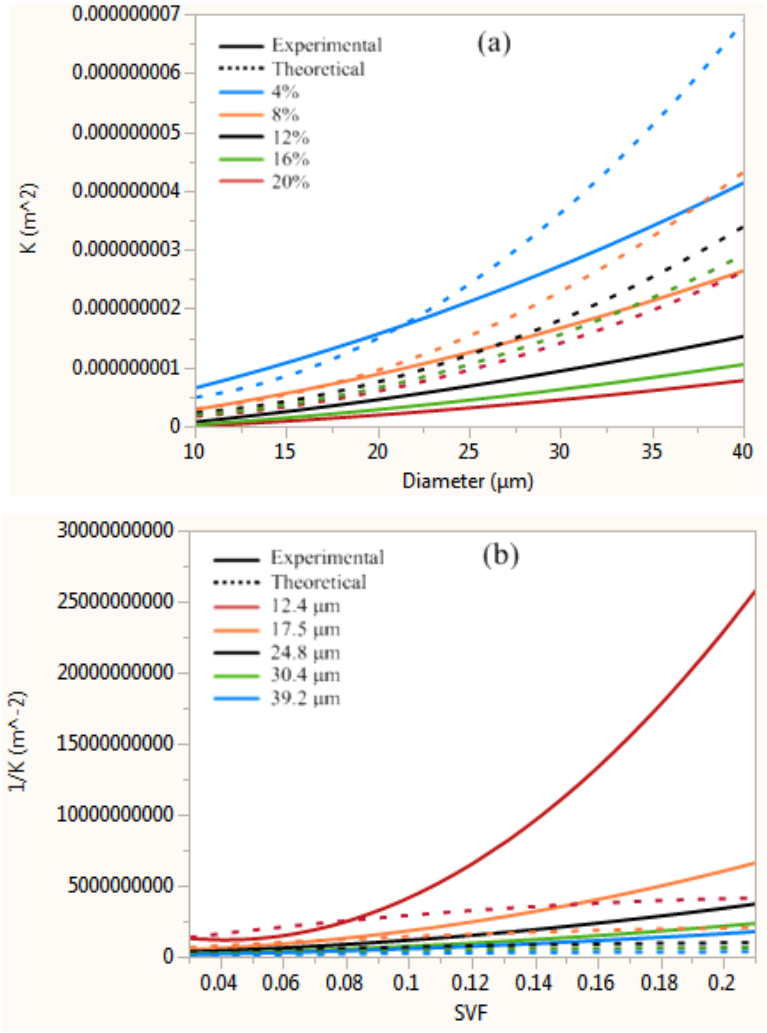

Figure 5.31: Comparison of the Experimental Air Permeability with the Higdon & Ford Theoretical (a) Air permeability by fiber diameter (b) The reciprocal of the air permeability by solid volume fraction

5.3.6 Lawrence & Liu

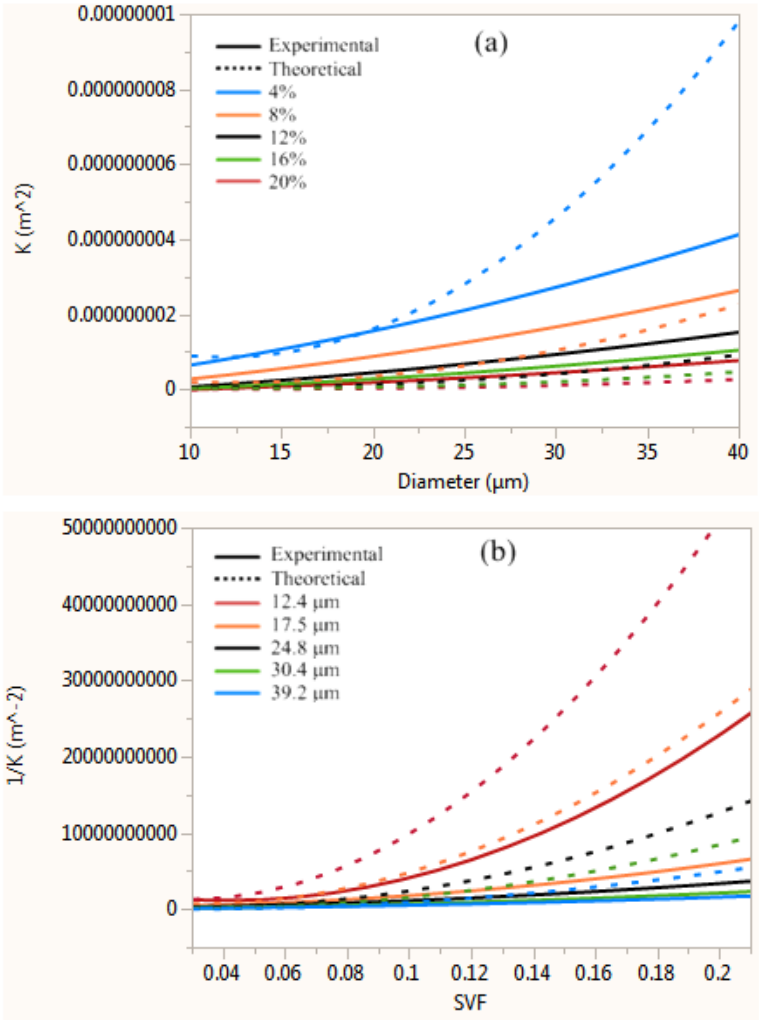

Figure 5.32: Comparison of the Experimental Air Permeability with the Lawrence & Liu Theoretical (a) Air permeability by fiber diameter (b) The reciprocal of the air permeability by solid volume fraction

5.3.7 Analysis

Figures 5.24 – 5.32 show that similar to the cell based analytical models; most of the non-cell based analytical theories also under predicted the air permeability of the samples. The exceptions to this were the Lawrence and Liu and the Higdon and Ford. The Lawrence and Liu model behaved similar to many of the cell-based models, under predicting a similar

trend to the experimental results for all but the 4% solid volume fraction samples with larger fiber diameters. This discrepancy could be because Lawrence and Liu's work did not extend below 5% solid volume fraction and to fabrics made of fibers with diameters above 23.5 microns. The Higdon and Ford model mostly over predicted the air permeability when compared with the experimental results except for the samples with smaller fiber diameters at lower solid volume fractions. It would appear that Higdon and Ford's model fails to predict the air permeability at lower solid volume fraction, since Tomadkis and Robertson (2015) reported that the Higdon and Ford model only agreed with their experimental data when the solid volume fraction was above 10%.

Other than model based on Pich's work, which severely under predicted the air permeability, the rest of the models, Spielman and Goren's models, Jackson and James' model, and the conduction based models, followed a similar trend with the experimental results. Of these, the Spielman and Goren model based on a three-dimensional structure and conduction based model for the transverse flow through a two dimensional structure, had trends most alike that of the experimental data. The Spielman and Goren's model for two-dimensional structures, Jackson and James' model and, the other two conduction based models failed to follow the trend at lower solid volume fraction and higher fiber diameters, following a pattern that would drift toward over predict the air permeability in such structures.

Since the model proposed in Das, Ishtiaque, Rao & Pourdeyhimi (2013), relied heavily on the two parameters "determined empirically from experimental data (Neckar &

Ibrahim, 2003, pg. 617),” it was not found to be practical in forecasting the air permeability of a fabric.

5.4 Empirical Based Models

5.4.1 Henry & Ariman

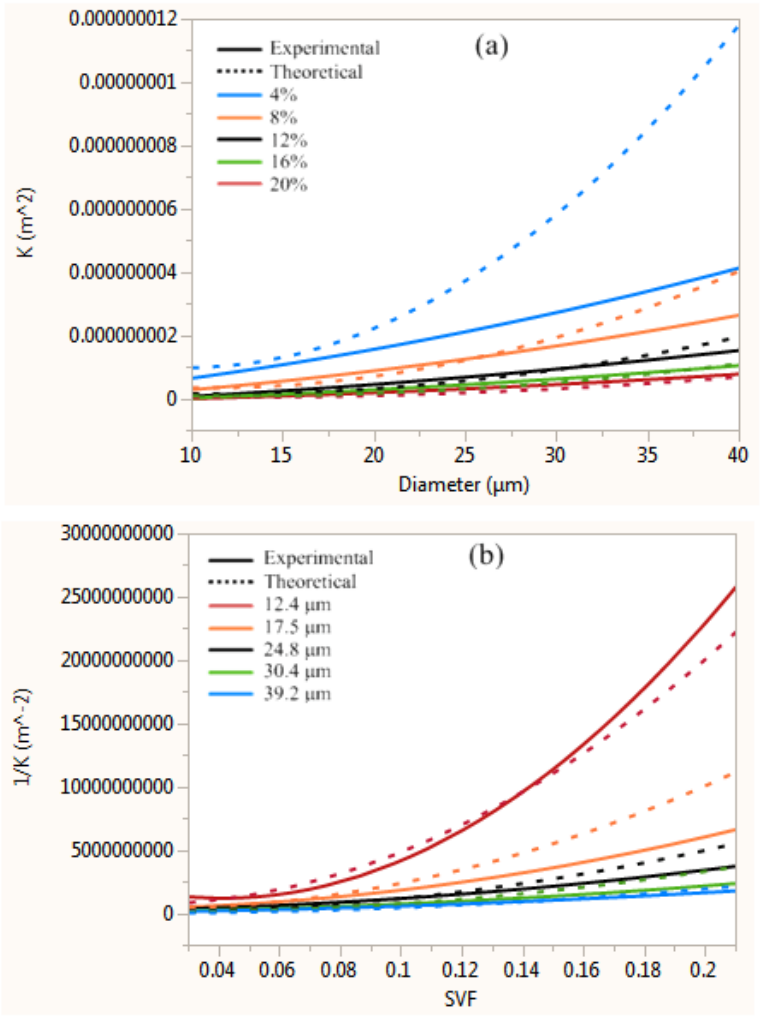

Figure 5.33: Comparison of the Experimental Air Permeability with the Henry & Ariman Theoretical (a) Air permeability by fiber diameter (b) The reciprocal of the air permeability by solid volume fraction

5.4.2 Rao & Faghri

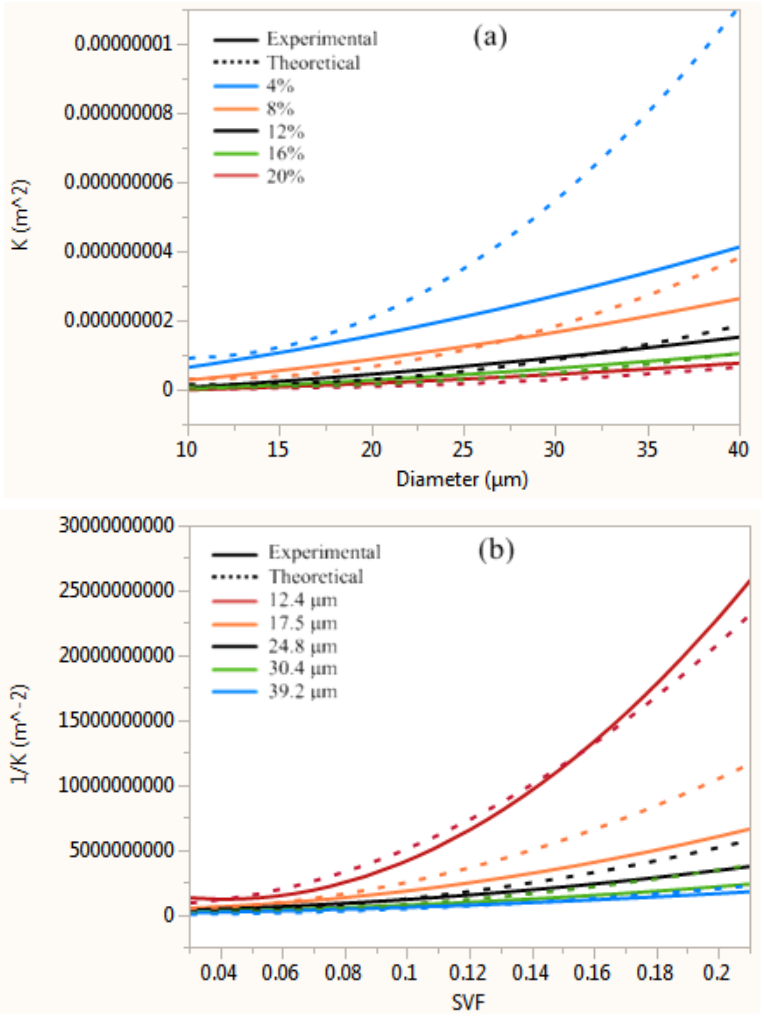

Figure 5.34: Comparison of the Experimental Air Permeability with the Rao & Faghri Theoretical (a) Air permeability by fiber diameter (b) The reciprocal of the air permeability by solid volume fraction

5.4.3 Johnston

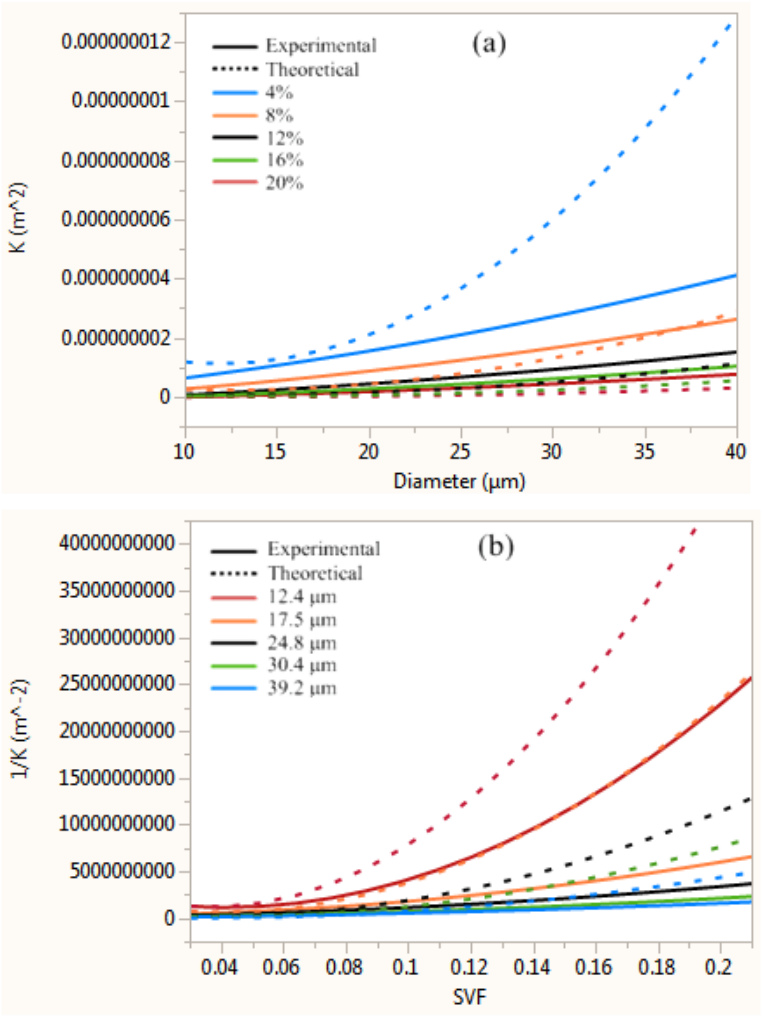

Figure 5.35: Comparison of the Experimental Air Permeability with the Johnston Theoretical
(a) Air permeability by fiber diameter (b) The reciprocal of the air permeability by solid volume fraction

5.4.4 Kopenen et al.

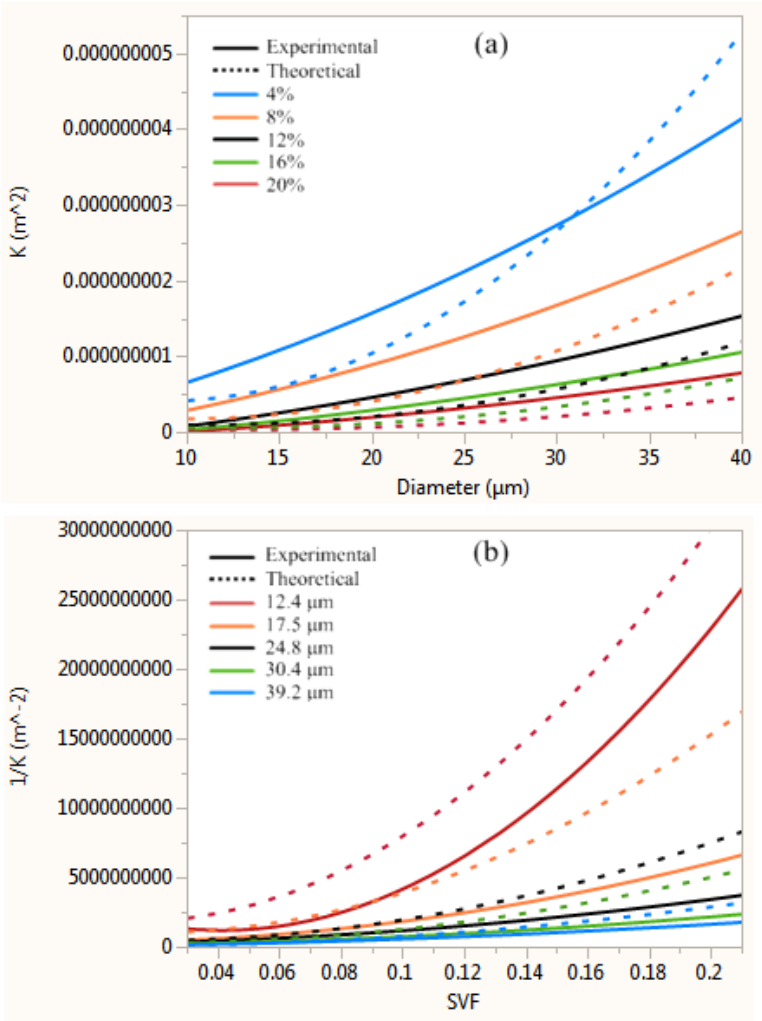

Figure 5.36: Comparison of the Experimental Air Permeability with the Kopenen et al. Theoretical (a) Air permeability by fiber diameter (b) The reciprocal of the air permeability by solid volume fraction

5.4.5 Navobati, Llewellin & Sousa

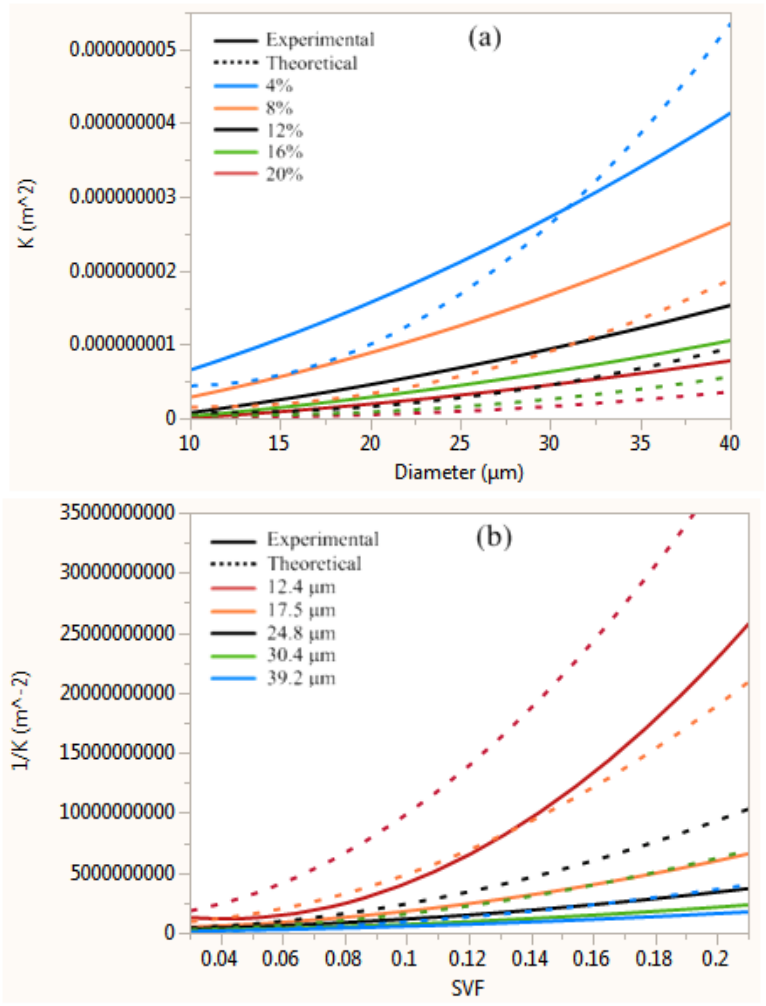

Figure 5.37: Comparison of the Experimental Air Permeability with the Navobati, Llewellin & Sousa Theoretical
(a) Air permeability by fiber diameter (b) The reciprocal of the air permeability by solid volume fraction

5.4.6 Vallabh, Banks-Lee & Seyam

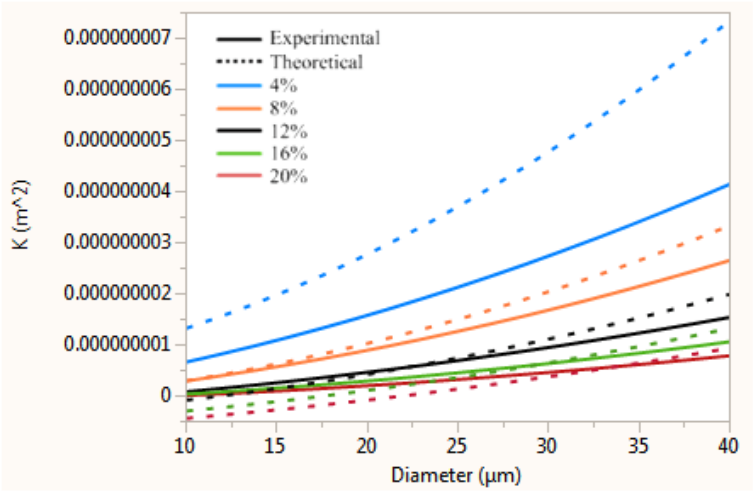

Figure 5.38: Comparison of the Experimental Air Permeability with the Vallabh, Banks-Lee & Seyam Theoretical

5.4.7 Analysis

All of the empirical based models neither completely under predict nor completely over predict air permeability, but rather did a little of each depending on the solid volume fraction and fiber diameter. The models by Henry and Ariman and Rao and Faghri agreed well each other and with the experimental data, but both models over predicted the samples that had a lower solid volume fraction and under predicted the samples that had a higher solid volume fraction. Johnston models followed a trend similar to that of Henry and Ariman's and Rao and Faghri's models but the air permeability predicted by Johnston's model deviated further from experimental result than that of Henry and Ariman's and Rao and Faghri's.

The models postulated by Kopenen et al. and Navobati, Llewellin & Sousa agreed well each other and with many of the cell based models for parallel flow, underestimating a similar trend with the experimental except for the samples with a solid volume fraction of 4% at larger fiber diameters (above 30 microns). This deviation from the trend of the

experimental results was expected since Kopenen et al. (1998) reported that their model worked in nonwovens with a solid volume fraction ranging from 5% to 60%, and Navobati, Llewellin, and Sousa reported that their model deviated at low solid volume fractions.

Though the model derived in the paper by Vallabh, Banks-Lee & Seyam tended to over-predict a trend comparable to that of the experimental data, this model failed to be able to predict the effect that smaller fiber diameters had on the air permeability at higher solid volume fractions. The negative projections for the samples composed of fibers with 12.401 and 17.537 microns at solid volume fractions of approximately 16% and 20% was very surprising, since both samples were well within the range (7.7-25.3 μm and 10-35% SVF) of fabrics the Vallabh, Banks-Lee and Seyam's empirical model were based upon. The thickness of the samples used in this research might account for the negative results by being slightly outside the range of Vallabh, Banks-Lee and Seyam's model, but all the samples tested in this research had a similar thickness around 4 millimeters and Vallabh, Banks-Lee and Seyam's experimental work included a sample with a thickness of 4.04 millimeters composed of 15.8 micron diameter fibers.

While some of the empirical based models were able to predict some of the effect solid volume fraction and fiber diameter had on the air permeability, they did so as long as the sample parameters were within the range the model was based upon. Outside of those ranges and sometimes even within those ranges, the empirical models had limited use to no use in predicting the trend of the air permeability when compared with the experimental results of this research. Due to the circumstantial usability and the inconsistency, under predicting at times and over predicting at others, the empirical based models were too limited

to be used dependably to predict the air permeability of a wide range of fabrics with varying structures, such as nonwovens.

6. CONCLUSION & FUTURE WORKS

The air permeability of a fabric is affected by numerous factors related to the qualities of the air and fabric used. The velocity and thickness of the air passing through fabric also plays a key role, since at higher flow rates and higher viscosities, the air is able to more easily force its way through the fabric. For this reason, when a fabric's air permeability is measured, the results will be affected by the testing parameter used. The structure of the fabric, the fiber shape and size, and the manufacturing processes used to create the fabric all have varying effect on the fabrics ability to limit air flow through the fabric. Thicker, denser fabrics with larger surface areas and less flow paths will be more readily able to impede air from flowing easily through it. Since the fabric structure dictates the method in which it was created, the manufacturing processes also plays a role in influencing the air permeability. For these reasons, it is extremely difficult to predict the air permeability of a fabric.

Predicting the air permeability of a nonwoven fabric is also particularly difficult because of the manufacturing processes that are used to create them. Not only are nonwoven fabrics non-uniform in nature. They are created using an assortment of methods used to combine and bind the fibers together using several methods that will affect the structure of nonwovens differently in particular needlepunching, which creates through channels allowing air to more easily pass through the nonwoven.

Due to the difficulty in predicting the air permeability of fabrics, a method or model has yet to be created to calculate the air permeability of all fabrics; instead numerous researchers have proposed various techniques to predict the air permeability. For the most part, these models have originated from studying the flow of air through defined structures,

analyzing the flow air around a fiber, or through empirical means. Though the models differ greatly, all of the research agrees that the two most important factors affecting air permeability is the solid volume fraction and the fiber diameter of the fabric.

To evaluate the effectivity of the various models, a dual approach was used to analyze carded and needle punched nonwoven fabrics composed of polyester fiber with diameters ranging from 12.401 to 39.214 microns. Using both an air permeability tester that measured the air permeability with a fixed pressure and an air permeability tester that used a fixed flow, a compression system was used to calculate the air permeability of samples with solid volume fractions ranging from about 4% to 20%. After the air permeability of the samples were collected using both instruments with and without the compression system, a conversation process was used to make the data comparable, and the results were back calculated to be aligned with that of the ASTM standard for air permeability of a fabric. Though the different testers and methods had highly correlated results, there was no direct equivalence between the different instruments and techniques and only after numerous measurements was it possible to establish a relationship between differing methods, further propagating the fact that the machine and testing method, fixed flow or fixed pressure, used had effect on the calculated air permeability of a fabric.

Agreeing well with the literature review, the back calculated results demonstrated that the solid volume fraction and fiber diameter greatly affected the flow air through the nonwoven samples. In the nonwoven samples tested, as fiber diameter decreased, air permeability started approaching zero and as fiber diameter increased, the air permeability grew exponentially. This was opposite of the solid volume fraction, where air permeability

increased exponentially as solid volume fraction was decreased and approached zero as solid volume fraction increased.

When the experimental results were compared the theoretical models, the general trend was for the models to under predict the air permeability of the nonwoven samples. The cell based models and some of the non-cell based models, hypothesized on the flow of air through defined structure, did an adequate job at predicting the flow of air through the nonwovens, but the nonwoven samples' non-uniformity and the lack of a defined structure limited their ability to be accurately used with nonwoven fabrics. The Kozeny-Carman and Das, Ishtiaque, Rao, and Pourdeyhimi models were limited in their ability to predict air permeability, since they relied heavily on constants or parameters, which could only be determined through experimental means. While some of the empirical based models were able to forecast trends of air permeability within certain ranges, in general, they had limited use since they were restricted by the realms in which they were created. The general trend of almost all the models under predicting the air permeability could be accounted for by the fact that the samples tested in this research were created through means of needlepunching, which naturally increases the air permeability of a nonwoven by punching through channels in the fabric during the needling mechanism.

Of all the models, some of the best were some of the first models created. Though created through empirical means, Davies model was reasonably accurate at calculating the air permeability of the nonwoven samples, since his model was created using a host of data from wide range of fabrics. While they were constructed after studying the flow around circular arrays, Happel's and Kuwabara's models did a great job at predicting the effect changing

solid volume fraction and fiber diameter had on the air permeability of the samples. Even one of the oldest non-cell based analytical models, Spielman and Goren's model accurately followed the trend of the air permeability of the nonwoven samples in the experimental work. Though these are some of the oldest models, this research proves that some of the earliest models are among the most robust for predicting the air permeability of a nonwoven fabric. It could even be postulated, that even the oldest model, the Kozeny-Carman model would be among this list, if the Kozeny constant could be forecasted accurately.

While a theoretical empirical based model could be created using the experimental results of this research, it was decided against, since such a model would only be applicable for a relatively small range of solid volume fractions and fiber diameters within carded and needle punched polyester fabrics. In general, there are too many impractical and limited models, particularly empirical based, for predicting the air permeability of fabrics, and one more with such a restricted window is unnecessary.

In future works, it is suggested that the air permeability of further nonwoven samples be analyzed. In this research, only one fiber in fabric from only one of the methods of nonwoven manufacturing was examined. A more accurate understanding of the air permeability of nonwovens could be expanded if various other methods of nonwoven manufacturing using a variety of fibers and a wider range of solid volume fractions were evaluated. In addition, further examination of the Kozeny-Carman equation and Kozeny constant is suggested. There are about as many methods for predicting the Kozeny constant as there are for predicting the air permeability of a fabric, so in-depth examination of these is warranted to truly test the accuracy of the Kozeny-Carman model.

REFERENCES

ASTM International. (2012). *ASTM D737-04*: *Standard test method for air permeability of textile fabrics.* (DOI: 10.1520/D0737-04R12). West Conshohocken, PA.

Benson, T. (2014). Air viscosity: Sutherland's formula. Retrieved from http://www.grc.nasa.gov/WWW/BGH/viscosity.html

Brown, G. (2005). *Darcy's law basics and more.* Retrieved from http://biosystems.okstate.edu/darcy/LaLoi/basics.htm

Cai, Z. (1992). Estimation of the permeability of fibrous preforms for resin transfer moulding processes. *Composites Manufacturing,* 3(4), 251-257.

Carman, P.C. (1956). *Flow of gases through porous media*. New York: Academic Press.

Chapman, R.A. (2010). *Applications of nonwoven in techinal textiles.* Oxford, UK: Woodhead Publishing

Clauge, D.S. & Phillips, R.J. (1997). A numerical calculation of the hydraulic permeability of three-dimensional disordered fibrous media. *Phys. Fluids*, 9(6), 1562-1572.

Darcy's law. (2015). In Encyclopædia Britannica. Retrieved from http://www.britannica.com/EBchecked/topic/151481/Darcys-law

Das, D., Ishtiaque, S.M., Ajab Rao, S.V., & Pourdeyhimi, B. (2013). Modelling and experimental studies of air permeability of nonuniform nonwoven fibrous porous media. *Fibers and Polymers,* 14(3), 494-499.

Dent, R.W. (1976). The air-permeability of nonwoven-fabrics-reply. *Journal of the Textile Institute,* 67(6), 220-224.

FracFocus. (2015). *Fluid flow in the subsurface (Darcy's Law).* Retrieved from https://fracfocus.org/groundwater-protection/fluid-flow-subsurface-darcys-law

Gebart, B.R. (1992). Permeability of unidirectional reinforcements for RTM. *Journal of Composite Materials,* 26(8), 1100-1133.

Gervais, P.C., Bardin-Monnier, N. & Thomas, D. (2012). Permeability modeling of fibrous media with bimodal fiber size distribution. *Chemical Engineering Science*, 73, 239-248.

Henry, F.S. & Ariman, T. (1983). An evaluation of the Kuwabara model. *Particulate Science and Technology: An International Journal,* 1(1), 1-20.

Higdon, J.J. & Ford, G.D. (1996). Permeability of three-dimensional models of fibrous porous media. *Journal of Fluid Mechanics*, 308(1), 341-361.

ISO. (2011). ISO 9092:2011 Textiles – Nonwovens – Definition. Geneva, Switzerland: ISO

Jackson, G.W. & James, D.F. (1986). The permeability of fibrous porous media. *The Canadian Journal of Chemical Engineering*, 64(3), 364-374

Jayaraman, K.A. (2005). *Acoustical absorptive properties of nonwovens* (unpublished doctoral dissertation). North Carolina State University, Raleigh, NC.

Johnston, P.R. (1993). Revisiting the most probable pore-size distribution in filter media: The gamma distribution. *Filtration & Seperation*, 35(3), 287-292.

Kato Tech Co., LTD. (2007). KES-F8 Air Permeability. Retrieved from http://english.keskato.co.jp/products/kes_f8.html

Koponen, A., Kandhai, D., Hellén, E., Alava, M., Hoekstra, A., Kataja, M., Niskanen, K., Sloot, P. & Timonen, J. (1998). Permeability of three-dimensional random fiber webs. *Physical Review Letters*, 80(4), 716-719.

Kothari, V.K. & Newton, A. (1974). The air-permeability of nonwoven-fabrics. *Journal of the Textile Institute*, 65(10), 525-531.

Kothari, V.K. & Newton, A. (1976). The air-permeability of nonwoven-fabrics-reply. *Journal of the Textile Institute*, 67(6), 224.

Labrecque, R.P. (1967). An investigation of the effects of fiber cross sectional shape on the resistance to the flow of fluids through fiber mats (Doctoral dissertation). Retrieved from George Institute of Technology. (http://hdl.handle.net/1853/5605)

Lamb, G.E.R., Costanza, P. & Miller, B. (1975). Influences of fiber geometry on the performance of nonwoven air filters. *Textile Research Journal*, 45(6), 452-463.

Lawrence, C.A. & Liu, P. (2006). Relation of structure, properties and performance of fibrous media for gas filtration. *Chemical Engineering & Technology*, 29(8), 957-967.

Mao, N. & Russell, S.J. (2000). Directional permeability in homogeneous nonwoven structures part 1: The relationship between directional permeability and fibre orientation. *Journal of the Textile Institute*, 91(2), 235-243.

Maze, B., Vahedia Tafreshi, H. Wang, Q. & Pourdeyhimi, B. (2007). A simulation of unsteady-state filtration via nanofiber media at reduced operating pressures. *Journal of Aerosol Science*, 38(5), 550-571.

Nabovati, A., Llewellin, E.W. & Sousa, A.C.M. (2009). A general model for the permeability of fibrous porous media based on fluid flow simulations using the lattice Boltzmann method. *Composites: Part A*, 40(6), 860-869.

Neckar, B. & Ibrahim, S. (2003). Theoretical approach for determing pore characteristics between fibers. *Textile Research Journal*, 73(7), 611-619.

Pich, J. (1966). Pressure drop of fibrous filters at small Knudsen numbers, *The Annals of Occupational Hygiene*, 9(1), 23-27.

Pich, J. (1971). Pressure characteristics of fibrous aerosol filters. *Journal of Colloid and Interface Science*, 37(4), 912-917.

Pradhan, A.K. (2013). *Studies on multi-consistutent nonwoven air filter media.* (Doctoral dissertation). Indian Institute of Technology Delhi, New Delhi, India.

Rao, N & Faghri, M. (1988). Computer modeling of aerosol filtration by fibrous filters. *Aerosol Science and Technology*, 8(2), 133:156.

Shim, E. (2012a). *Lecture 1: Introduction to Nonwovens* [PowerPoint slides]. Retrieved from NC State TT 504 Moodle website

Shim, E. (2012b). *Lecture 3:Structures of Nonwovens - 1* [PowerPoint slides]. Retrieved from NC State TT 504 Moodle website

Tamayol, A. & Bahrami, M. (2010). Transverse permeability of fibrous porous media. *Proceedings of the 3rd International Conference on Porous Media and its Applications in Science and Engineering*. Montecatini, Italy: ICPM3.

TexTest. (n.d.). Air Permeability Tester FX 3300 LabAir IV. Retrieved from http://www.textest.ch/en/FX3300-Lab-Air.html

Tomadakis, M.M. & Robertson, T.J. (2005). Viscous permeability of random fiber structures: Comparison of electrical and diffusional estimates with experimental and analytical results. J*ournal of Composite Materials*, 39, 163-188.

Vallabh, R., Banks-Lee, R., & Seyam, A. (2010). New approach for determining tortuosity in fibrous porous media. *Journal of Engineered Fibers and Fabrics*, 5(3), 7-19.

Wang, Q., Maze, B., Vahedi Tafreshi, H. & Pourdeyhimi, B. (2007a). A case study of simulating submicron aerosol filtration via lightweight spun-bonded filter media. *Chemical Engineering Science*, 61(15), 4871-4883.

Wang, Q., Maze, B., Vahedi Tafreshi, H. & Pourdeyhimi, B. (2007b). Simulating through-plane permeability of fibrous materials with different fiber lengths. *Modelling and Simulation in Materials Science and Engineering*, 15(8), 855-868.